Journal of Environmental Chemical Engineering 14 (2026) 122520

Contents lists available at ScienceDirect

Journal of Environmental Chemical Engineering

journal homepage: www.elsevier.com/locate/jece

Advancements in polysulfone membrane technology for efficient H_2S and CO_2 separation from CH_4: A comprehensive review

Waqar Hussain [a,b], Serene Sow Mun Lock [a,b,*,1], Syed Abdul Moiz Hashmi [a,b,h], Lydia Anggraini [c], Lian See Tan [d], Mee Kee Wong [e], Lam Ghai Lim [f], Suhaib Umer Ilyas [g], Mehtab Ali Darban [a,b]

[a] Chemical Engineering Department, Universiti Teknologi PETRONAS, Bandar Seri Iskandar, Perak 32610, Malaysia
[b] Centre of Carbon Capture, Utilisation and Storage (CCCUS), University Teknologi PETRONAS, Seri Iskandar, Perak 32610, Malaysia
[c] Department of Mechanical Engineering, President University, Jababeka Education Park, West Java 17550, Indonesia
[d] Department of Chemical and Environmental Engineering, Malaysia - Japan International Institute of Technology, Universiti Teknologi Malaysia, Kuala Lumpur, Malaysia
[e] PETRONAS Research Sdn Bhd, Lot 3288 & 3289, Off Jalan Ayer Hitam, Kawasan Institusi Bangi, Kajang, Selangor 43000, Malaysia
[f] Department of Electrical and Robotics Engineering, School of Engineering, Monash University Malaysia, Jalan Lagoon Selatan, Bandar Sunway, Selangor 47500, Malaysia
[g] Department of Chemical Engineering, College of Engineering, University of Jeddah, Jeddah 23890, Kingdom of Saudi Arabia
[h] School of Engineering, STEM College, RMIT University, Melbourne VIC 3000, Australia

ARTICLE INFO

Keywords:
Polysulfone membrane innovations
Molecular simulations
Polymeric or composite membranes
Hybrid membranes
Membrane synthesis
Characterization
And predictive framework & sensitivity analysis

ABSTRACT

Natural gas streams frequently contain carbon dioxide (CO_2) and hydrogen sulfide (H_2S), which cause corrosion, safety hazards, and environmental concerns, necessitating efficient separation technologies. Membrane-based processes have gained increasing attention due to their energy efficiency and operational simplicity, with polysulfone (PSF)-based membranes emerging as promising candidates because of their thermal stability, mechanical strength, and tunable transport properties. Despite their extensive studies on CO_2/CH_4 separation, research addressing the separation of CO_2 and H_2S from CH_4 under sour gas conditions remains limited and fragmented. This review critically evaluates recent advances in PSF-based membrane technologies for CO_2 and H_2S separation from natural gas, with particular emphasis on fabrication routes such as solution casting and phase inversion, characterization techniques, and gas permeation analysis. To address this gap, a literature calibrated predictive analytical framework is proposed that systematically links experimentally verifiable indicators like morphology, polymer-filler interfacial integrity, chemical interactions, chain mobility, thermal stability, and plasticization resistance to membrane design robustness. Recent findings demonstrate that hybrid architectures, particularly PSF-based mixed matrix membranes (MMM), incorporating functionalized fillers such as zeolitic imidazolate frameworks (ZIFs), graphene oxide, metal organic frameworks (MOFs), and ionic liquids, significantly enhance permeability, selectivity, and long term stability. The integration of molecular simulations and machine learning is highlighted as a promising pathway towards predictive membrane design and accelerated material screening for sour gas separation.

1. Introduction

Natural gas has been a popular energy source for decades, and its global demand as a fuel is steadily increasing [1,2] where methane (CH_4) is found in a significant ratio in natural gas [3,4]. The composition of natural gas varies significantly depending on its source, as illustrated in Fig. 1, which presents both the classification of natural gas resources and the typical composition of raw gas prior to processing [5–8]. Globally, many reserves consist of sour gas, containing substantial amounts of acid gases such as carbon dioxide (CO_2) (up to 90%) and hydrogen sulfide (H_2S) (up to 15%) [4,9,10]. These components not only reduce the calorific value of natural gas but also pose serious operational

* Corresponding author at: Chemical Engineering Department, Universiti Teknologi PETRONAS, Bandar Seri Iskandar, Perak 32610, Malaysia.
E-mail address: sowmun.lock@utp.edu.my (S.S.M. Lock).
[1] ORCID: 0000–0003-2285–0308

https://doi.org/10.1016/j.jece.2026.122520
Received 31 January 2026; Received in revised form 29 March 2026; Accepted 1 April 2026
Available online 4 April 2026

challenges. In the presence of moisture, CO_2 and H_2S form corrosive acidic species that can damage pipelines and processing equipment [11, 12], thereby complicating purification and downstream operations [13]. Moreover, CO_2 emissions contribute significantly to greenhouse gas accumulation and climate change, further emphasizing the need for efficient CO_2 removal technologies [14].

Moreover, various industrial processes need to purify natural gas by extracting H_2S contaminants from methane as it is crucial for safety and product quality [15,16]. According to the National Institute for Occupational Safety and Health (NIOSH), exposure to H_2S concentrations as low as 100 ppm is classified as an immediate danger to life and health (IDLH) [17] and at these levels, H_2S can cause rapid respiratory distress, unconsciousness, or even death with only a brief exposure. Further details underlying hazardous effects of H_2S at varying exposure concentration is summarized in Table S1 in supplementary document. Such concentrations require immediate protective measures to prevent severe health hazards in industrial environments [18]. Industries such as oil & gas, power, and construction increasingly prioritize safety across processes, equipment, workforce, and the environment, encouragement the development of management systems to ensure compliance with regulations [19–22].

Considering the processing and health and safety risks, the gas must be processed to remove these pollutants before it can be made commercially viable. Simultaneously, due to the rising costs and growing demand for natural gas, numerous governments have shifted their attention to exploiting low quality gas sources with higher content of acid gases. This trend is fueled by a need to diversify energy sources and meet growing energy demand, especially in the face of a potential supply shortfall projected by 2030 [2,23,24].

To tackle the above mentioned issues, gas separation technologies including adsorption, absorption, cryogenic separation, and membrane technology play an important part in addressing both environmental concerns and fulfilling crucial requirements for industrial applications in an energy-efficient and environmental friendly manner [25,26]. Among these, membrane technology stands out as a promising approach [27–31] because of its energy efficiency [32], reduced operational cost [33], supportive in reducing environmental impacts [34,35], simplicity, and modularity [36], compactness, ease in operations, and capabilities to control the thermodynamics [37]. Further, the comparative analysis of gas separation technologies is tabulated in Table S3 in supplementary document.

Beyond pipeline corrosion, H_2S presents an additional challenge to membrane-based separation systems due to its potential chemical interaction with polymeric materials. When dissolved in condensed water, H_2S forms weak acidic species and under oxidative conditions, it can generate sulfur-containing compounds that may induce polymer chain scission, oxidative degradation, or plasticization. In membranes based on materials such as polysulfone (PSF), these interactions can alter the microstructure, free volume distribution, and mechanical stability, ultimately affecting gas permeability and selectivity. Therefore, understanding both the compositional variability of natural gas and the chemical stability of membrane materials is essential for the effective design of systems capable of CO_2 and H_2S removal from methane in natural gas sweetening applications.

The use of membranes for gas separation began in the late 1970s [38, 39]. Over the past few decades, significant advancements have been made in gas separation technologies through the development of various membrane types, including polymeric membranes [40,41], MMMs [42], carbon molecular sieve (CMS) membranes [43], and inorganic membranes [44]. These membranes are generally categorized into three main groups: polymeric, inorganic, and MMMs [45], as illustrated in Fig. 2.

The gas separation performance of a membrane is typically evaluated by two key parameters: permeability and selectivity. Permeability is also known as the permeation coefficient [46] and refers to the rate at which a gas permeates through the membrane and is usually expressed in Barrer, while selectivity is the membrane's ability to discriminate between two gases. A higher permeability allows for faster processing, while higher selectivity ensures better separation efficiency. CO_2/CH_4

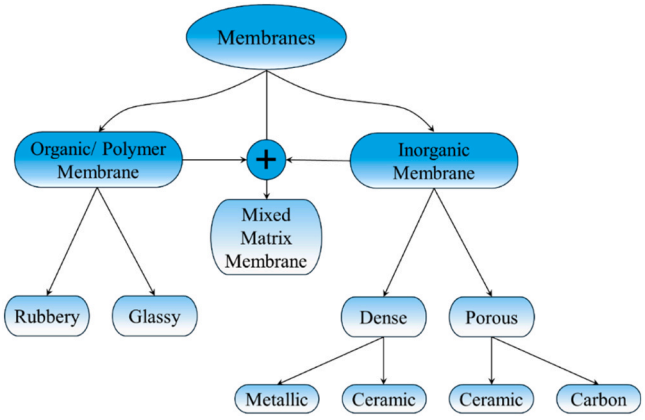

Fig. 2. Schematic overview of membrane classification based on structural characteristics and material composition.

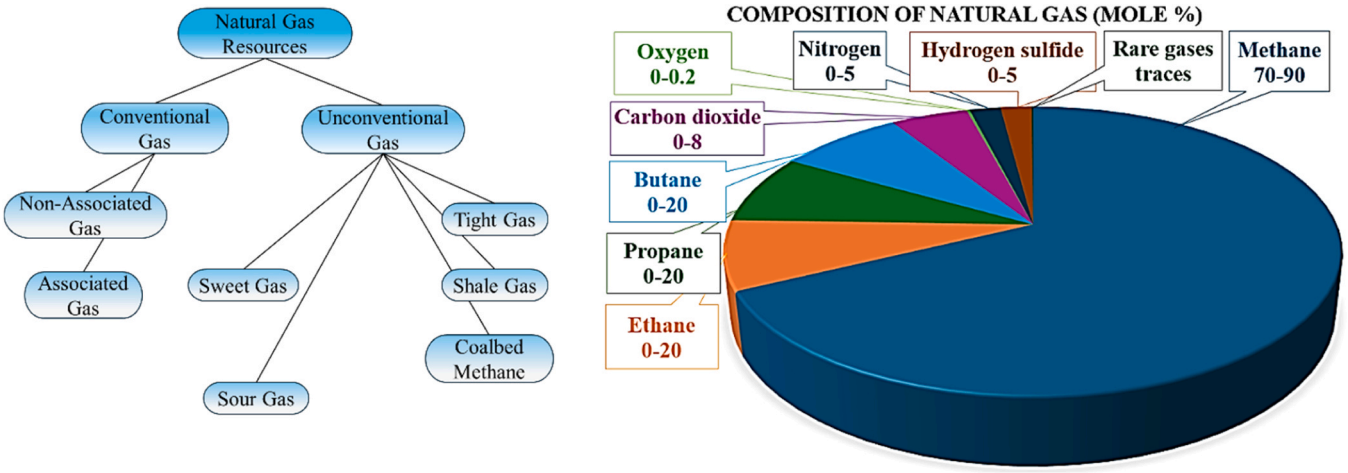

Fig. 1. (a) Resources of natural gas, (b) Composition of natural gas (mole %).

separation is extensively studied due to its importance in natural gas purification and carbon capture [47], while H_2S is highly toxic and corrosive, making its handling and separation more challenging compared to CO_2. This has led to fewer studies focusing on H_2S/CH_4 separation [48]. However, recent investigations have begun to address this gap by exploring H_2S-selective membranes and evaluating their performance under realistic sour gas conditions, including mixed-gas and high-pressure environments [40,49–51]. Recent studies highlight advances in materials that offer improved gas permeability and selectivity, particularly for CO_2/CH_4 and H_2S/CH_4 separation [52,53]. More recently, research has focused on the development of advanced MMMs incorporating novel fillers such as MOFs, graphene-based materials, ionic liquids, and covalent organic frameworks to overcome the permeability-selectivity trade-off [54–57]. In addition, emerging studies have explored the integration of machine learning and molecular simulation techniques to accelerate membrane design and predict gas transport behavior with improved accuracy [58,59]. These developments highlight a shift toward data-driven and hybrid material design strategies for next-generation gas separation membranes. The trade-off between permeability and selectivity is commonly represented by the Robeson upper bound relationship, which sets the benchmark for gas separation performance [60]. Fig. 3 is the schematic diagram showing the gas separation process of membrane.

In membrane technology, various polymers such as PSF, polyethersulfone (PES), polyvinylidene fluoride (PVDF), and cellulose acetate (CA) etc. have been used for gas separation. While polymers such as PSF are widely used for their mechanical strength and stability, a promising solution to overcome inherent limitations in polymer-only membranes is the development of MMMs, which integrate inorganic fillers into polymer matrices. Its relatively low cost and high reproducibility further contribute to its widespread use in industrial membrane production. Table S3 in supplementary document presents a comparison of the key properties of commonly used polymers, highlighting the superior characteristics of PSF for membrane fabrication. Table 3 shows a progression from high strength, thermally stable glassy polymers with moderate permeability (e.g., PSF, PES, PEI) to more permeable but less durable materials such as Poly(ether-block-amide) (PEBAX) and Poly(1-trimethylsilyl-1-propyne) (PTMSP), reflecting the ongoing challenge of balancing permeability-selectivity trade-offs with mechanical and aging performance. PSF stands out as a superior choice because it simultaneously offers excellent processability, high aging and swelling resistance, and strong thermal and mechanical stability, providing a more balanced and industrially reliable performance compared to polymers that sacrifice durability for permeability. Furthermore, recent studies emphasize the importance of long term stability, anti-plasticization behavior, and resistance to aggressive contaminants in membrane materials, particularly for industrial sour gas applications [61–64]. These factors are increasingly recognized as critical performance indicators beyond conventional permeability and selectivity metrics. While numerous experimental and modeling studies have reported performance enhancements in PSF-based membranes for CO_2/CH_4 separation, most investigations remain focused on isolated material modifications or single-gas performance metrics. Furthermore, existing reviews largely discuss polymeric membranes or MMMs independently, without systematically addressing CO_2 and H_2S separation under sour gas conditions, where plasticization, interfacial instability, and long term durability become critical challenges.

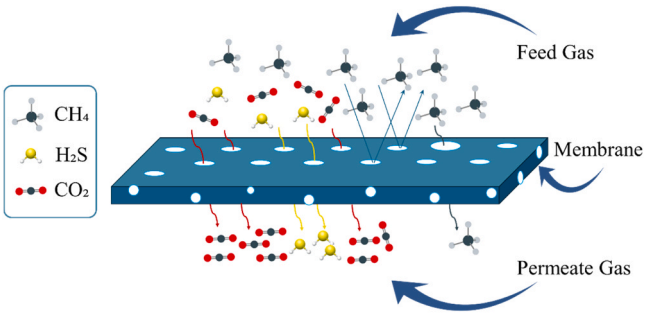

Fig. 3. Schematic illustration of membrane-based gas separation process.

In contrast, the present review introduces a literature calibrated predictive analytical framework that bridges experimental characterization outcomes (morphology, interfacial compatibility, chemical interactions, thermal stability, and plasticization resistance) with membrane design robustness. Rather than merely summarizing permeability-selectivity trends, this work provides a multidimensional evaluation strategy that links analytically measurable parameters to sour gas stability. This integrative approach distinguishes the current review from prior modeling and experimental reports by transforming fragmented performance data into a structured, design-oriented evaluation methodology for next-generation PSF-based membranes.

2. PSF properties, performance and applications

PSF is a high-performance thermoplastic polymer composed of para-linked aromatic rings interconnected by sulfone (–SO_2–) and ether (–O–) linkages, with partial incorporation of alkyl groups within its backbone structure [65]. PSFs are rigid, high strength, and transparent thermoplastics, exhibiting high resistance to chemicals, exceptional mechanical properties and dimensional stability across a wide temperature range [66]. These materials maintain their structural integrity between −100 °C and 150 °C, demonstrating high strength and stiffness even under extreme conditions [67]. An overview of significant industrial polysulfone variants and their chemical abstract service (CAS) numbers are provided in Table 1.

PSF and chemically modified derivatives exhibit significant success in membrane applications, spanning diverse fields such as fuel cells, wastewater treatment, gas separation, clinical dialysis, wastewater separation, and support for composite membranes [69–71] as shown in Fig. 4.

Further, Table 2 demonstrates the evolution of PSF from a fundamental membrane forming polymer toward a high-performance, multifunctional material optimized through structural modification and composite reinforcement. Over time, improvements such as enhanced anti-fouling behavior, increased permeation flux, and stronger gas separation capability have significantly enhanced the performance of PSF membranes. These advancements have expanded their applications from basic water treatment to advanced biomedical, nanofiltration, and gas separation systems, demonstrating their adaptability and technological progression.

3. Synthesis and characterization of PSF-based membrane

Characterization of PSF membranes highlights the strong link between synthesis methodology and resulting performance in gas separation applications. Variations in fabrication approaches directly affect gas permeability and selectivity [73], while material synergy plays a vital role, particularly when PSF interacts with fillers or undergoes functionalization during synthesis [87]. Structural parameters such as pore formation [88] and surface hydrophilicity/hydrophobicity [89] further determine gas diffusion pathways and interaction with target gases, influencing overall separation efficiency. Optimization of synthesis conditions, including temperature, pressure, and processing time is equally important to ensure consistent and reproducible performance [90]. Moreover, the morphology of the active layer, which governs transport behavior and mechanical integrity, remains a critical factor in enhancing permeability without sacrificing selectivity [91]. Together, these insights demonstrate that tailoring synthesis strategies and correlating them with characterization outcomes provides a robust foundation for PSF membrane development. This approach enables

Table 1
Chemical structures and CAS numbers of PSF, PES, PPSF [68].

Polymer	Abbreviation	Repeating unit structure	CAS No.
Polysulfone	PSF	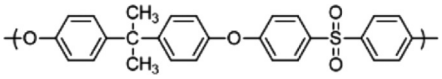	25135–51–7
Polyether sulfone	PES	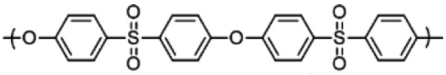	25608–63–3
Polyphenylsulfone	PPSF	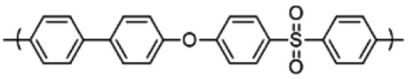	25608–64–4

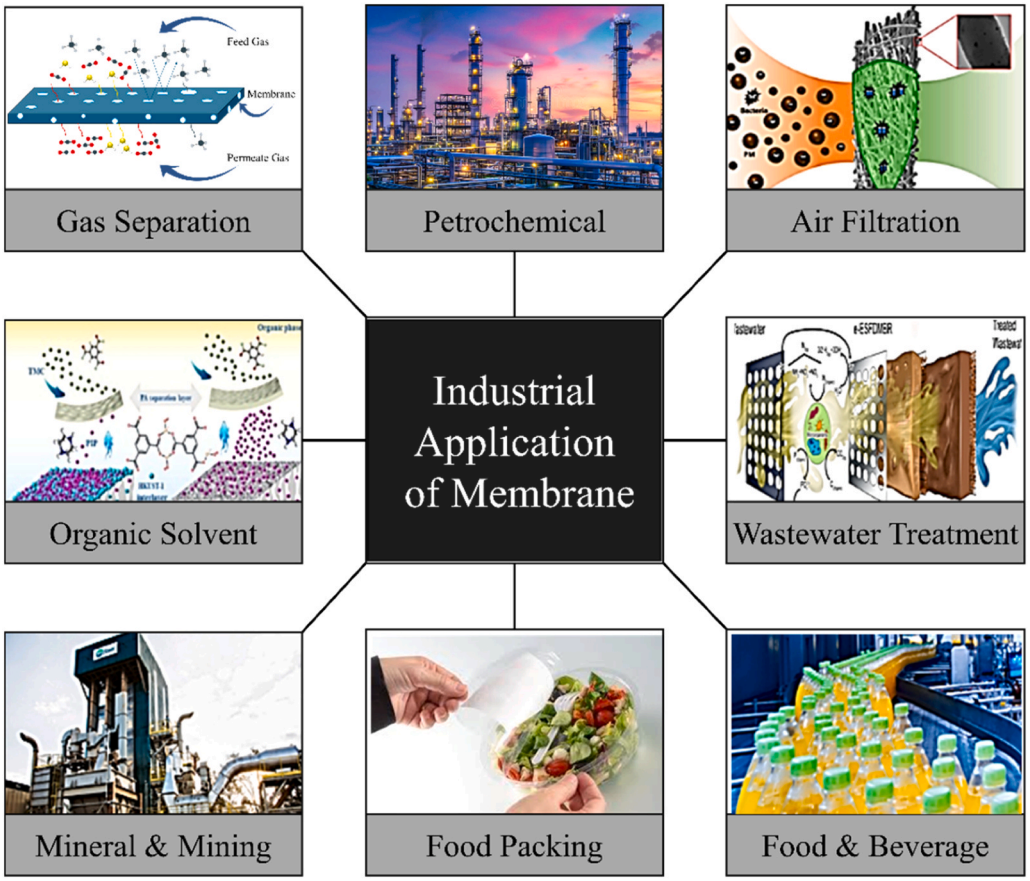

Fig. 4. Key industrial applications of membrane technology across various sectors.

improved separation efficiency and operational stability in natural gas purification.

3.1. Synthesis methodology

The fabrication of gas separation membranes based on PSF encompasses various methodologies:

3.1.1. Solution casting method

PSF is first dissolved in high-polarity solvents such as N,N-Dimethylformamide (DMF) or N,N-Dimethylacetamide (DMAC) because these solvents effectively disrupt the rigid aromatic backbone and sulfone linkages of PSF, ensuring complete solubilization. This step is crucial for achieving defect-free PSF membranes with consistent morphology and gas separation performance [92]. The polymer dissolution step is typically assisted by sonication or vigorous stirring to ensure complete solubilization and uniform dispersion of any added fillers, followed by degassing to remove entrapped air and avoid membrane defects. For PSF-based MMM, achieving homogeneous filler distribution is essential, as the chemical structure of PSF promotes good compatibility with functionalized fillers, minimizing interfacial voids and enhancing gas separation performance. The resulting solution is then cast onto a flat substrate with controlled thickness and subjected to phase inversion, during which the polymer transitions into a solid membrane matrix. Owing to PSF's high glass transition temperature and rigid aromatic backbone, the membrane retains structural integrity during this process. The resulting membrane is typically peeled off and further dried or post-treated as needed, yielding stable morphologies with reliable selectivity and permeability for gas separation applications [93,94]. Fig. 5 illustrates the schematic flow of the solution casting method as applied to membrane fabrication.

Almuhtaseb *et al.* (2021) prepared two PSF-based membranes via

Table 2
Properties, Performance and applications of PSF.

Properties / Performance	Applications	References
Membrane Forming Ability PSF is frequently used to make membranes because of its excellent membrane forming capacity.	Used in filtration processes	[72,73]
Mechanical Properties The mechanical attributes, such as strength and tensile modulus, play a crucial role in determining the effectiveness of PSF. PSF exhibits favorable mechanical properties, rendering it well suited for applications in water treatment.	Water treatment application	[73–75]
Anti-Compaction Properties PSF exhibits anti-compaction characteristics that improve membrane application performance and durability.	Membrane manufacturing/ application	[72]
High Permeation Flux/ Ultrafiltration Utilizing PSF in the fabrication of ultrafiltration membranes through methods like phase inversion enhances its effectiveness in filtration processes.	Sewage purification and desalination	[76,77]
Nanofiltration The physicochemical attributes of PSF support influence the performance of thin-film composite nanofiltration membranes, showcasing its versatility across various filtration techniques.	Nanofiltration Membranes	[78]
Biocompatibility The hydrolytic, thermal, and oxidative stability of PSF makes it unique. These characteristics make it a good option for implants and medical devices.	Biomedical applications	[79,80]
Composite Reinforcement PSF can be better by adding different materials to it to make changes to the surface and structure of PSF, like using carbon-fabric composites.	Composite processing	[81]
Surface Charge/ Hydrophilicity and Anti-fouling Properties Materials such as polyaniline may also be included to boost performance. The incorporation of these components results in enhanced hydrophilicity and anti-fouling characteristics.	Protein separation/ Liquid separation	[82,83]
Gas Separation Properties/ Structural Robustness The literature extensively examines how well PSF separates CO_2 from CH_4 due to its good mechanical strength, thermal stability, and chemical resistance. To achieve efficient gas separation, it's crucial to understand how different polymeric materials affect the membrane's performance.	Gas separation processes	[84–86]
Chemical Modification/ Influences Physicochemical Properties Cleaning changes how polymers are made and affects how well membranes work. Modifying the chemicals allows customization of the characteristics of the materials for specific uses.	Membrane manufacturing/ application	[83]

solution casting to evaluate chloroform (CF) and tetrahydrofuran (THF) as solvents for CO_2/CH_4 gas separation. Both solvents effectively dissolved PSF, producing homogeneous solutions at a concentration of 0.3 g/ML. The solutions were cast onto glass plates, dried for 24 h, and the resulting membrane thicknesses were measured. Fig. 6 illustrates the formation of the PSF membrane structure before and after solvent evaporation. [86].

3.1.2. Phase inversion

Phase inversion, first introduced in the 1960s by Loeb and Sourirajan, led to the development of anisotropic CA membranes for reverse osmosis [95]. This milestone laid the foundation for modern desalination and membrane separation technologies. Although initially developed using CA, PSF later became widely used for asymmetric membrane fabrication due to its excellent thermal stability, mechanical strength, and chemical resistance.

Among phase inversion techniques, immersion precipitation, commonly known as non-solvent induced phase separation (NIPS), is the most widely employed method for the industrial fabrication of asymmetric polymer membranes. In this approach, a polymer dope solution is cast onto a suitable support and immersed in a non-solvent coagulation bath, where rapid solvent–non-solvent exchange triggers thermodynamic instability, leading to phase separation and polymer solidification. PSF is particularly well suited for NIPS processing due to its favorable rheological properties and broad compatibility with common coagulation media, including water and alcohols. The rapid demixing process produces the hallmark asymmetric membrane structure, characterized by a dense selective skin layer over a porous support sublayer. Membrane morphology and separation performance are governed by the interplay of dope formulation parameters (polymer concentration, solvent system, and additives), coagulation bath conditions, and processing variables such as evaporation time and immersion kinetics [96–98]. The general phase inversion synthesis scheme for PSF membranes is illustrated in Fig. 7. To elucidate the mechanisms governing membrane formation, numerous mass transfer models have been proposed to describe solvent–non-solvent exchange during phase inversion [99]. Seminal contributions by Cohen *et al.* [100], the McHugh group [101], and Reuvers *et al.* [102] provided fundamental insights into the kinetics and thermodynamics of asymmetric membrane formation. These models have been further adapted to PSF systems to better predict skin layer development and pore evolution based on PSF's molecular characteristics. Alternative theoretical approaches have also been introduced, including the spinodal decomposition model proposed by Kim *et al.* [103], MC diffusion simulations by Termonia [104], and dynamic modeling studies by Wang *et al.* [105] examining the influence of polymer chain length and solvent molecular size. Despite these advances, the precise mechanism responsible for selective skin layer formation remains incompletely understood, as highlighted by Peng. Beyond NIPS, other phase inversion techniques have been explored to tailor PSF membrane morphology. Thermal-induced phase separation (TIPS) relies on cooling the polymer solution to reduce solubility and induce solidification, and has demonstrated promising gas separation performance [88,106,107]. In contrast, NIPS is achieved by immersing the polymer solution into a non-solvent coagulant bath typically water or alcohol which rapidly extracts the solvent and triggers phase separation [108]. Evaporation-induced phase separation (EIPS) promotes gradual solvent loss from the cast film, increasing polymer concentration until phase separation occurs [109]. In contrast, vapor-induced phase separation (VIPS) involves exposing the polymer solution to a vapor phase, such as water vapor, leading to controlled gelation and phase transformation [110]. Collectively, these techniques provide versatile routes for tuning membrane structure and separation properties.

Recent studies further underscore the adaptability of PSF membranes fabricated via phase inversion. Yousef *et al.* (2023) demonstrated that PSF membranes prepared by NIPS using PVP and NMP exhibited distinct sponge-like or finger-like morphologies depending on casting thickness, alongside enhanced mechanical and thermal stability [111]. Similarly, modifications in casting solution composition have been shown to significantly influence the performance of gas separation membranes produced by wet phase inversion [112]. Overall, phase inversion remains the cornerstone of PSF membrane fabrication, offering robust control over membrane morphology and performance for a wide range of separation applications.

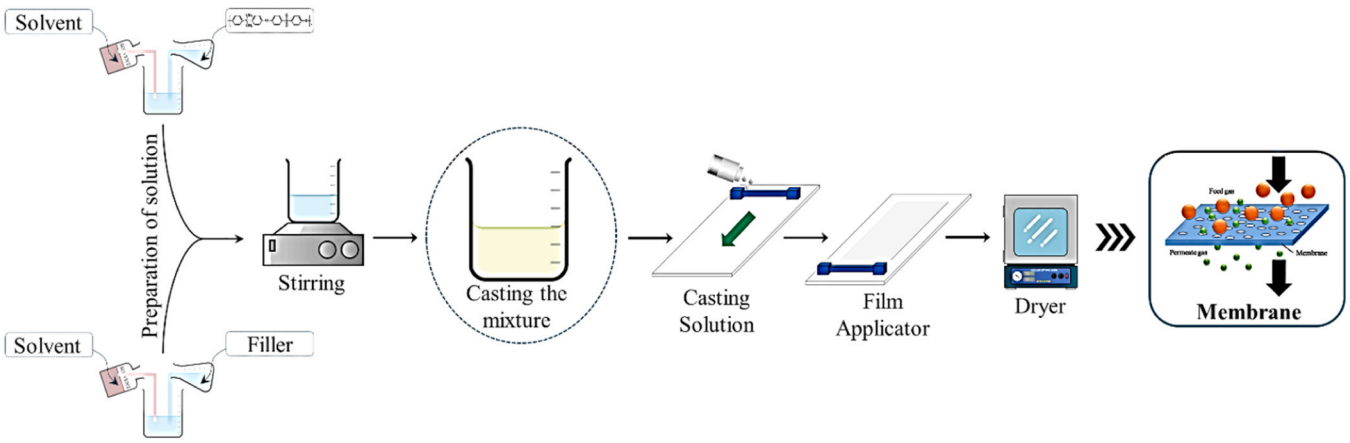

Fig. 5. Schematic overview of the solution casting method employed for PSF membrane synthesis.

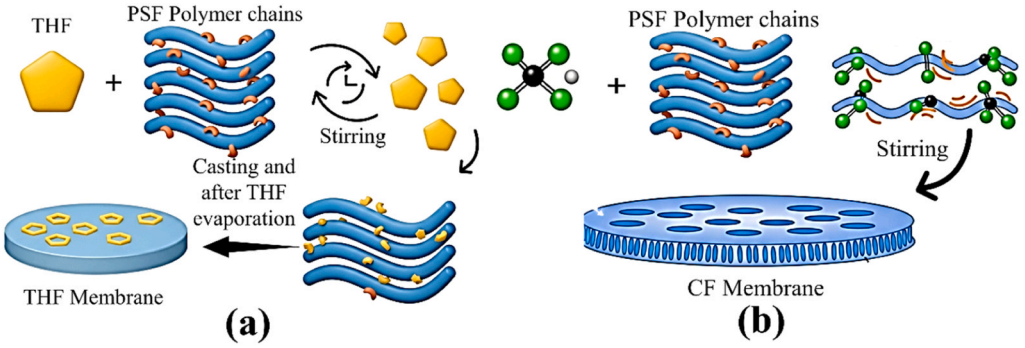

Fig. 6. The formation of PSF membranes via solution casting using (a) THF and (b) CF solvents.

3.1.3. *Interfacial polymerization*

Interfacial polymerization (IP), also referred to as polycondensation, is a membrane fabrication technique in which polymer formation occurs at the interface between two immiscible liquid phases, typically an aqueous and an organic phase. In this process, reactive monomers are dissolved separately in each phase and undergo rapid polymerization upon contact, usually on the surface of a porous support membrane. PSF is one of the most widely used support materials for IP due to its excellent mechanical strength, thermal stability, and compatibility with both aqueous and organic solvents. A defining feature of IP is its self-limiting reaction mechanism, whereby the growing polymer layer restricts further monomer diffusion, resulting in the formation of an ultrathin and uniform selective film, often on the order of ~50 nm [113–116]. Thin-film composite (TFC) membranes fabricated on PSF supports are commonly produced via IP between complementary monomers. As illustrated in Fig. 8, the process typically involves impregnating a porous PSF support with an aqueous amine solution, followed by contact with an organic solution containing an acid chloride monomer, leading to the formation of a polyamide (PA) selective layer at the interface. The physicochemical properties of the PSF support, including porosity, surface hydrophilicity, and roughness, critically influence the morphology, continuity, and adhesion of the PA layer. Post-treatment steps, such as thermal curing, are often employed to enhance layer stability and interfacial adhesion. Owing to its ability to independently optimize the ultrathin selective layer and the porous support, IP has enabled the commercial realization of a wide range of high-performance membranes for industrial separation applications [117]. Plasma polymerization represents an additional complementary approach and is discussed separately in the context of surface modification.

3.1.4. *Laser ablation*

Laser ablation has emerged as a promising and versatile technique for membrane fabrication and surface engineering, offering precise control over surface modification and material integration. In this approach, a high-energy laser beam is directed onto a solid target, often immersed in a liquid medium, a process known as laser ablation in liquid (LAL) resulting in the ejection of material in the form of nanoparticles or thin films. PSF has attracted increasing attention as a suitable substrate for laser ablation-based membrane engineering due to its thermal stability, chemical resistance, and compatibility with advanced surface functionalization strategies. Laser-generated nanomaterials produced via this method have been shown to enhance critical membrane properties, including permeability, selectivity, and mechanical robustness, thereby improving overall separation performance [118–120]. Recent studies further demonstrate the potential of laser ablation for functional membrane design. Mintcheva *et al.* (2023) reported the synthesis of hybrid TiO_2-ZnO nanomaterials using PLAL, in which sequential laser ablation of metal targets in a liquid environment enabled the controlled formation of layered oxide nanostructures with enhanced functional properties, as schematically illustrated in Fig. 9 [121]. Although primarily investigated for gas sensing, this approach highlights the capability of PLAL to generate tailored nanomaterials suitable for membrane modification.

In the context of gas separation, Mishra *et al.* (2021) demonstrated a rapid and scalable strategy for integrating laser-induced graphene (LIG) onto PSF membranes using CO_2 laser irradiation as presented in Fig. 10. The resulting LIG/PSF membranes exhibited markedly improved hydrogen selectivity compared to pristine PSF membranes, underscoring the effectiveness of laser ablation in tailoring PSF surface chemistry and transport characteristics [122]. Laser ablation offers a clean and efficient route for developing next-generation PSF-based membranes due to

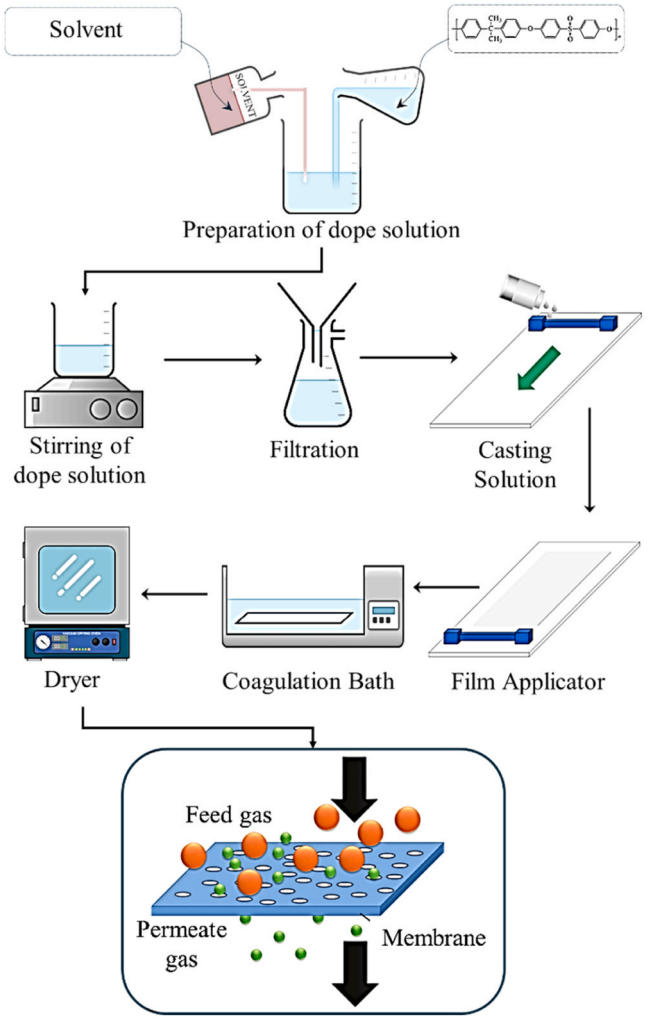

Fig. 7. Schematic of the phase inversion process for the fabrication of PSF membranes.

its solvent-free nature, minimal chemical requirements, and precise spatial control. This approach is particularly suitable for advanced gas separation and surface functionalization applications.

Although current LIG/PSF studies primarily report improvements in hydrogen selectivity, the structural characteristics introduced by laser ablation may also offer advantages for sour gas applications. The in-situ formation of graphene nanostructures creates a defect-minimized, chemically stable carbon layer that is covalently integrated with the PSF substrate, thereby reducing interfacial voids commonly observed in solution-blended MMMs. Since H_2S-induced degradation often initiates at weak polymer-filler interfaces, the absence of physically dispersed filler phases may improve resistance to corrosion and plasticization under CO_2/H_2S environments. Compared to conventional solution blending, laser ablation represents a surface engineering strategy that enhances structural integrity without introducing agglomeration risks, potentially offering improved stability in dual acid gas separation systems. However, further dedicated studies under mixed CO_2/H_2S conditions are required to fully validate this potential.

3.1.5. *Surface modification techniques*

PSF membranes are highly amenable to surface modification due to their stable backbone, tunable porosity, and compatibility with diverse chemical and physical treatments, making surface engineering critical

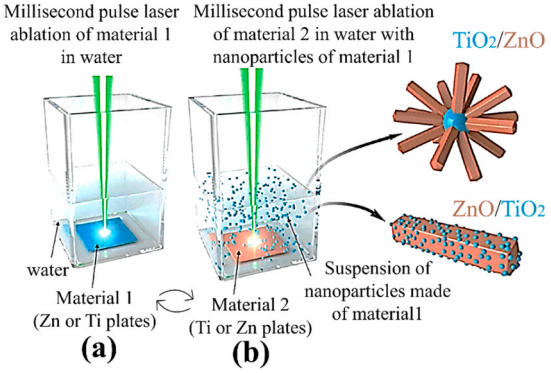

Fig. 9. Illustration of the synthesis pathway for ZnO/TiO_2 and TiO_2/ZnO hybrid nanomaterials via PLAL [121] (Reprinted from N. Mintcheva et al., 2023, MDPI, under CC BY 4.0).

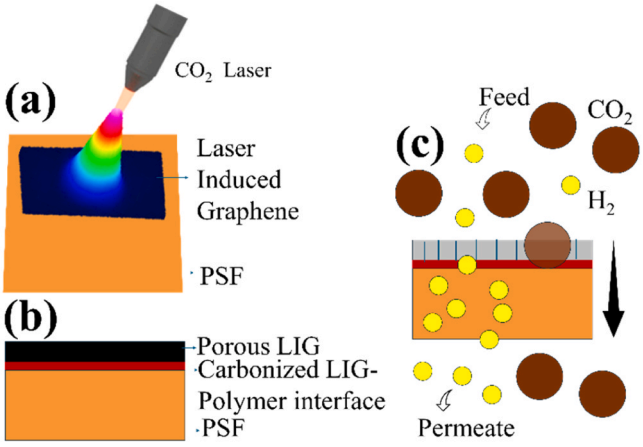

Fig. 10. (a) Schematic of CO_2 laser set up used to make LIG on PSF film, (b) Schematic of cross-section of LIG/PSF membrane, (c) Gass separation process.

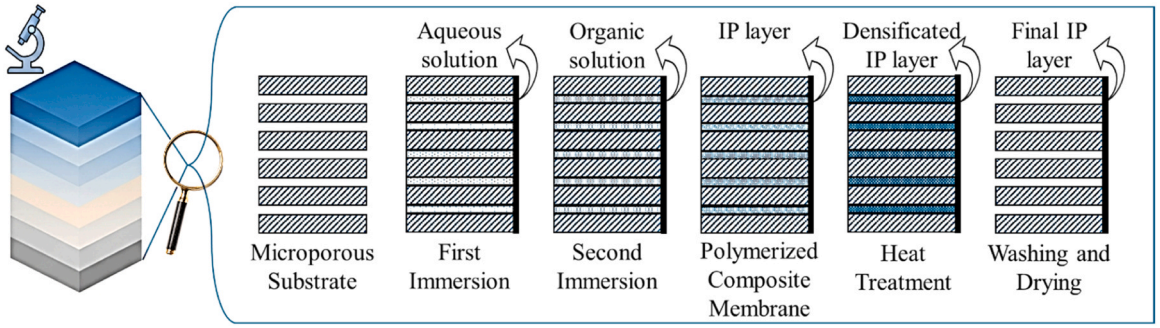

Fig. 8. Schematic illustration of the conventional IP process used for the fabrication of TFC membranes.

for enhancing gas separation and water purification performance. Techniques such as layer-by-layer (LbL) assembly, chemical functionalization, and plasma treatment allow precise control over surface chemistry and transport properties. LbL assembly enables the controlled deposition of oppositely charged functional layers, fine-tuning surface charge, hydrophilicity, fouling resistance, and gas selectivity without affecting the bulk membrane [123,124]. Complementary chemical and plasma treatments, particularly plasma modification, introduce oxygen-containing polar groups that increase surface energy and convert the hydrophobic PSF surface to hydrophilic [124]. This modification improves compatibility with polar gases and enhances anti-fouling performance in aqueous environments. The effectiveness of these surface engineering strategies has been widely validated. Surface-modified PSF hollow fiber membranes have demonstrated significant improvements in CO_2/CH_4 and O_2/N_2 separation, reflecting concurrent gains in permeability and selectivity [125]. Kadirkhan *et al.* (2021) reported PSF hollow fiber membranes for natural gas sweetening that exhibited stable CO_2 permeation under elevated temperatures and pressures, with negligible plasticization even at CO_2 concentrations up to 70%, highlighting their suitability for industrial deployment [61]. Furthermore, multilayer-coated PSF membranes were shown to outperform single-layer systems, including those coated with polydimethylsiloxane (PDMS) and polyether-block-amide (PEBAX), in terms of separation efficiency [156]. Additional performance enhancements have been achieved through nanofiller incorporation within the PSF matrix. The integration of amine-modified SiO_2/ZIF-8 (A@S/ZIF-8) nanofillers strengthened polymer-filler interfacial interactions, yielding hollow fiber MMM with a CO_2 permeability of 4.25 Barrer and markedly improved CO_2/N_2 and CO_2/CH_4 selectivities. These improvements, attributed to the strong affinity of amine functionalities toward CO_2, positioned the modified PSF membranes near the Robeson upper bound, underscoring the effectiveness of combined surface modification and nanofiller integration in advancing PSF-based membrane technologies [126]. Fig. 11 illustrates the multilayer coating method on flat sheet and hollow fiber membranes.

3.1.6. *Comparative analysis of fabrication techniques*

To evaluate the trade-offs between fabrication complexity and membrane performance, a comparative framework is presented in Fig. 12. This scatter plot maps eight fabrication methods across two axes: complexity of fabrication techniques (x-axis) and membrane performance (y-axis). The x-axis ranges from very low to very high complexity, reflecting the degree of process control, equipment sophistication, and operational demands. The y-axis spans from very low to very high-performance, based on metrics such as selectivity, permeability, and structural precision. Each method is represented by a circular marker, where green indicates conventional, low-complexity techniques and red denotes advanced, high-performance approaches. Solution casting and phase inversion appear in the lower-left quadrant, offering ease of implementation but limited selectivity and structural control [127,128]. IP occupies the upper-middle region, reflecting its moderate-to-high complexity and strong performance in TFC membranes [129]. Surface

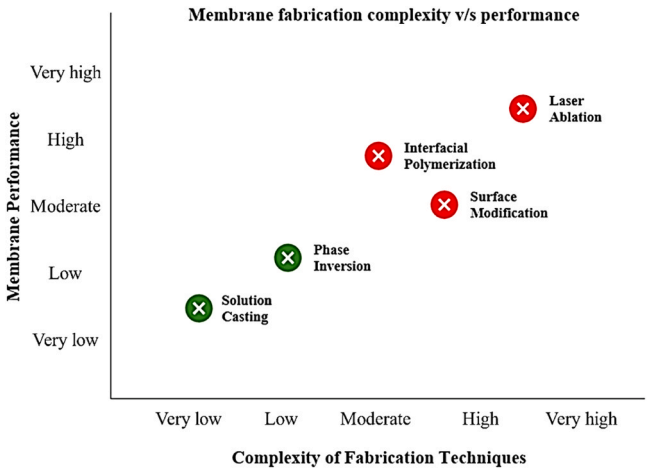

Fig. 12. Visualization of the trade-off between membrane fabrication complexity and separation performance.

modification techniques, including plasma treatment and grafting, are positioned in the high complexity zone but yield only moderate performance gains, highlighting that increased fabrication effort does not always result in proportionally higher functionality [130]. Laser ablation is located at the top-right corner, representing the frontier of membrane engineering with high complexity and high-performance [131]. This visualization underscores the versatility of PSF across the fabrication spectrum. PSF membranes are commonly produced via phase inversion and IP, and are increasingly modified through plasma treatment, nanofiller integration, and laser patterning. Their adaptability makes PSF a central material in both scalable industrial processes and emerging high-performance applications. This observation is consistent with prior studies where membrane synthesis techniques, particularly phase inversion and solution casting, significantly influence membrane morphology and separation performance. For example, PSF-based MMMs fabricated via phase inversion have shown improved dispersion of fillers and enhanced gas separation properties, provided that interfacial compatibility is well controlled [132]. To complement this framework, Table S4 in the supplementary document provides a comparative overview of fabrication techniques based on complexity, cost, membrane format, application suitability, environmental impact, and scalability.

3.2. *Characterization techniques*

Characterization of PSF membranes is essential for evaluating their structural, thermal, mechanical, and gas separation properties. Techniques such as scanning electron microscopy (SEM) and Fourier transform infrared spectroscopy (FTIR) provide critical information on morphology, interfacial defects, and polymer-filler interactions. In addition, thermogravimetric analysis (TGA) and differential scanning

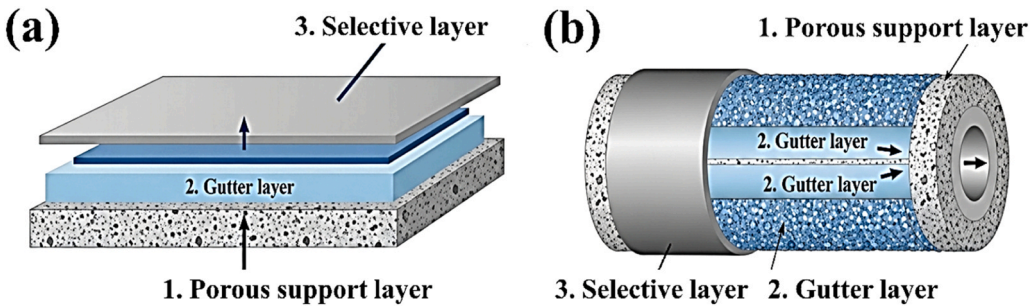

Fig. 11. The schematic diagram of the multilayer coating method on (a) flat sheet and (b) hollow fiber membrane.

calorimetry (DSC) offer insights into thermal stability and polymer network behavior through systematic application. Systematic application of these methods enables a comprehensive understanding of membrane performance, including permeability, selectivity, mechanical robustness, and operational stability.

3.2.1. SEM and field emission SEM (FESEM)

SEM and FESEM are indispensable techniques for analyzing the morphology of PSF and PSF-based MMMs [93,133]. These imaging tools provide crucial information on surface roughness, pore structure, cross-sectional architecture, and the distribution of fillers within the polymer matrix [134,135]. Such insights are vital because gas transport performance in MMMs is closely tied to microstructural features such as pore size, the continuity of selective layers, and the presence or absence of interfacial voids. In a recent study, Fadaly *et al.* investigated PSF/$LaFeO_3$ MMMs and used SEM to visualize the effect of filler loading on membrane morphology. At 1 wt% $LaFeO_3$, the SEM cross-sections revealed a homogeneous distribution of filler particles within the PSF matrix, with no apparent interfacial voids (Fig. 13a) [136]. This uniform dispersion was directly linked to an increase in CO_2/CH_4 selectivity. However, as the filler content increased beyond the optimal loading, SEM images clearly showed particle agglomeration and the development of voids at the polymer-filler interface (Fig. 13b). These structural defects compromised the selective pathways for gas transport, causing a decline in selectivity even though permeability continued to increase. To highlight this trend, cross-sectional SEM images of PSF/$LaFeO_3$ membranes at low and high loadings should be incorporated here, illustrating the transition from well-dispersed to agglomerated morphologies. A similar observation was reported for PSF/activated carbon nano-fiber (ACNF) MMMs, where SEM cross-sections revealed that increasing the ACNF content transformed the internal morphology of the membrane [137]. At lower ACNF loadings (Figs. 13c, 13d & 13e), membranes exhibited predominantly sponge-like structure, whereas higher filler concentrations promoted the formation of finger-like pores (Fig. 13 f & 13 g). This morphological evolution was shown to influence both permeability and selectivity, with finger-like structures favoring higher flux at the expense of separation efficiency [137]. The inclusion of SEM images comparing sponge-like and finger-like pore structures provides an effective visual demonstration of how synthesis conditions and filler content can drive morphological transitions.

Further evidence of the critical role of SEM in evaluating filler dispersion was provided by a study on PSF/KIT-6 MMMs. FESEM cross-sections of these membranes demonstrated that up to 2 wt% filler loading, KIT-6 particles were evenly distributed within the polymer matrix without voids (Figs. 18h, 18i & 18j) [138]. However, at loadings above 4 wt%, pronounced particle agglomeration and the emergence of interfacial gaps were observed (Fig. 18k & 18 l). These defects created non-selective pathways for gas molecules, ultimately diminishing the CO_2/CH_4 separation performance. Including FESEM images from this study comparing the void-free morphology at 2 wt% with the defective structure at higher loadings would effectively illustrate the optimal filler threshold concept.

Taken together, SEM and FESEM studies consistently demonstrate that while low to moderate filler loadings enhance dispersion and strengthen interfacial compatibility, excessive filler incorporation leads to agglomeration, interfacial voids, and reduced selectivity. Beyond filler concentration, synthesis method also plays an important role in determining morphology. Membranes fabricated via solution casting typically display smoother surfaces and better filler dispersion at low concentrations, whereas dry-wet phase inversion methods often produce finger-like porous substructures that favor permeability but can reduce selectivity unless carefully controlled. Surface modification of fillers, such as amine functionalization, has been shown to mitigate void formation and improve compatibility, and these improvements are directly visible in SEM micrographs.

3.2.2. Transmission Electron Microscopy (TEM)

TEM provides a direct, real-space view of nano- to sub-micron features that control transport in PSF-based MMMs, including the dimensions of 2D fillers, crystallite size of MOFs and zeolites, and polymer-filler interfacial gaps at the tens of nanometers scale. Additionally, when ultramicrotomed cross-sections are prepared, it reveals the continuity of dispersed domains through the membrane thickness. In practice, two complementary TEM modes show the most value for PSF systems: (i) conventional bright-field TEM of the filler (and, when possible, of membrane cross-sections) to quantify particle morphology and agglomeration; and (ii) high-resolution TEM (HRTEM) or STEM-EDX to verify crystallinity and local composition at the interface.

For 2D carbonaceous fillers, Zahri *et al.* [139] fabricated GO/PSF hollow fiber MMMs by dry-jet wet spinning and used TEM alongside Atomic Force Microscopy (AFM) (see Fig. 14 d & 14e) to verify that GO is present as few-layer nanosheets with lateral sizes of hundreds of nanometers, rather than restacked platelets. This confirmation was decisive, as TEM revealed thin, well-exfoliated GO that correlated with improved gas transport, including higher CO_2 permeance without significant loss of selectivity. Together with cross-sectional SEM, these findings suggest that nanosheet aspect ratio, captured by TEM/AFM, is a key structural factor in the phase inversion route.

For MOF-filled PSF membranes, Nordin *et al.* [140] combined solution casting with ZIF-8 loadings and reported TEM micrographs of the ZIF-8 nanocrystals used to formulate the MMM dope (see Fig. 14a). Although these images are of the filler rather than the membrane cross-section, they quantify a narrow primary particle size distribution (tens of nanometers) and well-faceted morphology. Those attributes, verified by TEM, were consistent with dense packing and minimized polymer-filler gaps seen later in SEM and with the selective CO_2/CH_4 performance trend they reported. The methodological point is important: when the synthesis method targets small, uniformly faceted MOF seeds (e.g., by modulator-assisted crystallization), TEM of the filler before dope preparation is often the most predictive indicator that a solution-cast PSF-MMM will avoid non-selective interfacial voids [140].

Where TEM genuinely changes the interpretation relative to SEM is in diagnosing interfacial quality after more aggressive processing. In the study conducted by Zahri *et al.* [139] hollow fiber spinning, for example, risks shear-induced stacking of GO or formation of nanovoids that are invisible in SEM at moderate magnification. TEM groundwork showing few-layer GO (not thick tactoids) supports their claim that spinning did not catastrophically restack the nanosheets, had TEM instead revealed multilayer stacks, the same permeance gains could have been attributed to microdefects rather than 2D-filler tortuosity. Likewise, when casting PSF/ZIF-8 with rapid solvent exchange, TEM-sized MOF seeds improve the odds of conformal wetting; if TEM had revealed polydisperse, micron-scale ZIF-8, the solution-cast route would be prone to the classic “rind” and gap formation often misread in SEM [141].

Two cautions reappear across PSF systems. First, TEM contrast between an amorphous PSF matrix and low-Z fillers can be poor; meaningful interfacial imaging typically requires ultramicrotomy (room temperature or cryo) and, ideally, STEM-EDX line scans to detect filler-derived elements along the polymer-filler boundary [141] (See Fig. 14b & 14c). Second, filler-only TEM (e.g., ZIF-8 powders, GO sheets) is necessary but not sufficient: it reduces uncertainty about the starting morphology but cannot, by itself, rule out processing-induced aggregation inside the membrane. The strongest studies therefore pair TEM with FESEM/SEM on fractured cross-sections and with gas permeation to triangulate structure property links [142]. Reviews and methods papers on polymeric membrane microscopy echo these points and recommend ultramicrotomy plus low-dose imaging to avoid beam damage to PSF [142].

From a synthesis perspective, solution-cast PSF MMMs benefit from TEM when filler synthesis produces small, uniform particles (e.g., ZIF-8, UiO-type) or thin sheets (e.g., GO). TEM-confirmed narrow size or thickness distribution correlates with fewer interfacial voids and a

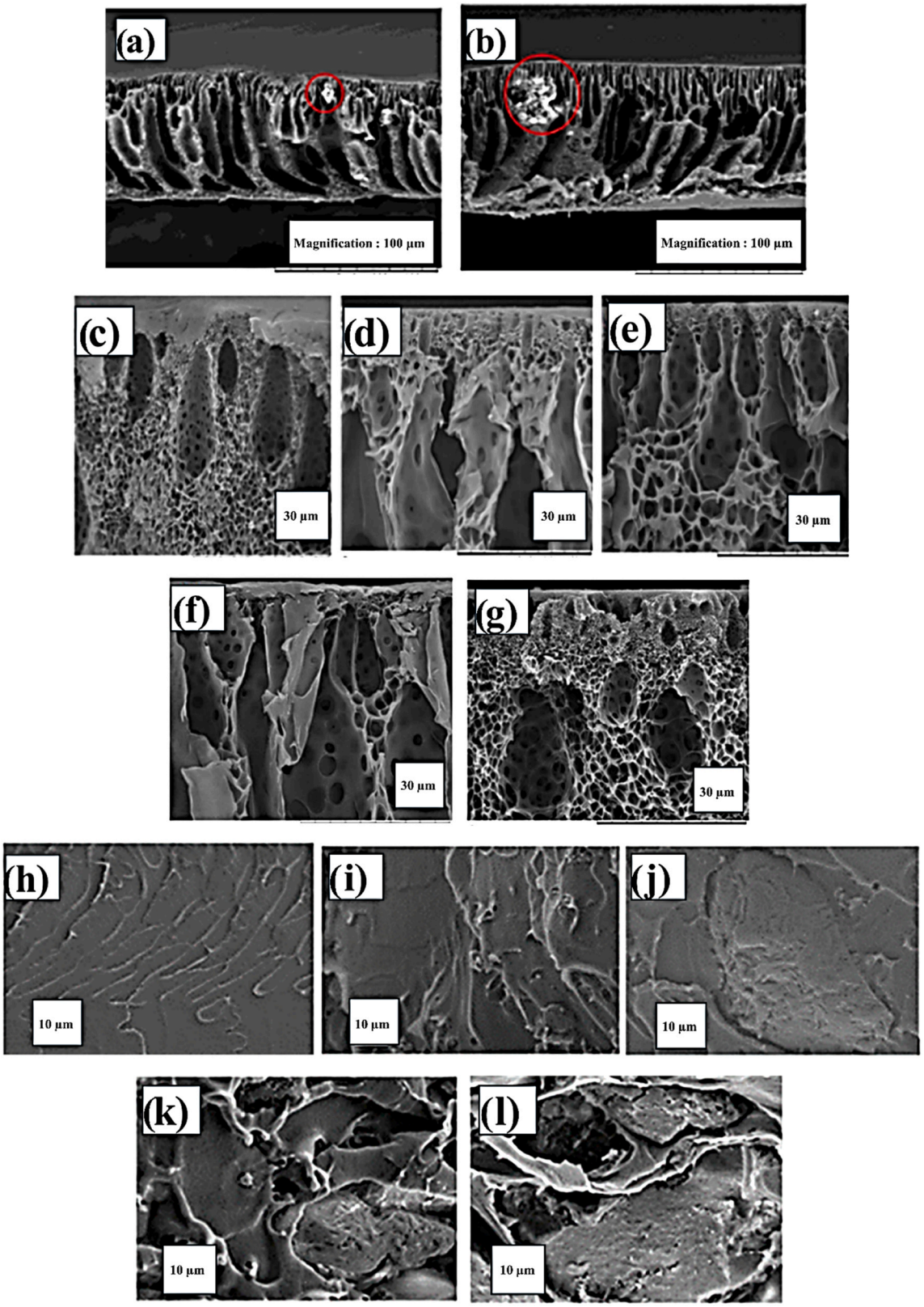

Fig. 13. SEM images of membrane cross-sections with (a) 1 wt% LaFeO3 loading [136]. Reprinted from Fadaly & Aziz (2020) under the Creative Commons Attribution (CC BY 4.0) license, (b) 1.5 wt% LaFeO3 loading [136], SEM images of cross-sections of polysulfone containing different concentration of ACNF (c) 0 wt %, (d) 0.1 wt%, (e) 0.5 wt%, (f) 1.0 wt%, (g) 1.5 wt% reproduced with permission from [137], The cross-sectional images of (h) pristine PSF membrane; (i) 2%-KIT-6/PSF; (j) 4%-KIT-6/PSF; (k) 6%-KIT-6/PSF; and (l) 8%-KIT-6/PSF reproduced with permission from [138]. Reproduced from Ding et al., (2019). Polymers, 11, 1732, under CC BY 4.0.

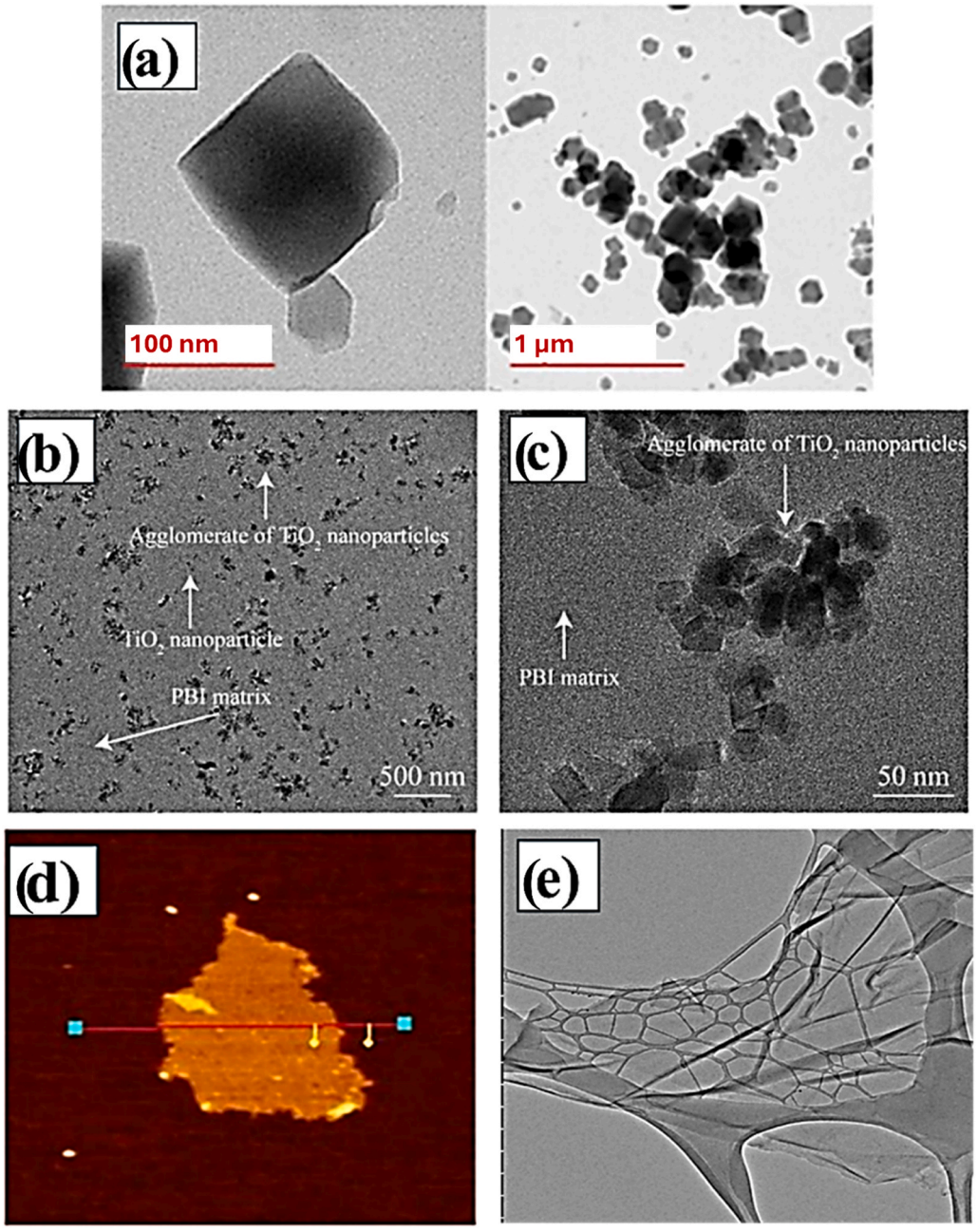

Fig. 14. TEM images of the ZIF-8 filler synthesized in the study done by Nordin *et al.* [140]. Copyright 2015, RSC Advances, (a) TEM images of TiO_2 nanoparticles on polybenzimidazole (PBI) membrane with the addition of TiO_2 nanoparticles: (b) At a magnification of 500 nm, (c) at a magnification of 50 nm synthesized by Akhtar *et al.* [143], (d) AFM topography image of the GO nanosheets, (e) TEM image of the GO nanosheets synthesized by Zahri *et al.* [139]. Copyright 2016, RSC Advances.

higher likelihood of true selectivity gains rather than defect-driven permeance. In phase-inverted/hollow fiber PSF MMMs, the value of TEM is in disproving nanosheet restacking or MOF aggregation under shear/antisolvent exchange interpretations that SEM alone can over- or under-call. Across both routes, TEM observations of few-layer GO or sub-100 nm MOF crystallites with clean facets are often associated with improved CO_2-selective transport. In contrast, when TEM reveals thick tactoids or polydisperse, irregular MOF particles, selectivity benefits become inconsistent and may diminish once defects are sealed [140].

3.2.3. *Fourier Transform Infrared Spectroscopy (FTIR)*

FTIR is a key technique for probing the chemical interactions between PSF and inorganic or organic fillers in MMMs and to identify the functional group found in PSF membrane [93]. By monitoring vibrational frequencies, FTIR provides evidence of whether fillers are successfully incorporated, whether functional groups remain chemically active, and whether new interfacial interactions are established. Since interfacial compatibility strongly affects filler dispersion and gas transport behavior, FTIR is indispensable for understanding the chemical dimension of structure property relationships [93]. There are many other studies in which FTIR is used for analysis [144–146]. In PSF/ACNF MMMs, FTIR-ATR spectra revealed the emergence of a new band at approximately 1750 cm^{-1} , corresponding to the stretching vibration of carboxyl groups [137]. This peak was absent in pristine PSF but became increasingly pronounced with higher ACNF content, demonstrating that the nanofibers were not merely physically dispersed but chemically integrated into the polymer matrix. The growing intensity of this band was correlated with higher CO_2 permeability and CO_2/CH_4 selectivity,

showing that chemical interactions enhanced interfacial adhesion and reduced the likelihood of non-selective voids (see Fig. 15a). In contrast, FTIR analysis of PSF/$LaFeO_3$ MMMs showed no new absorption bands beyond the characteristic peaks of PSF, such as the sulfone (S═O) and ether (C–O–C) stretching modes [136]. The absence of new peaks indicated that $LaFeO_3$ was incorporated physically without strong chemical bonding to the PSF matrix (see Fig. 15b). Despite the lack of chemical signatures, membranes with low $LaFeO_3$ loadings exhibited enhanced selectivity due to morphological effects confirmed by SEM.

Amine-functionalized fillers provide a different picture. For example, in a study conducted by Alsaady *et al.* [147] on PSF/NH_2-MIL-125(Ti) MMMs, FTIR spectra displayed additional broad bands at 3457 cm^{-1} and 3331 cm^{-1} (O–H and N–H stretching), as well as new peaks at 1661 cm^{-1} (C═O) and 1259 cm^{-1} (C–N stretching). These features confirmed the presence of amine functionalities from the MOF and their successful incorporation into the polymer matrix. Importantly, the backbone peaks of PSF remained intact, demonstrating that chemical integration was achieved without degrading the polymer. These new vibrational features explain the stronger polymer-filler interactions and the significant improvements in CO_2 permeability and CO_2/CH_4 selectivity reported in gas permeation tests (see Fig. 15c).

Zeolite-based MMMs show similar confirmation of filler incorporation. In a study conducted by Anbealagan *et al.* [148] PSF membranes loaded with RHO and NH_2-RHO zeolites were investigated, FTIR-ATR spectra displayed both the characteristic sulfone band of PSF (~1295 cm^{-1}) and the framework vibrations of zeolites in the 1080–960 cm^{-1} range. The amine-functionalized NH_2-RHO also produced distinct shoulder peaks at 1075–1020 cm^{-1} and an Si–O–C vibration at ~1012 cm^{-1} , confirming stronger polymer-filler interactions compared to unmodified RHO. These spectral differences align with performance data showing that NH_2-RHO membranes outperformed their non-functionalized counterparts in CO_2/CH_4 separation (see Fig. 15d).

Collectively, FTIR studies highlight the decisive role of functionalization in determining chemical interactions at the polymer-filler interface. Unmodified fillers, such as $LaFeO_3$, generally preserve the polymer's vibrational profile, suggesting physical embedding with limited chemical bonding. In contrast, functionalized fillers, ACNF with surface carboxyl groups, NH_2-MOFs, and NH_2-zeolites introduce new peaks that confirm stronger interfacial compatibility. These findings correlate directly with enhanced filler dispersion, improved selectivity, and higher thermal and morphological stability observed in

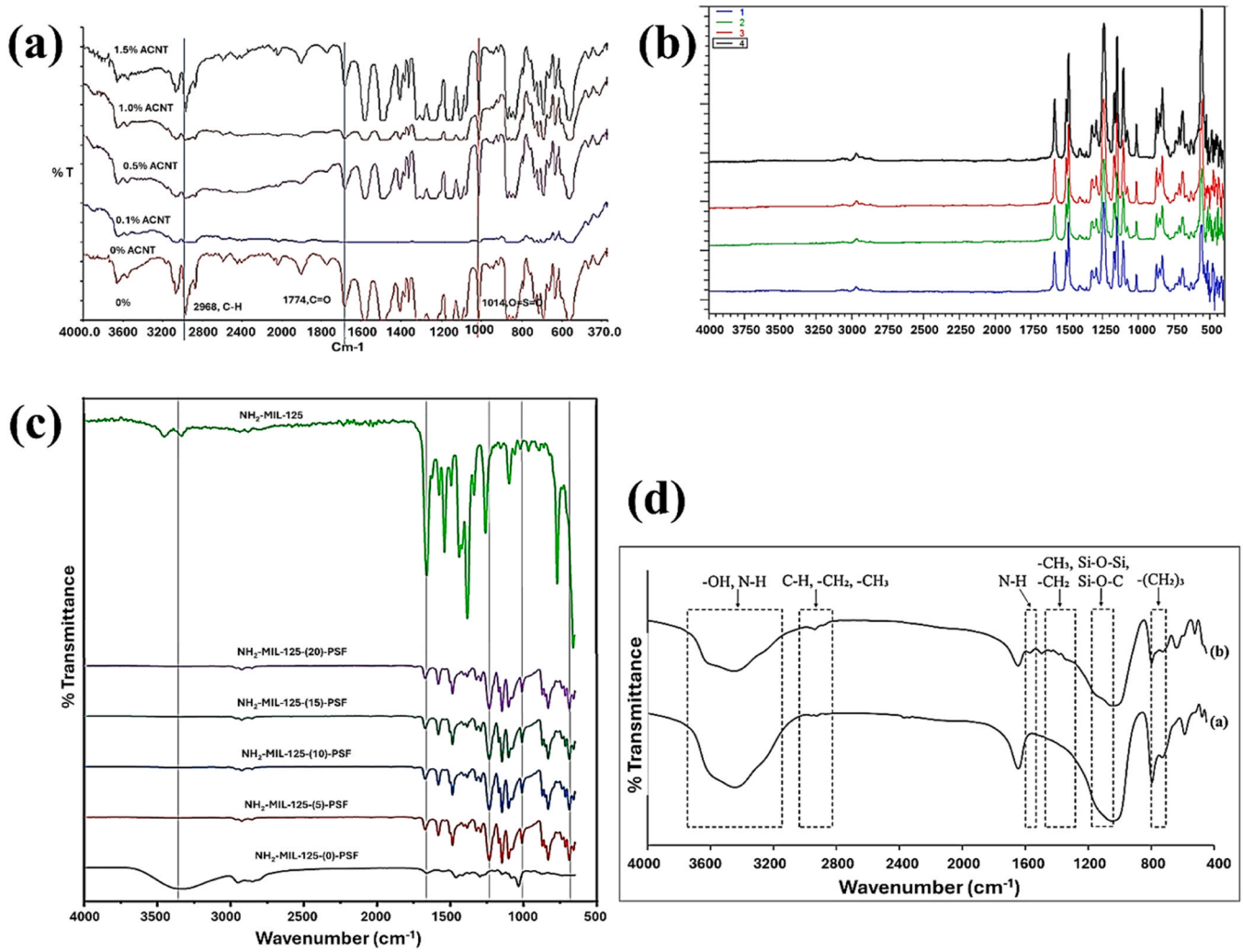

Fig. 15. (a) overlay FTIR spectra of pristine PSF and PSF/ACNF MMMs at increasing loadings, synthesized by Jamian *et al.* [137], (b) FTIR spectra of pristine PSF and $LaFeO_3$-loaded MMMs, showing the persistence of PSF's sulfone/ether bands without new vibrational features at increasing $LaFeO_3$ loadings (1) 0 wt%, (2) 0.5 wt%, (3) 1.0 wt% (4) 1.5 wt% synthesized by fadaly *et al.* [136]. Reprinted from Fadaly & Aziz [136] under the Creative Commons Attribution (CC BY 4.0) license, (c) FTIR spectra of PSF, pure NH_2-MIL-125(Ti), and PSF/NH_2-MIL-125(Ti) MMMs, synthesized by Alsaadi *et al.* [147]. Adapted from M. Alsaady *et al.* (2025), ACS Omega, DOI:10.1021/acsomega.4c09251. CC BY 4.0, (d) comparative FTIR spectra of PSF, RHO-MMM, and NH_2-RHO-MMM, focusing on sulfone and framework peaks, synthesized by Anbealagan et al. [148]. Mdpi, 10.3390/membranes11080630. CC BY 4.0.

complementary characterization techniques.

3.2.4. Thermogravimetric Analysis (TGA) and DSC

TGA and DSC are indispensable techniques for evaluating the thermal properties of PSF and PSF-based MMMs. TGA provides insight into decomposition behavior, residual mass, and overall thermal stability [138], while DSC measures thermal transitions such as the glass transition temperature (T_g) [149,150], which reflects polymer chain mobility [144,151,152]. Together, they establish the durability of the membranes and clarify how fillers alter polymer dynamics, which is essential for predicting long term stability and separation performance in natural gas purification.

The study focuses on the most important test for characterizing interfacial membrane quality and suitability to other high-temperature applications. Although similar weight loss was observed during the primary and secondary degradation stages of pure PSF and PSF/GO/CNT membranes, different thermal stability for these two types of mass reduction stages. As a result, higher residual masses after carbonization at elevated temperatures, 520°C or above (Fig. 16), which makes them more promising candidates for other rigorous applications. The curves reveal that the second stage of weight loss in the MMMs is significantly lower than in the pure PSF membrane, with a higher residual mass [93].

A representative perovskite-filled PSF system underscores typical TGA responses. Fadaly and Aziz [136] prepared PSF/$LaFeO_3$ MMMs by solution casting and found that incorporating 0.5–1.0 wt% $LaFeO_3$ slightly delayed the main mass loss step and increased residual mass, indicating a barrier and char-promoting effect of the inorganic phase. However, higher loading (1.5 wt%) caused agglomeration and performance deterioration, showing that thermal benefits can plateau or reverse when dispersion is poor. The obtained TGA curves make this point visually (see Fig. 17a), while the companion gas separation data show how the "thermal stability gain up to an optimum loading" accompanies permeability/selectivity improvements before turning over at higher loadings due to packing inefficiency and interfacial voiding. These features; earlier dryness, a single dominant decomposition step centred ~500–550°C, and a slightly higher char fraction in MMMs are typical of well-integrated, low-loading inorganics in PSF [136].

Rigidification trends are clearest in MOF-PSF MMMs where coordinated or H-bonding interfaces suppress local segmental mobility. In an indium-MOF series, Aditya and Bhanu [153] compared 3D MIL-68 (In)-NH_2 with a 2D In(aip)$_2$ within PSF and reported DSC-measured T_g increases upon filler incorporation. The authors attributed the T_g rise to interfacial interactions that immobilize PSF segments near the MOF surface; notably, the magnitude and sign of T_g shifts differed between the 3D and 2D architectures, reflecting distinct polymer-filler contact areas and packing constraints. These DSC signatures paralleled gas transport changes selectivity gains at moderate loadings where rigidified interphases suppress larger gas diffusivity more than CO_2, reinforcing the structure property link that DSC helps to quantify. Building on these observations in composites, Gómez-Avilés *et al.* [154] examined the intrinsic thermal stability of the amine-functionalized MOF NH_2-MIL-125(Ti). Their TGA data showed that the material remains structurally intact up to ~300°C, with a major weight loss only between 300°C and 350°C due to ligand decomposition (see Fig. 16b). Establishing this thermal baseline is important because it explains why such fillers can be incorporated into PSF without compromising the host matrix: the MOF itself is thermally robust within the processing and operating range of membranes. Thus, while DSC highlights how amine-MOFs rigidify the polymer matrix once embedded, TGA confirms that the resilience of the filler contributes to the long term stability of the hybrid. While such MOFs highlight how intrinsic thermal robustness of the filler can underpin composite stability, other porous phases such as zeolites show that the outcome is equally sensitive to surface chemistry and the synthesis route employed.

Porous zeolite derivatives in PSF provide a useful counterpoint where both synthesis route and surface chemistry steer the thermal outcome. In a silane-modified zeolite RHO series, Anbealagan *et al.* [148] compared unmodified RHO with NH_2-RHO prepared and cast by phase inversion. Their TGA/Differential thermogravimetric (DTG) analysis (see Fig. 16c & 16d) shows that adding either filler slightly raises the temperature of maximum mass loss and increases char yield, but the amino-silane-modified particles give the cleaner one-step profile, and the larger thermal stability increment evidence of better interfacial adhesion and reduced micro-voiding relative to unmodified RHO. That thermal "tightening" mirrors the separation data where NH_2-RHO outperforms RHO at the same loading even classical ZIF-8/PSF systems often prepared by dry/wet phase inversion; display the same pattern at low-loading: Nordin *et al.* [155] reported improved thermal and mechanical stability even at $\leq$ 1 wt% ZIF-8, with diminishing returns and morphological defects at higher loadings (see Fig. 16e). While their results emphasize mechanical/TGA outcomes more than DSC, it reinforces the synthesis-sensitivity of thermal metrics: gentle dope preparation and low filler content yield the cleanest TGA baselines and the most reproducible decomposition curves.

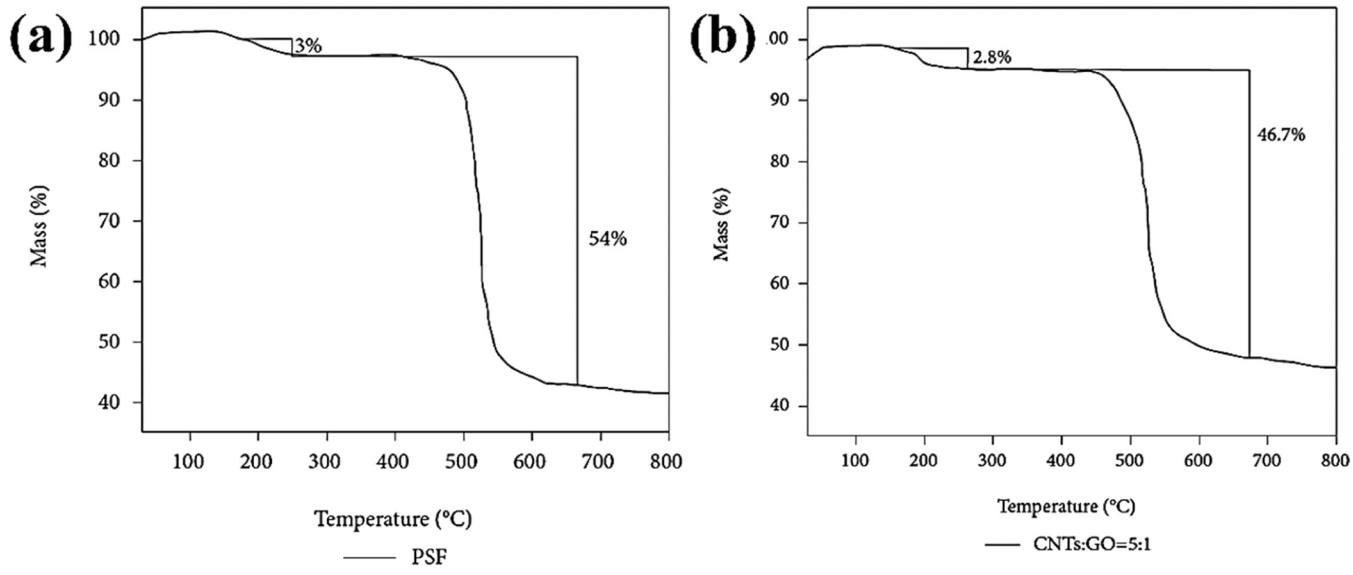

Fig. 16. TGA of (a) PSF and (b) PSF/GO/CNTs [93]. Reproduced from L. Jiang et al. (2021), Journal of Nanomaterials, Article ID 9934118, under CC BY 4.0.

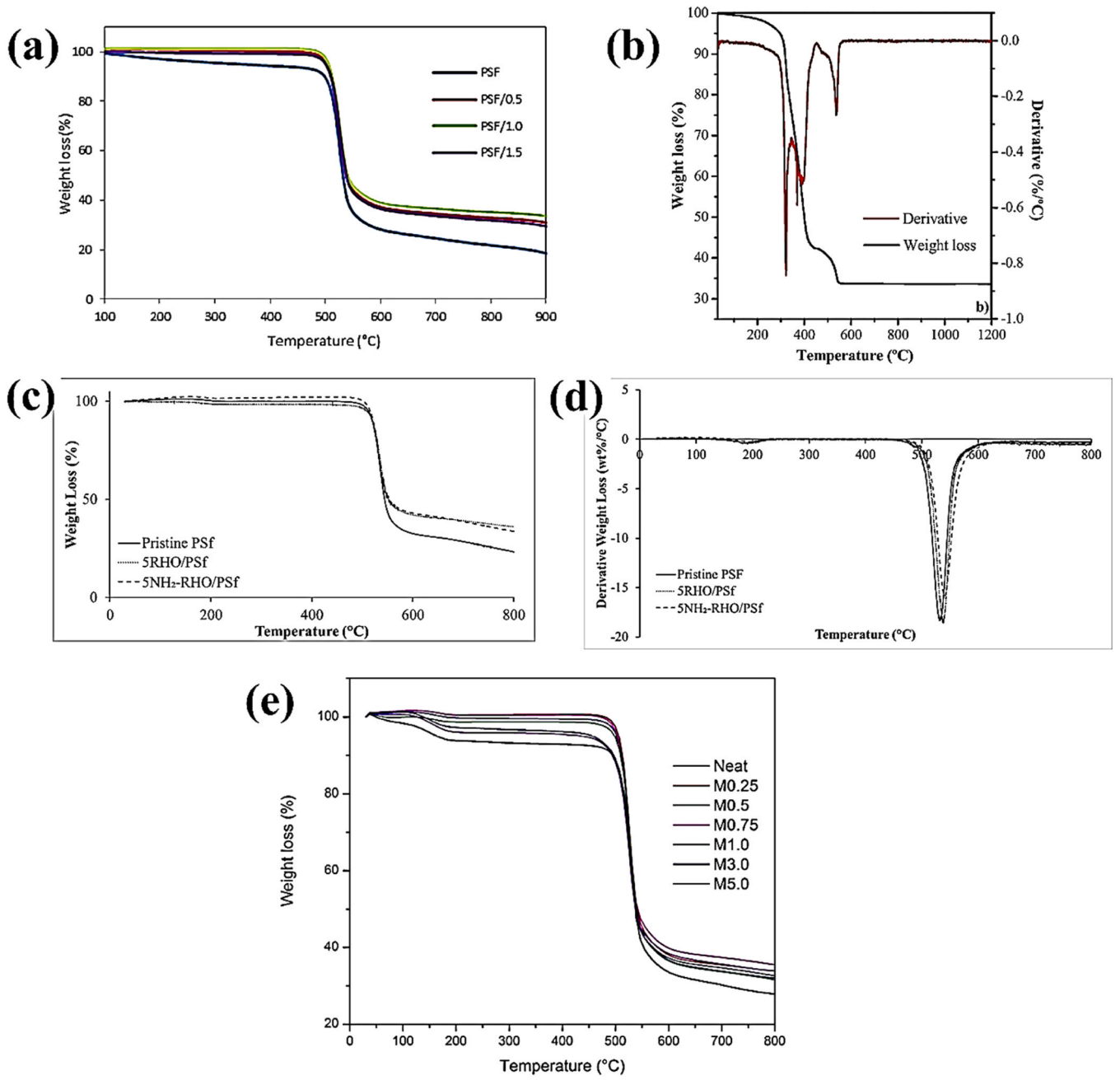

Fig. 17. (a) TGA analysis of the PSF/LAFeO$_3$ membrane study conducted by Fadaly and Aziz [136]. Reprinted from Fadaly & Aziz [136] under the Creative Commons Attribution (CC BY 4.0) license, (b) thermogravimetric analysis in air of NH_2-MIL-125(Ti) and its corresponding derivative study conducted by Gomez et al. [154]. Reproduced from Gómez-Avilés et al., (2020), Catalysts, 10(6), 603. CC BY 4.0., (c) TGA thermograms of pristine PSF membrane, 5RHO/PSF, and 5NH_2-RHO/PSF MMMs., (d) DTG thermograms of pristine PSF membrane, 5RHO/PSF, and 5NH_2-RHO/PSF-MMMs. Study conducted by Anbealagan et al. [148]. Mdpi, 10.3390/membranes11080630. CC BY 4.0., (e) TGA curves of the prepared ZIF-8/PSF membranes with increasing ZIF-8 loading synthesized by Nordin et al. [140]. Copyright 2015, RSC Advances.

In conclusion, these studies highlight that TGA consistently demonstrates incremental improvements in thermal stability and char residue with well-dispersed, low to moderate filler loadings. DSC provides complementary evidence by detecting shifts in T_g, which are most pronounced when fillers are functionalized to promote stronger interactions with PSF. Functionalized MOFs and zeolites reliably increase T_g and stability, while unmodified fillers often provide weaker or inconsistent benefits. These techniques therefore offer a dual diagnostic perspective: TGA defines safe operating temperature ranges, while DSC reveals how fillers alter polymer chain dynamics, which in turn controls permeability and selectivity.

3.2.5. *Gas permeation test*

Gas permeation testing remains the definitive method for evaluating the performance of MMMs developed for gas separation applications [93,149]. This method yields critical quantitative data on permeability, selectivity, and the impact of operational parameters such as filler type, loading, pressure, and gas composition on membrane behavior. Robeson invented the Robeson upper bound curves, which are a useful tool for coordinating data on selectivity and permeability in membrane separation procedures [156]. Gas separation qualities, such as permeability and selectivity, were also investigated for gas permeation measurements [157,158]. Over the past decade, considerable advancements have been

achieved in PSF-based MMMs designed for CO_2/CH_4 separation, where the choice and dispersion of fillers have been shown to profoundly influence membrane transport properties and long term stability. A key insight from these studies is the delicate balance between improving permeability through filler incorporation and maintaining or enhancing selectivity by preventing filler agglomeration. For instance, PSF hollow fiber membranes incorporated with $LaFeO_3$ perovskite particles demonstrated remarkably high CO_2 permeability (~47.7 GPU) and a CO_2/CH_4 selectivity of about 28 at a relatively low filler loading of 1 wt % under pressures ranging from 8 to 16 bar. Beyond this concentration, increased filler agglomeration led to reduced selectivity, highlighting the critical importance of controlling particle dispersion within the polymer matrix [61]. This example illustrates how modest addition of well-dispersed fillers can significantly enhance gas transport performance without detrimental morphological effects. Building on this principle, PSF membranes incorporating amino-functionalized MIL-125 (Ti) MOFs showcased a significant increase in CO_2 permeability from 6.1 to 19.1 Barrer at an optimal filler loading of 15 wt%, coupled with selectivity peaking near 31.9. However, exceeding this loading threshold introduced particle agglomeration verified by SEM, which diminished performance. Such observations exemplify the fine threshold in filler loading where the benefits of enhanced gas pathways balance against the drawbacks of heterogeneous filler distribution [147]. Together with the $LaFeO_3$ studies, these results underscore the intricate interplay of filler content and dispersion quality in realizing high-performance MMMs [136]. Explorations with indium-based MOFs such as MIL-68(In)–NH_2 and In(aip)$_2$ further underscore this relationship. At 20 wt% In(aip)$_2$ incorporation, PSF MMMs manifested a dramatic increase in CO_2 permeability (~144 Barrer), almost 24 times that of the pure PSF matrix, while concurrently enhancing selectivity. FESEM imaging confirmed uniform filler dispersion at lower loadings, yet also revealed agglomeration as filler content increased, reinforcing the critical role of filler morphology and loading in determining membrane efficacy and durability [153]. Additionally, pressure dependence of gas transport properties is another key consideration, as observed with PSF MMMs comprising PEG-grafted carbon nanotubes (PEG-g-CNTs). At 7.5 wt% loading, both CO_2 permeability and selectivity were found to increase with rising pressure, with permeability showing a 38% enhancement. This pressure-responsive behavior points to favorable interactions between the polymer matrix and nanofillers, which optimize gas transport pathways under realistic operating conditions, emphasizing the need for variable-pressure testing to fully delineate membrane performance [159]. The complexity of real-world applications is further reflected in mixed-gas experiments, such as those involving PSF/ZIF-8 MMMs exposed to CO_2/CH_4 blends containing 800 ppm H_2S. These membranes exhibited pressure-dependent permeability consistent with dual-mode sorption models, where both Henry's law dissolution and Langmuir-type adsorption mechanisms contribute. The observed selectivity variations correlated closely with structural changes detected via advanced characterization, demonstrating that testing membranes under relevant mixed-gas conditions is essential to predict in-field operation accurately [153]. Beyond these MOF and carbon-based fillers, investigations into other fillers such as SiO_2 nanoparticles, activated carbon nanofibers, mesoporous silica KIT-6, graphene derivatives, ILs, and functionalized MOFs have expanded understanding of how filler chemistry and structure influence PSF membrane performance. For example, SiO_2 nanoparticles improved CO_2 permeability and selectivity up to moderate loadings, though sorption saturation caused slight permeability reductions at higher pressures [160]. Activated carbon nanofibers enhanced selectivity at lower loadings but void formation at elevated filler concentrations diminished separation capabilities [137]. Meanwhile, graphene-based fillers and ILs contributed to improved plasticization resistance and transport properties, illustrating the multifaceted roles that filler properties play in customization of PSF MMMs [159].

Critically, the long term operational stability of PSF MMMs has been demonstrated in multiple studies, with some crosslinked polymer membranes maintaining CO_2 permeability and selectivity over 10,000 h under mixed-gas and vacuum conditions. Such durability is pivotal for industrial deployment, validating the synthesis approaches that optimize polymer-filler interactions and membrane morphology [147,153]. The observed permeability-selectivity trends can be physically interpreted through the solution-diffusion mechanism governing gas transport in glassy polymers. Incorporation of well-dispersed fillers modifies the fractional free volume and introduces preferential sorption sites, thereby enhancing CO_2 solubility and diffusivity. At optimal loadings, improved polymer-filler interfacial adhesion reduces non-selective voids while increasing tortuosity for larger gas molecules such as CH_4, resulting in enhanced selectivity. However, excessive filler loading leads to agglomeration and interfacial defects that create non-selective transport pathways, explaining the simultaneous increase in permeability and decline in selectivity. Under high CO_2 pressure, plasticization further increases chain mobility, enlarging free volume elements and reducing size-sieving capability, which accounts for pressure-dependent selectivity loss.

4. Predictive analytical framework for PSF-based membranes under sour gas conditions

Despite extensive experimental efforts to enhance PSF-based membranes for CO_2 and H_2S separation, membrane development for sour gas environments remains largely empirical. Improvements achieved through filler incorporation, surface functionalization, or processing modification are often reported as isolated studies, which limits the ability to generalize outcomes or predict design robustness under aggressive gas conditions. To address this limitation, a predictive analytical framework is proposed that systematically links experimentally measurable characteristics to membrane design suitability, enabling a theoretical assessment rather than trial-and-error optimization.

To enhance methodological clarity, Fig. 18 provides a schematic overview of the analytical framework and workflow adopted in this study. The process begins with systematic literature compilation of experimentally reported PSF-based membrane performance under sour gas conditions. Governing stability indicators are then identified based on recurring structure property correlations, followed by literature calibrated threshold definition. Ordinal scoring is applied using a 0–3 scale, and composite robustness scores are generated through equal weighting of all indicators. The resulting classification enables comparative evaluation of membrane architectures. Finally, limited quantitative consistency checks and sensitivity analysis are performed to assess robustness of ranking outcomes.

Fig. 19 presents the core of this framework in the form of a literature calibrated predictive matrix. The matrix integrates six analytically verifiable indicators that are repeatedly identified in PSF membrane studies as governing performance stability in the presence of acidic gases: morphological dispersion (SEM), polymer-filler interfacial integrity (TEM), chemical interaction strength (FTIR), changes in chain mobility reflected by glass transition shifts (DSC), thermal stability under elevated temperature exposure (TGA), and resistance to gas-induced plasticization. Each indicator is evaluated on an ordinal scale from 0 to 3, where 0 denotes high-risk or failure-prone behavior and 3 represents analytically strongest and design-ready characteristics. The scoring thresholds and classification criteria used to assign these values are derived from experimentally observed trends reported across PSF and PSF-based MMM literature and are summarized in Supplementary Information (Tables S6-S8).

The six governing indicators incorporated in the predictive matrix were selected based on repeatedly established structure property correlations in the PSF and MMM literature. Specifically, (i) filler dispersion has been shown to directly influence selectivity retention by minimizing non-selective voids [161]; (ii) polymer-filler interfacial compatibility

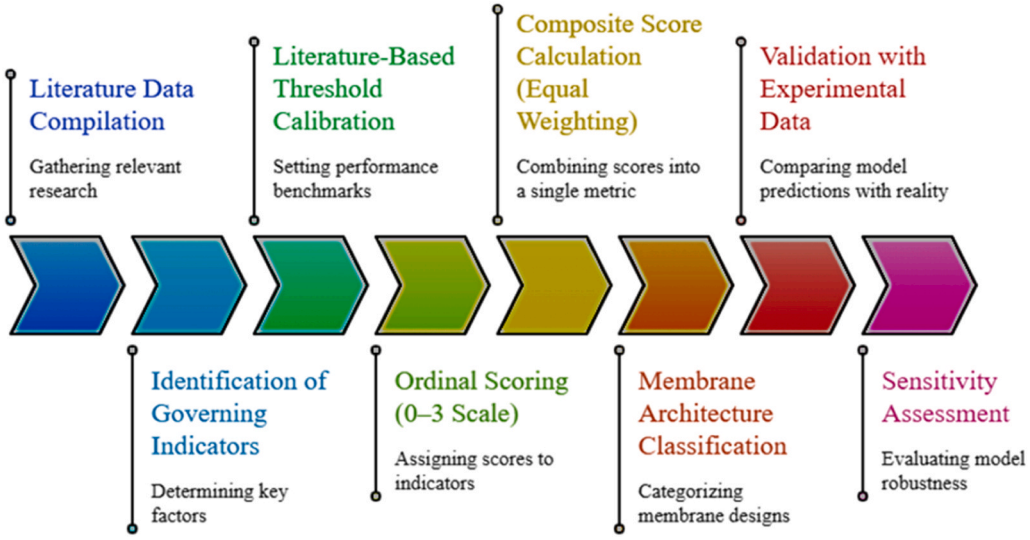

Fig. 18. Schematic illustration of the analytical modeling framework and workflow adopted in this study.

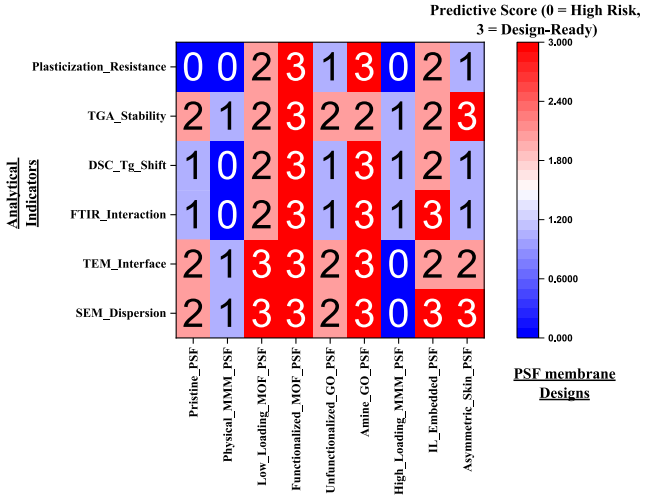

Fig. 19. Literature calibrated predictive analytical matrix for PSF-based membrane design under CO_2/H_2S (sour gas) conditions.

governs defect suppression and stress distribution; (iii) chemical functionalization enhances CO_2 affinity and interfacial adhesion [162]; (iv) shifts in glass transition temperature (T_g) reflect changes in chain mobility and resistance to pressure-induced swelling; (v) decomposition onset temperature correlates with long term thermal durability; and (vi) resistance to CO_2-induced plasticization strongly determines permeability stability under high-pressure sour gas conditions [163].

The ordinal scoring scale (0−3) was adopted to provide a semi-quantitative and transparent classification framework capable of accommodating variability in reported experimental datasets. Rather than relying on empirical fitting, threshold criteria were literature calibrated based on consistent experimental trends reported across PSF and MMM systems. Equal weighting of indicators was intentionally applied to reflect the coupled and interdependent degradation mechanisms observed in sour gas environments, where morphological, thermodynamic, and interfacial factors collectively determine membrane robustness.

The predictive matrix reveals clear differentiation among PSF membrane design architecture types. Pristine PSF and physically blended MMMs consistently exhibit low composite scores, reflecting weak interfacial compatibility and susceptibility to plasticization under CO_2 and H_2S exposure. In contrast, chemically engineered systems, particularly those incorporating functionalized fillers or amine-modified nanostructures exhibit consistently elevated scores across multiple analytical domains. This observation suggests that improvements in sour gas stability arise not from a single modification, but from the concurrent mitigation of interfacial defects, chain mobility enhancement, and plasticization resistance. In this respect, Fig. 18 functions as a diagnostic tool, enabling identification of dominant failure mechanisms while simultaneously highlighting design strategies that address them.

While the full predictive matrix provides comprehensive analytical insight, its multidimensional nature can limit rapid design decision-making. To enhance practical use, the framework is projected into a reduced design space in Fig. 20. Fig. 20 represents a condensed architectural interpretation derived directly from the composite scoring matrix shown in Fig. 19. While Fig. 19 presents individual indicator scores across membrane types, Fig. 20 synthesizes these multidimensional outcomes into broader robustness categories by considering aggregate composite scores and recurring performance patterns. Thus, Fig. 19 provides the analytical scoring basis, whereas Fig. 20 translates these scores into a practical membrane design landscape, highlighting relative stability under sour gas conditions.

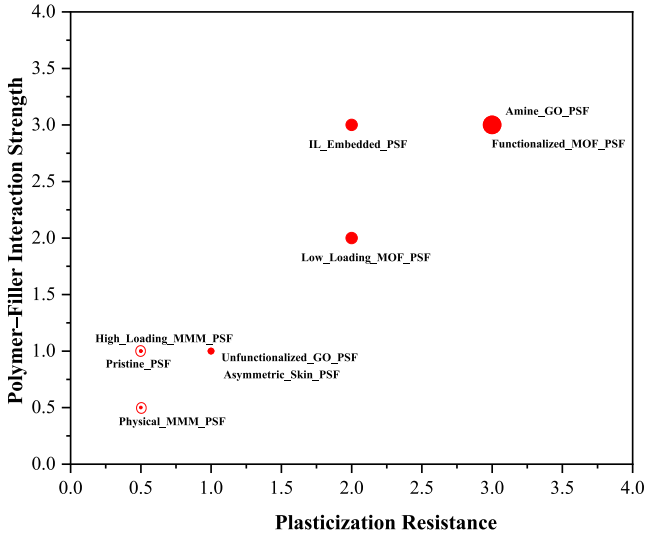

Fig. 20. Reduced design space projection of PSF-based membrane archetypes based on plasticization resistance and polymer-filler interaction strength.

In Fig. 20, each membrane design is represented as a point within this reduced space, while the bubble size corresponds to a suitability score for CO_2 and H_2S separation, derived from the cumulative analytical evaluation summarized in Fig. 18. Larger bubbles represent designs that simultaneously satisfy multiple robustness criteria and are thus more likely to exhibit long term operational stability. Several data points are marked by red-outlined circles; these correspond to designs that received a zero score for one or more governing indicators. Such points are intentionally retained to preserve their spatial positioning within the design space, ensuring that failure-prone designs remain visually represented without implying enhanced suitability.

Together, Figs. 19 and 20 illustrate how analytically grounded indicators can be translated into actionable design guidance. Fig. 19 establishes the structural and chemical basis for membrane suitability through multidimensional evaluation supported by literature calibrated criteria (Tables S6-S8), while Fig. 20 further coincizes this information into a design space map that facilitates rapid comparison among competing strategies. Membrane designs clustering in the upper-right region of Fig. 20, characterized by strong polymer-filler interactions and high plasticization resistance, consistently correspond to large bubble sizes. On the contrary, designs located in low-interaction, low-resistance regions are associated with minimal suitability, reinforcing the predictive consistency of the proposed framework.

Fundamentally, the framework does not aim to predict permeability or selectivity directly, nor does it rely on empirical fitting. Instead, it provides a rational methodology for interpreting analytical data in the context of membrane design decisions. By formalizing the relationship between characterization outcomes and sour gas stability, and by grounding scoring criteria explicitly in published experimental evidence, the framework offers a transferable and extensible approach for guiding the development of PSF-based membranes capable of operating under chemically aggressive conditions.

While the proposed predictive analytical framework provides a structured method for correlating characterization indicators with membrane robustness, certain limitations must be acknowledged. The model is semi-quantitative and literature calibrated, relying on reported experimental trends rather than first-principles molecular simulations. It assumes relatively uniform filler dispersion and does not explicitly resolve three-dimensional morphological heterogeneity or interfacial stress distribution. Additionally, long term physical aging, time-dependent plasticization kinetics, and multicomponent competitive sorption effects under realistic process conditions are not directly incorporated. Therefore, the framework should be interpreted as a design guidance and screening tool rather than a substitute for detailed molecular-level modeling or process scale simulations.

4.1. Sensitivity analysis of the predictive framework

To evaluate the validity of the proposed analytical matrix, a limited sensitivity assessment was conducted by systematically varying key indicator scores and weighting factors within reasonable bounds. Since the framework is based on ordinal scoring (0−3) and equal weighting of six governing indicators, the analysis focused on two critical parameters identified as dominant in sour gas separation environments: plasticization resistance and polymer-filler interfacial compatibility.

4.1.1. Variation of plasticization resistance score

For high-performing systems such as NH_2-functionalized MMMs, the plasticization resistance score (baseline = 3) was reduced to 2 and subsequently to 1 while maintaining other indicators constant. This adjustment resulted in an approximate 6–12% reduction in composite score. However, the overall ranking hierarchy among membrane archetypes remained unchanged

NH_2-functionalized MMMs > ZIF-based MMMs > metal oxide-filled MMMs > pristine PSF

4.1.2. Alternative weighting scenarios

To assess the impact of weighting assumptions, individual indicators were varied by ±20% relative to the baseline equal-weight scheme, while absolute composite scores shift by approximately 5–11% depending on the parameter variation, the overall ranking hierarchy of membrane architectures remains unchanged. The modified weighting was applied separately to plasticization resistance, interfacial compatibility and thermal stability

Under all tested scenarios, ranking stability was preserved. While absolute composite values shifted slightly, membrane classification into low-, moderate-, and high-robustness categories remained consistent. Furthermore, the representative outcomes of the sensitivity analysis are summarized in Table 3.

4.2. Preliminary quantitative consistency with experimental data

To assess the consistency of the proposed framework with reported experimental performance, a limited quantitative comparison was conducted using representative PSF-based membranes discussed in this review. Membranes were scored according to the analytical matrix (Fig. 19), and their composite scores were compared against reported CO_2 permeability, CO_2/CH_4 selectivity, and plasticization resistance behavior.

The analysis reveals that membranes exhibiting stronger polymer-filler interactions, improved T_g shifts, and enhanced thermal stability consistently achieve higher composite scores and correspond to superior selectivity retention and pressure stability in experimental studies. In contrast, pristine PSF and physically blended systems with limited interfacial engineering yield lower composite scores and demonstrate susceptibility to plasticization under elevated CO_2 concentrations.

These results indicate that the framework successfully captures experimentally observed performance hierarchies across PSF-based membrane architectures, supporting its utility as a rational screening tool. It is emphasized that the framework does not predict exact permeability values but rather evaluates relative robustness under sour gas conditions. Furthermore, a quantitative comparison between predictive framework score and experimentally reported gas separation performance has been presented in Table 4.

The limited quantitative comparison demonstrates a consistent hierarchy between framework composite scores and experimentally reported performance. Membranes assigned higher analytical robustness scores, particularly those incorporating chemically functionalized fillers (e.g., NH_2-MIL-125(Ti)), exhibit improved CO_2/CH_4 selectivity and enhanced plasticization resistance. Conversely, pristine PSF, which receives lower composite scoring due to limited interfacial and thermal reinforcement, demonstrates earlier onset of pressure-induced plasticization. While the framework is not intended to predict absolute permeability values, it successfully captures experimentally observed robustness trends across PSF membrane architectures. Compared to

Table 3
Sensitivity of membrane ranking under parameter variation.

Scenario	NH_2-MOF MMM	ZIF MMM	$LaFeO_3$ MMM	Pristine PSF	Ranking Stability
Baseline (equal weights)	High	Moderate-High	Moderate	Low	Reference
Plasticization −1 score	High	Moderate-High	Moderate	Low	Unchanged
Plasticization weight + 20%	High	Moderate-High	Moderate	Low	Unchanged
Interfacial weight + 20%	High	Moderate-High	Moderate	Low	Unchanged

Table 4
Limited quantitative comparison between predictive framework score and experimentally reported gas separation performance.

Membrane System	Approx. Composite Score (Framework)	CO_2 Permeability	CO_2/CH_4 Selectivity	Plasticization Resistance	Reference
Pristine PSF	Low (≈6–7)	~6 Barrer	~28	Poor (4–6 bar)	[147,164]
PSF/$LaFeO_3$ (1 wt%)	Moderate (≈10–11)	47.7 GPU	28	Moderate	[61,136]
PSF/ZIF-8 (≤1.25 wt%)	Moderate-High	Enhanced vs PSF	Improved	Improved	[140,165]
PSF/NH_2-MIL-125(Ti) (15 wt%)	High (≈15–16)	19.17 Barrer	31.95	High (≤14 bar)	[147]

existing studies [166], which primarily rely on empirical correlations or isolated modeling approaches, the present framework offers a more integrated perspective by linking structural, chemical, and thermo-mechanical parameters to membrane performance. Recent data-driven and machine learning-assisted studies have demonstrated the strong potential of predictive modeling in membrane design; however, these approaches often lack direct integration with experimental characterization [[167–170]. The current framework bridges this gap by combining experimental insights with predictive analysis, providing a more practical and transferable design methodology.

Case. Study: Framework-Guided Design of PSF-Based MMM

To demonstrate the practical applicability of the proposed analytical framework, a design-oriented case study is presented for a PSF-based MMM intended for high-pressure CO_2/CH_4 separation under sour gas conditions (≥15 bar, presence of H_2S).

Based on Fig. 19, membrane robustness under such conditions requires high scoring in three dominant indicators: plasticization resistance (≥2–3), polymer-filler interfacial compatibility (≥2), and enhanced CO_2 affinity through chemical functionalization (≥2). Fig. 20 further indicates that chemically functionalized MMM architectures consistently occupy the high-stability design region.

Following this logic, incorporation of amine-functionalized MOFs (e.g., NH_2-modified frameworks) into PSF would be expected to:

- Increase CO_2 affinity via specific acid-base interactions
- Improve interfacial adhesion through hydrogen bonding
- Elevate resistance to pressure-induced plasticization
- Maintain thermal stability above 450°

Applying the scoring matrix provides an estimated composite robustness score in the high-performance category (≈15–17), consistent with experimental observations for functionalized PSF/MOF systems discussed in this review. In contrast, a physically blended metal-oxide-filled PSF membrane would score moderately due to limited chemical reinforcement at the interface and lower plasticization resistance.

This case study demonstrates how the framework can guide reasonable membrane design by identifying critical structural features necessary to achieve performance targets rather than relying solely on empirical optimization.

5. Recent advances in the study of PSF-based membrane

In the previously discussed sections, different classes of membranes including organic (polymeric), inorganic, and MMMs have been outlined, their comparative properties, such as composition, permeability, selectivity, thermal stability, chemical resistance, mechanical strength, fabrication cost, scalability, application, advantages and disadvantages are summarized in Table S5 of the supplementary document, to provide a clear understanding of their relative performance and application potential.

In the proceeding sections, recent advances will be explored in membrane technology in greater detail, focusing on the development and enhancement of PSF-based membranes.

5.1. Polymeric blend or composite membrane

Polymeric blending, the first generation of gas separation technology, involves combining two compatible polymers and offers advantages in simplicity and fabrication efficiency [171,172]. Polymer membranes are typically classified as glassy or rubbery, depending on whether their glass transition temperature (Tg) is above or below room or operating temperature [173]. Additionally, membranes can be categorized as anisotropic or isotropic based on morphology, and further distinguished by geometry and fabrication method [174]. Tan and Rodrigue (2019) reviewed five principal methods for polymeric membrane fabrication, namely NIPS, VIPS, electrospinning, track-etching, and sintering, highlighting their respective mechanisms and applicability in membrane production [175]. Alkandari *et al.* (2024) reported that sustainable manufacturing strategies for polymer-based membranes can markedly improve gas separation performance through the integration of advanced fabrication techniques, green solvents, and hybrid material systems [127]. Fig. 21 summarizes the classification of polymeric membranes and their synthesis methodologies, including the fabrication techniques discussed in 3.1.

Polymeric membranes and are increasingly recognized as a promising technology for natural gas sweetening, due to their modularity, energy efficiency, and relatively low operational costs compared to conventional absorption processes [176]. Dong *et al.* (2020) investigated multilayer composite membranes for CO_2 separation, in which polysulfone (PSF) served as the porous support layer. The PSF substrate provided the necessary mechanical strength and structural integrity to sustain successive coating layers without pore collapse, while maintaining adequate porosity for gas transport. This support configuration contributed to the scalability, durability, and industrial feasibility of the multilayer membrane design for CO_2 separation applications [46,177]. Kadirkhan *et al.* (2022) reviewed challenges and emphasized that in CO_2/CH_4 separation, polymers such as PSF, CA, PI, and polyethylene oxide (PEO)-based blends exhibit high CO_2 solubility, which enhances selectivity, but their performance is often compromised by plasticization at high CO_2 pressures and physical aging that reduces permeability over time. The review also discusses the importance of future studies in mixed-gas scenarios for large-scale applications, addressing issues such as pore blockage, plasticization, and aging [63]. Roafi *et al.* (2024) reported that PSF/cellulose triacetate (CTA) blend membranes exhibit enhanced CO_2 solubility and gas separation performance relative to pristine PSF, demonstrating the effectiveness of polymer blending in mitigating plasticization and aging effects. The blended membranes achieved a CO_2/CH_4 selectivity of 30.70 at 4 bar, markedly higher than that of pristine CTA (9.82) and PSF (10.35), while maintaining a reasonable CO_2 permeability of 11.12 Barrer, indicating no significant trade-off between selectivity and permeability [164]. Maghami *et al.* (2021) demonstrated that PSF membranes prepared with NMP exhibited the highest CO_2 permeability, which was further enhanced by propionic acid incorporation (106% increase). The addition of 30 wt% γ-alumina nanoparticles, improving CO_2/CH_4 selectivity by 13%, highlighting the effectiveness of solvents and additives in boosting CO_2 separation performance [178]. Further Karimi *et al.* (2019) examined PEG-blended PSF membranes for gas separation, confirming their dense, asymmetric, and amorphous structure via XRD, FTIR, and SEM analyses. CO_2 permeability initially decreased up to 4 bar feed pressure but increased at higher pressures, with the most pronounced enhancement observed at

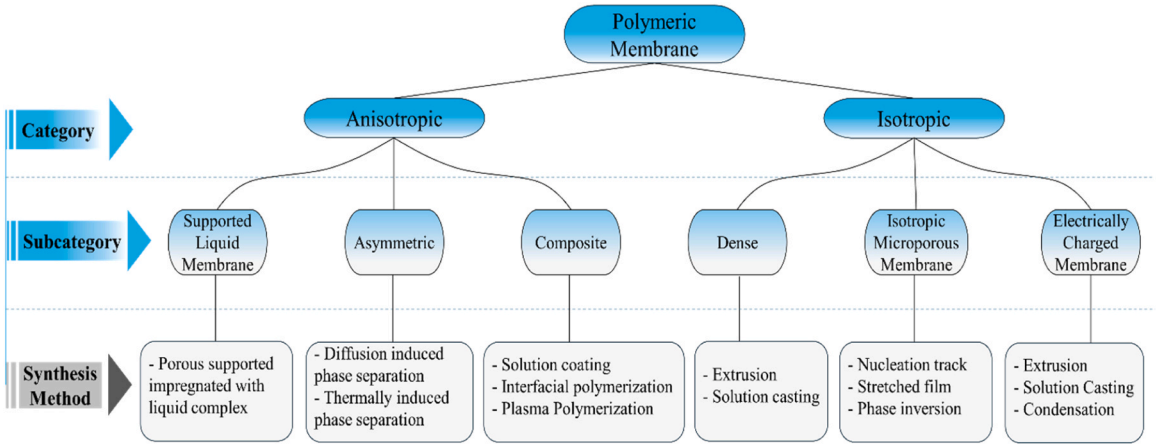

Fig. 21. Overview of polymeric membrane types and the methods employed for their synthesis.

20 wt% PEG. This behavior is attributed to CO_2-induced plasticization, which enhances polymer chain mobility and gas sorption, indicating that PEG incorporation can effectively improve PSF membrane permeability under varying pressures [179]. Nasirian *et al.* (2020) also investigated PEG/PSF membranes prepared with varying PEG loadings and reported that PEG incorporation significantly enhanced gas separation performance. The optimal composition, PSF/PEG10000 at 20 wt %, increased CO_2 permeability from 5.61 to 7.64 Barrer, attributed to improved polymer miscibility, increased free volume, and enhanced tensile strength, while maintaining resistance to CO_2 induced plasticization [180]. Abd. Hamid *et al.* (2018) demonstrated PSF blending with PI (specially 60w%) presents increase in CO_2 permeability to 86 GPU [181]. Further PSF is also playing important role in TFC membranes with their enhanced selectivity, permeability, and mechanical strength, extensively applied in gas separation [182]. The permeabilities and selectivities of the different PSF-based membranes studied in literature are tabulated in Table 5.

Table 5 summarizes the reported gas separation performance of various PSF- and PES-based polymeric membranes modified with different additives, solvents, blends, and ionic liquids. Most studies primarily report CO_2 permeability and CO_2/CH_4 selectivity, demonstrating that the incorporation of additives such as PEG, PDMS, ionic liquids, and polymer blends can significantly enhance CO_2 transport properties. For example, ionic liquid-modified membranes (e.g., [EMIM][BF_4] and [EMIM][Tf_2N]) exhibit substantially higher CO_2 permeability compared to conventional solvent-modified systems, while maintaining moderate selectivity. However, H_2S permeability and H_2S/CH_4 selectivity data are rarely reported, with only limited studies providing H_2S transport performance. This indicates that, despite extensive research on CO_2/CH_4 separation, systematic investigation of H_2S/CH_4 separation in PSF-based membranes remains insufficient, highlighting the need for further studies on acid gas removal.

The performance of membranes is commonly evaluated against Robeson's upper limit, which serves as a benchmark for selective gas permeability versus selectivity. This comparison allows for a clearer understanding of how effectively a polymeric membrane can separate different gases while adhering to theoretical performance boundaries established by Robeson in 2008. By analyzing the data presented in Table 3, the gas separation efficiency of PSF-based polymeric membranes is presented in Fig. 22.

5.2. Hybrid membranes

A promising direction to overcome the inherent limitations of current membrane technologies is the development of hybrid membranes, which include blends, composites, and MMMs. These hybrid systems aim to enhance both selectivity and permeability by integrating inorganic fillers or modifying polymer matrices [191–193]. Among various approaches, the incorporation of nanomaterials has gained attention due to their tunable properties and potential for improving dispersion

Table 5
Permeabilities and selectivities of the polymeric or composite membrane.

Polymeric membrane	Additive / Feature	Permeability (Barrer)		Selectivity		Reference
		P_{CO_2}	P_{H_2S}	P_{CO_2}/P_{CH_4}	P_{H_2S}/P_{CH_4}	
PSF/PEG10000	PEG10000	7.64	—	28.56	—	[180]
PSF/THF	THF	30.04	—	50	—	[86]
PSF/CF	CF	24.76	—	35	—	[86]
PES/NMP	—	0.51	—	25.5	—	[183]
PES/dimethylacetamide	dimethylacetamide	29.7	—	7.13	—	[86]
CA/PSF (2 wt%)	CA	80.51	—	—	—	[172]
PSF/CTA(6 wt%)	CTA(6 wt%)	11.12	—	30.70	—	[164]
PSF/DMAC	DMAC solvent	—	119000	—	1.56	[92]
PSF/PEG	PEG	5.61	—	27	—	[179]
PES/[emim][Tf2N]	[emim][Tf2N]	298.84	—	57.53	—	[184]
PSF/[EMIM] [BF4] (30 wt%)	[EMIM] [BF4] (30 wt%)	601.98	—	25.87	—	[185]
PSF/[APTMS][Ac] (30 wt%)	[APTMS][Ac] (30 wt%)	16.00 ± 0.80	—	39.00 ± 0.98	—	[186]
T-PPPS/PDMS/PSF	PDMS coating	9.29	—	34	—	[177]
PSF/PDMS30	PDMS (30%)	52 GPU	—	56.7	—	[187]
PSF/PES	PES blend	25 GPU	—	3.8	—	[188]
PSF/PI-60	PI blend	—	—	4.4 (H_2/CO_2)	—	[181]
PSF/PI	PI blend	1.3624	—	4.80	—	[189]
PSF/PEBAX	PEBAX	11GPU	—	16	—	[190]

"—" data is not available (limited literature)

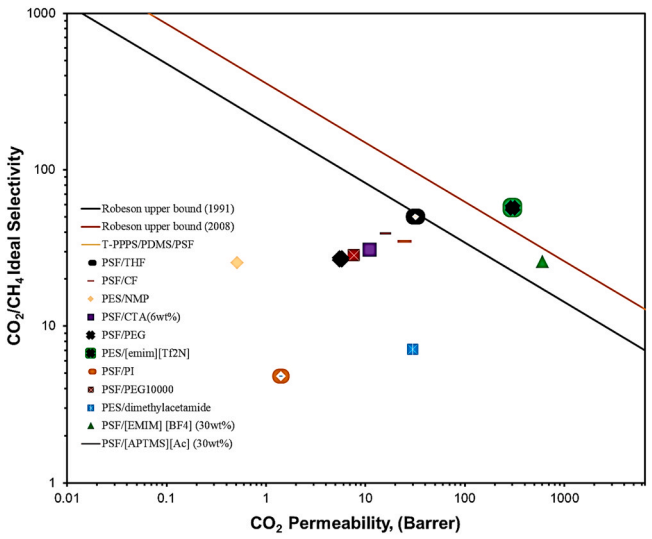

Fig. 22. Separation performance of polymeric membranes with Robeson's upper limit.

and compatibility across diverse applications [194]. These advancements offer economical and scalable solutions for next-generation membrane technologies. MMM are composite structures that integrate inorganic or organic fillers within a polymer matrix to combine the mechanical flexibility of polymers with the high selectivity of molecular sieving materials [164,192,195,196]. This design aims to overcome the trade-off between permeability and selectivity inherent to conventional polymeric membranes, thereby improving gas separation performance [197,198]. Fig. 23 schematically illustrates the interaction between fillers and the polymer matrix in a typical MMM structure.

5.2.1. *Functionalized MMM*

Functionalized MMMs combine a polymer matrix with active or modified fillers to improve interfacial compatibility, reduce non-selective voids, and enhance gas transport performance. PSF is a preferred polymer matrix due to its durability, mechanical strength, and easy processability.

Saqib *et al.* (2021) fabricated PSF-based MMM containing 5–20 wt% porphyrin fillers via solution casting. The membranes showed uniform filler dispersion, microporosity, and improved thermal stability due to π-π interactions, Lewis basic sites, and the nitrogen-rich porphyrin structure, resulting in enhanced CO_2 permeability and selectivity for both single and binary gas systems. However, long term stability under dynamic operating conditions remains to be further evaluated [199]. Dey *et al.* (2019) dissolved PSF in chloroform with covalent triazine framework (CTF-1) fillers (0–24 wt%), producing defect-free membranes with uniform CTF-1 dispersion. The CO_2 permeability rose from 7.3 Barrer (pure PSF) to 12.7 Barrer (24 wt% CTF-1), while CO_2/N_2 selectivity increased to 26, deviating from the Maxwell model and suggesting cooperative contributions from both polymer and filler [165]. Several studies incorporated MOFs and ZIFs to improve CO_2 separation. Alsaady *et al.* (2025), demonstrated that at the optimal 15 wt % loading of NH_2-MIL-125(Ti) into PSF/NH_2-MIL-125(Ti)-based membranes exhibited enhanced CO_2/CH_4 separation, achieving a CO_2 permeability of 19.17 Barrer and selectivity of 31.95 far surpassing pristine PSF. They also showed strong resistance to CO_2-induced plasticization up to 14 bar, compared to only 4–6 bar for the unmodified membrane. Structural analyses confirmed uniform filler dispersion at this loading, while higher amounts led to agglomeration and reduced efficiency [147]. Shafiq *et al.* (2021), synthesized ZIF-95/PSF MMMs at varying loadings (8–32 wt%), and at 24 wt% achieving maximum CO_2 permeability by 67.2% [200]. ZIF-8 has also gained attention due to its tunable microporous structure and srong interfacial compatibility with PSF. Neat PSF and MMMs with $\leq$ 1.25 wt% ZIF-8 loading showed excellent potential for natural gas purification [201]. Saikumar *et al.* (2020) synthesized amine-modified SiO_2/ZIF-8 (A@S/ZIF-8) nanofillers and incorporated them into PSF to fabricate MMMs, which exhibited enhanced CO_2/CH_4 and CO_2/N_2 separation performance through improved polymer-filler adhesion [202]. Negi and Suresh (2024), reported that incorporating ZIF-8 nanoparticles into PSF-MMM significantly improved gas separation performance under ideal conditions, with an optimal loading of 1 wt% yielding a increasing CO_2 permeability (56.8%) and CO_2/CH_4 selectivity (41%). However, higher filler loadings caused particle agglomeration and reduced transport efficiency. Under realistic biogas mixtures containing CO_2, CH_4, N_2, O_2, and trace H_2S, membrane performance declined due to competitive sorption and H_2S-induced degradation of ZIF-8, highlighting the importance of evaluating MMMs under practical feed conditions [203]. Mei *et al.* (2020) incorporated nanosized ZIF-8 into PSF membranes, achieving higher H_2 and CO_2 permeance up to 10 wt% loading; subsequent polydopamine (PDA) coating increased H_2/CO_2 selectivity to approach the Robeson upper bound [204]. Sutrisna *et al.* (2020) produced PSF/CA MMMs containing TiO_2 and ZIF-8 particles, ZIF-8 showed better polymer compatibility, leading to uniform dispersion and reduced aggregation compared to TiO_2. As a result, ZIF-8 incorporation enhanced CO_2

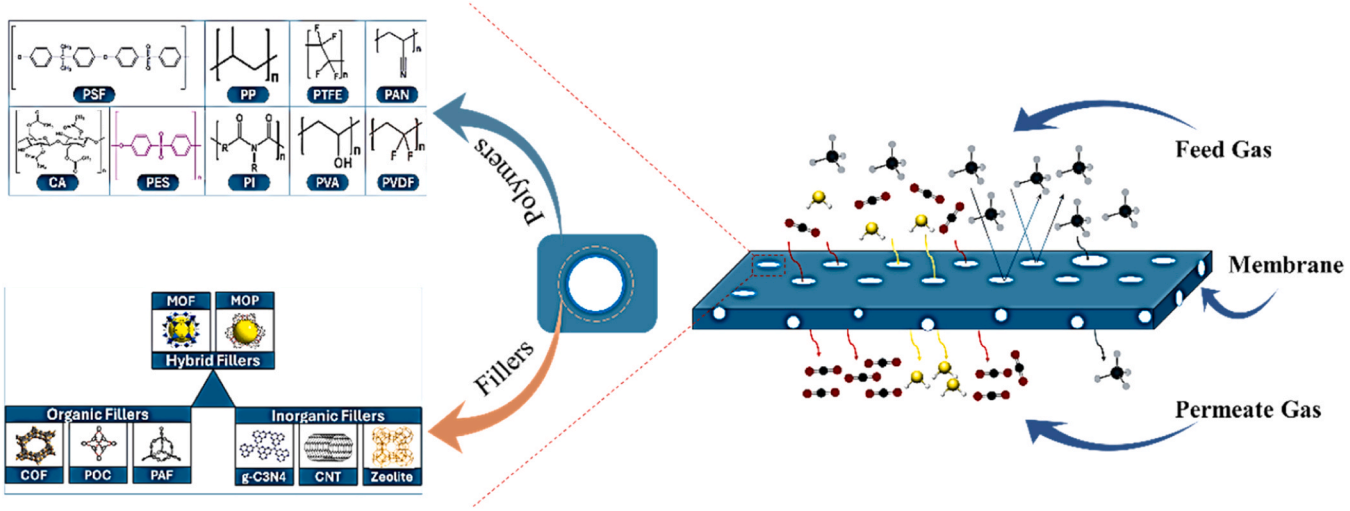

Fig. 23. Schematic illustration of hybrid membrane formation through the incorporation of fillers into a polymer matrix to enhance separation performance.

permeability in both matrices, increasing PSF membrane permeability from 17.1 to 20.3 Barrer at 10 wt% loading [205]. Bio-based and functional nanofillers have also been explored by Ishaq *et al.* (2019) introduced Bio-MOF-1 into PSF for the first time, achieving high separation performance and highlighting its potential in combination with high-permeability polymers [206]. Amusa *et al.* (2021) incorporated amine-functionalized and pretreated lignin-free date pit cellulose (DPC-NH_2) fillers into PSF membranes demonstrating increased porosity and amine functionalization enhanced CO_2 transport and selectivity through additional hydrogen bonding [207]. Raouf *et al.* (2020) incorporated PEG(5–10 wt%) into PSF and observed an increased CO_2 permeability (from 15.9 Barrer for neat PSF to 28.2 Barrer for PSF/PEG at 10 wt%). CO_2/CH_4 selectivity also improved slightly at 2 bar and 35 °C (from 12.23 for neat PSF to 12.81 for PSF/PEG at 10 wt%), while additional graphene hydroxyl (G–OH) nanoparticles further enhanced CO_2/CH_4 separation efficiency at 5 wt% loading [208]. Natarajan *et al.* (2021) incorporated Fe-pillared Cloisite 15 A clay (P–C15A) into PSF, yielding MMMs with enhanced CO_2 and O_2 permeability and selectivity near the Robeson upper bound [151]. There are other studies discussing functionalized PSF-based membranes for olefin and paraffin separation. Gholamipour *et al.* (2019) reported that silica nanoparticle addition improved both permeability and selectivity due to altered solubility and diffusion coefficients, with olefins showing higher diffusion rates than paraffins [209]. Najafi *et al.* (2020) reported that the incorporation of reduced graphene oxide (rGO) into polysulfone MMMs significantly enhanced olefin permeability at 2 bar and 30°C. At 1 wt% rGO loading, ethylene and propylene permeabilities increased by 143% and 193%, respectively. Although propylene/propane selectivity improved by 18%, ethylene/ethane selectivity decreased by 23%, indicating that rGO markedly enhances olefin productivity while exerting gas-pair-dependent effects on separation selectivity [210].

Overall, functionalized MMMs have shown substantial improvements in CO_2 permeability and CO_2/CH_4 selectivity through tailored filler functionalization and strong polymer-filler interfacial bonding. Nevertheless, ensuring uniform filler dispersion, minimizing microvoids, and evaluating long term stability remain critical for practical deployment.

5.2.2. *Ionic liquid based MMMs*

Incorporating ILs or IL-functionalized components into polymer matrices offers an effective route for enhancing CO_2 capture due to their intrinsic CO_2 affinity [211], tunable polarity, and ability to plasticize the polymer structure. These features typically increase CO_2 solubility and diffusivity while maintaining adequate membrane integrity [212,213]. The operation mechanism of ionic liquid MMMs (ILMMMs) is illustrated in Fig. 24.

Farrokhara and Dorosti (2020) prepared PSF/[EMIM][BF_4] membranes with 10–40 wt% ionic liquid, achieving up to 98.3% higher CO_2 permeability due to increased free volume and strong CO_2 affinity. Optimal performance occurred at 30 wt% IL, delivering ~602 Barrer permeability and ~25.9 selectivity, while excessive IL loading reduced separation efficiency [134]. Khraisheh *et al.* (2020) examined the incorporation of Diisopropylamine 1-alkyl-3-methylimidazolium ([DIP-C_4mim][NTf_2]) ILs into PSF matrices. Broadband dielectric spectroscopy (BDS), DSC, and TGA analyses confirmed the membranes' thermal stability, with Tg values decreasing gradually due to IL-induced plasticization effects [214]. Ortiz-Albo *et al.* (2022) [215], proved that including cyano-based ILs with dicyanamide ([DCA]−) and tricyanomethanide ([TCM]−) anions with ZIF-8 PSF MMMs increased CO_2 permeability, selective behavior, and mechanical strength compared to conventional MMMs, with a substantial reliance on intrinsic IL CO_2 selectivity. Liu *et al.* (2022) synthesized a Schiff base network/polysulfone MMM (SNW-3/PSF) that demonstrated intensified CO_2 capture capacity and over a 400% increase in CO_2 permeability relative to pristine PSF. Positron annihilation spectroscopy revealed higher fractional free volume and dynamic free volume changes during CO_2 exposure and desorption, confirming the strong influence of IL-like plasticization behavior on gas transport [216]. Hybrid IL-based systems also exhibit remarkable separation performance. A layered double hydroxide/-fluoroalkylsilane–polydimethylsiloxane hybrid ((LDH/FAS)$_{25}$-PDMS) membrane achieved an exceptionally high CO_2 permeability of 7748 GPU, with selectivity factors of 43, 86, and 62 for CO_2/H_2, CO_2/N_2, and CO_2/CH_4 mixtures, respectively [217].

In addition to filler selection, interfacial engineering plays a decisive role in MMM performance. Conventional systems often rely on physical blending, where weak filler-polymer interactions may result in interfacial voids and non-selective defects. In contrast, amine-functionalized SiO_2/ZIF-8 systems introduce surface –NH_2 groups that promote hydrogen bonding and acid-base interactions with the sulfone groups of PSF, thereby enhancing compatibility and suppressing interfacial defects. Similarly, GO/PSF systems benefit from oxygen-containing functional groups that facilitate hydrogen bonding and π–π interactions, improving dispersion and interfacial adhesion. Unlike conventional designs that rely primarily on filler porosity, these systems integrate chemical interface modulation with enhanced gas affinity, particularly toward acidic gases such as CO_2 and H_2S. In MMMs, separation performance depends on both filler properties and filler-polymer interfacial compatibility. Poor interfaces can cause voids, rigidification, and agglomeration, reducing gas transport efficiency. Therefore, recent studies focus on interface engineering strategies such as surface functionalization, coupling agents, polymer blending, and two dimensional

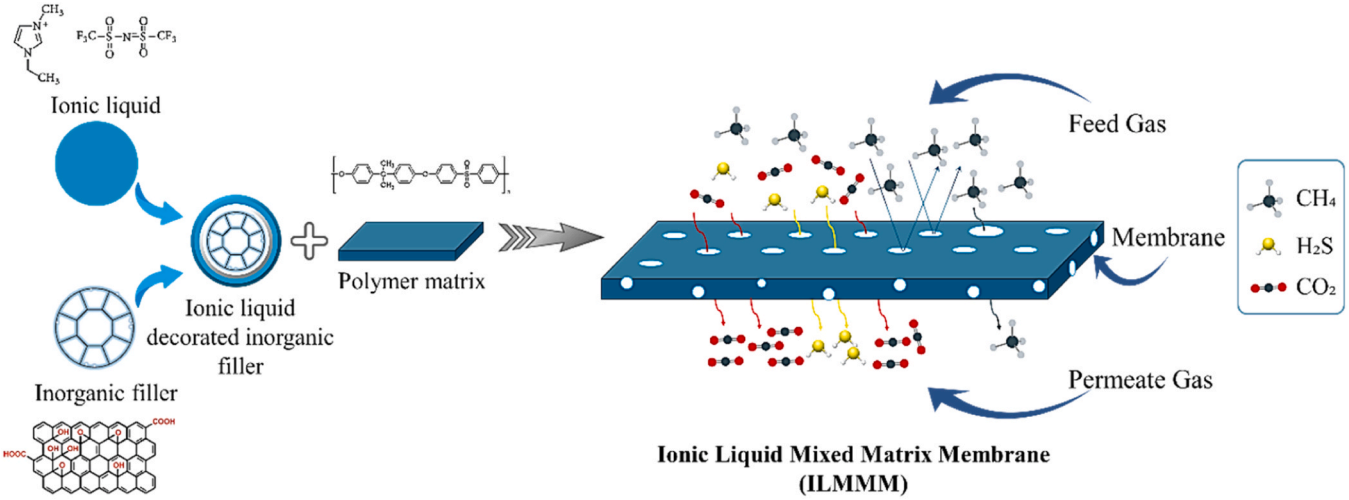

Fig. 24. Three-component ILMMM that incorporates inorganic filler, ILs, and polymer matrix for enhanced gas transport performance and structural compatibility.

(2D) nanosheet incorporation. Table 6 compares interfacial design strategies in conventional systems and highlights key features of amine-functionalized SiO_2/ZIF-8 and GO/PSF membranes.

As summarized in Table 6, conventional MMMs primarily rely on physical blending, where weak interfacial interactions often result in non-selective voids and limited control over gas selectivity. In contrast, advanced interface engineering strategies aim to strengthen filler-polymer compatibility through chemical bonding, hydrogen bonding, or acid-base interactions. The amine-functionalized SiO_2/ZIF-8 systems distinguish themselves by simultaneously improving interfacial adhesion and enhancing acid gas affinity via $–NH_2$ functional groups, which interact favorably with CO_2 and H_2S molecules. Similarly, GO/PSF systems leverage two dimensional confinement effects and polar functional groups to suppress defects while increasing selective transport pathways. The essential difference between conventional interface design and the reported systems lies in the deliberate integration of chemical affinity enhancement with structural defect suppression, rather than relying solely on filler porosity or loading. This dual-function interface modulation provides a more effective pathway for achieving improved CO_2/CH_4 and H_2S/CH_4 separation performance.

Following the discussion on interface engineering, it is essential to evaluate how these strategies affect actual gas separation performance. Therefore, Table 7 presents the reported permeability and selectivity of PSF-based MMMs, illustrating the impact of different fillers and interfacial modifications on gas transport behavior.

By analyzing the data presented in Table 7, the gas separation efficiency of PSF-based MMM is presented in Fig. 25.

The Robeson plot illustrates the trade-off between CO_2 permeability and CO_2/CH_4 selectivity for various PSF-based MMMs. Most membranes exhibit performance within the conventional upper bound region, while selected filler-incorporated systems approach the 2008 Robeson limit, indicating enhanced separation efficiency. The distribution of data points confirms that filler type and loading significantly influence the permeability-selectivity balance. The literature shows that PSF-based membranes are widely studied and well established for CO_2/CH_4 separation because of their good mechanical stability, processability, and reliable CO_2 selectivity. These observations are consistent with previous studies on CO_2/CH_4 separation, where PSF-based and composite membranes typically exhibit a trade-off between permeability and selectivity under mixed-gas conditions [51,243,244]. For instance, composite membranes incorporating MOF-based fillers have demonstrated enhanced CO_2 permeability but often at the expense of selectivity at higher CO_2 concentrations [51,244]. In contrast, studies focusing on H_2S-containing systems highlight additional challenges related to chemical stability, competitive sorption, and plasticization effects, which are less pronounced in CO_2-only systems [49]. These findings emphasize the importance of evaluating membrane performance under realistic sour gas conditions. However, studies addressing the removal of CO_2 and H_2S from CH_4 using PSF-based membranes are very limited. Most PSF research focuses exclusively on CO_2/CH_4 performance, while H_2S separation is either investigated separately, addressed using other polymers, or handled through hybrid systems such as membrane contactors combined with chemical absorbents. This scarcity is largely attributed to the aggressive and reactive nature of H_2S, which introduces challenges related to polymer stability, plasticization, and long term membrane durability. Consequently, despite extensive CO_2/CH_4 data, PSF membranes specifically engineered for concurrent CO_2 and H_2S removal from natural gas remain underexplored in the literature.

5.3. Benchmarking PSF-based membranes for H_2S/CH_4 and CO_2/CH_4 separation against other membrane materials

Although PSF membranes have been extensively investigated for CO_2/CH_4 separation in natural gas sweetening, their application toward H_2S/CH_4 separation either as a single acid gas system or under mixed-gas conditions with CO_2 remains limited. Most available PSF-based studies focus primarily on CO_2 permeability and CO_2/CH_4 selectivity, while direct permeability and selectivity data for H_2S are rarely reported. This limitation is primarily due to:

- The corrosive and toxic nature of H_2S, which complicates experimental evaluation.
- Plasticization and swelling effects in glassy polymers at elevated acid gas pressures.
- The industrial preference for facilitated transport or chemical absorption systems for selective H_2S removal.

Table 8 compares representative PSF studies with CA, polyimides (PI), polymers of intrinsic microporosity (PIMs), and supported ionic liquid membranes (SILMs).

The comparative results show that PSF membranes deliver extremely high H_2S permeability, particularly the DMAC-cast variant, but suffer from very low H_2S/CH_4 selectivity, limiting their practical use. In contrast, CA and PI membranes provide more balanced performance, with moderate permeability and selectivity values suitable for industrial applications. PIM-1 and rubbery polymers such as PEG and PEO demonstrate higher selectivity, especially for H_2S, while SILMs stand out with exceptional H_2S/CH_4 selectivity, highlighting their strong affinity for acidic gases. Overall, the Table emphasizes that PSF offers unmatched throughput but requires hybrid or composite designs to overcome its selectivity limitations.

5.4. Role of computational chemistry in membrane technology

Computational chemistry has progressively transformed membrane science by providing atomistic and molecular-level understanding of transport, sorption, and structural phenomena in polymeric and MMMs. The field began in the 1960s-70s with the solution-diffusion paradigm, rationalizing transport through dense polymers and reverse osmosis membranes [248,249]. In the 1980s, molecular mechanics and MD were applied to polymer glasses, elucidating chain mobility, free volume distributions, and their effects on gas diffusion [250,251]. The 1990s saw wider use of ab initio and density functional theory (DFT) methods to link polymer chemistry to transport parameters, particularly in glassy

Table 6
Comparison of interface design strategies in PSF-based MMM.

System	Interface Strategy	Nature of Filler-PSF Interaction	Interfacial Defect Control	Gas Affinity Enhancement	Key Distinction
Conventional inorganic filler/PSF [218]	Physical blending	Weak van der Waals interaction	Limited control; possible void formation	Minimal	Primarily mechanical reinforcement
MOF/PSF (non-functionalized) [219]	Direct incorporation	Partial compatibility; possible rigid interface	Moderate; may form non-selective gaps	Intrinsic MOF porosity	Separation driven mainly by filler porosity
Amine-functionalized SiO_2/ZIF-8/PSF [220]	Surface amination ($–NH_2$ groups)	Hydrogen bonding & acid-base interaction with PSF sulfone groups	Reduced interfacial voids; improved adhesion	Enhanced CO_2/H_2S sorption via acid-base interaction	Chemical interface engineering + dual functionality
GO/PSF [139]	Oxygenated functional groups (–OH, –COOH)	π–π interaction + hydrogen bonding	Improved dispersion; suppressed agglomeration	Increased CO_2 affinity via polar interactions	2D confinement + interfacial polarity tuning

Table 7
Permeabilities and selectivity of PSF-based MMM for gas separation.

Membrane Type	Composition	Additive / Feature	Permeability (Barrer)		Selectivity		Reference
			P_{CO_2}	P_{H_2S}	P_{CO_2}/P_{CH_4}	P_{H_2S}/P_{CH_4}	
MMMs/ Functionalized MMM	PSF/Porphyrin	Porphyrin (5–20 wt%)	129.8	—	93.38	—	[202]
	PSF/CTF-1	Covalent Triazine Framework (8–24 wt%)	12.7	—	26	—	[205]
	PSF/MCM-41 (20 wt%)	MCM-41 (20 wt%)	11.4	—	18.90	—	[221]
	PSF/PPS(10 wt%)	PPs10wt%	11.35	—	9.11	—	[222]
	PSF/SNW-3	Schiff Base Network (30 wt%)	28.63	—	21.37	—	[216]
	PSF/PI (50/50)/ ZSM-5(10 wt%)	ZSM-5 (10 wt%)	1.513	—	4.4253	—	[189]
	PSF/ Aminopropy ltrimethoxysilane/ acrylate-zeolite (15 wt%)	acrylate-zeolite (15 wt%)	18.36	—	10.28	—	[208]
	PSF/PES/GO((10 wt%)	GO (10 wt%)	17.54	—	14.31	—	[208]
	PSF/10 wt% PEG/G-OH (5 wt%)	Graphene Hydroxyl (5 wt%)	36.50	—	22.39	—	[223]
	PVA/PES-amine/GO (5 wt%)	GO (5 wt%)	18.65	—	15.47	—	[223,224]
	PSF/SO_3H-UiO-66	SO_3H-UiO-66	20	—	27	—	[225]
	PSF/UiO-66	UiO-66	14	—	27	—	[225]
	PSF/ZIF-95	Zeolitic Imidazolate Framework (8–32 wt%)	11.11	—	28.49	—	[200]
	PSF/ZIF-8	ZIF-8 (0.5–10 wt%)	29.22–47.75 GPU	—	23.16–27.72	—	[140,201, 202,204]
	PSF/ZIF-8 (0.5 wt%)	ZIF-8 (0.5 wt%)	1.374	—	1.192	—	[226]
	PSF-30/ZIF-8	ZIF-8 (10 wt%)	36.60	—	27.72	—	[204]
	PSF/A@S/ZIF-8 (0.5 wt%)	Amine-modified SiO_2/ZIF-8 (0.5 wt%)	4.25	—	22.25	—	[126]
	PSF/ZIF-67 (1 wt%)	ZIF-67 (1 wt%)	37 GPU	—	18.5	—	[227]
	PSF/ZIF-67 (2 wt%)	ZIF-67 (2 wt%)	64 GPU	—	11	—	[227]
	PSF/ZIF-67/GO	ZIF-67 grown on PSF/GO HFMs (0.25 wt%)	39.25 GPU	—	44.94	—	[228]
	PSF/CuBTC@GO (10 wt%)	CuBTC@GO (10 wt%)	8.70	—	26.94	—	[229]
	PSF/Cu-BTC (1 wt%)	Cu-BTC (1 wt%)	32 GPU	—	19	—	[230]
	PSF/Bio-MOF-1	Bio-MOF-1 (30 wt%)	16.57	—	42.6	—	[206]
	PSF/NH_2KIT-6	Amine-modified KIT-6 (0–2 wt%)	5.4	—	32.4	—	[146]
	PSF/KIT-6 silica	KIT-6 (0–2 wt%)	5.4	—	47.95	—	[138]
	PSF/Zeolite NH_2-RHO	Zeolite NH_2-RHO (1–3 wt%)	5.4	—	37	—	[148]
	PSF/ZTC	Zeolite Templated Carbon (0.4–0.7 wt%)	58.5 GPU	—	9.99	—	[231]
	PSF/G–OH/PEG	Graphene Hydroxyl + PEG (5–10 wt%)	30.6–36.5	—	19.78–22.39	—	[208]
	PSF/alumina	γ-Alumina (30 wt%)	15.6 ± 0.4	—	33.3	—	[178]
	PSF/GO	Graphene Oxide (0.25–8 wt%)	2.98–74.47 GPU	—	16.67–29.90	—	[139,232]
	PSF/GO(5 wt%)	GO (5 wt%)	19.43	—	16.38	—	[208]
	PSF/GO	GO	86.80 GPU	—	25.98	—	[233]
	PSF/Silica-ZIF-8	Silica-ZIF-8 (32 wt%)	24.4	—	31	—	[234]
	PSF/0.4 wt%zeolite-templatedcarbon	zeolite-templatedcarbon (0.4 wt %)	6.8	—	9.9	—	[235]
	PES/silica/MOF (15 wt%)	Silica/MOF (15 wt%)	30.92	—	48.31	—	[236]
	PSF/PEG-g-CNT	PEG-grafted CNTs (5 wt%) at 1.5 bar	7.24	—	13.4	—	[159]
	PSF/PEG-g-CNT	PEG-grafted CNTs (5 wt%) 2.5 bar	9.27	—	10.2	—	[159]
	PSF-Kapton/8 wt% oxidizingacid-treated MWCNTs	8 wt% oxidizingacid-treated MWCNTs	6.2	—	17.7	—	[237]
	PSF/5 wt%alkyl amine-functionalized SWCNTs	5 wt%alkyl amine-functionalized SWCNTs	5.1	—	18.9	—	[238]
	PSF/0.04 wt% carboxylicacid-functionalized MWCNTs	0.04 wt%carboxylicacid-functionalized MWCNTs	21.02 GPU	—	18.45	—	[239]
	PSF/CNF (1 wt%)	CNF (1 wt%)	4.8	—	12.1	—	[240]
	PSF/0.5 wt%amine-functionalized CNF	amine-functionalized CNF (0.5 wt %)	3.5	—	7.7	—	[241]
	PSF/LDH/FAS-PDMS	LDH–FAS hybrid PDMS (25 wt%)	7748 GPU	—	62	—	[217]
	PSF/2%MIL-53(Al)	2%MIL-53(Al)	37GPU	—	12.5	—	[220]
	PSF/2%IL@MIL-53(Al)	2%IL@MIL-53(Al)	34GPU	—	28	—	[220]
	PSF/PEG10000/Silica	PEG10000 + Silica (20 wt%)	13.36	—	36.63	—	[242]
	PSF/SWCNT (ODA-functionalized)	Single-walled CNTs (ODA)	5.19	—	18.41	—	[238]
	PSF/Porous silica	Silica nanoparticles	—	—	↑ selectivity	—	[209]
	PSF/rGO	Reduced graphene oxide	—	—	↑ olefin selectivity	—	[210]
	PSF/P-C15A	Fe-pillared Cloisite 15A (1 wt%)	19.47 GPU	—	—	—	[151]
	0.5 wt%MX@Pebax/PSF	0.5 wt%MX	23GPU	—	30.05	—	[190]
	PSF/Bio-based filler	Amine-functionalized delignified biomass (0–5 wt%)	—	—	↑ performance	—	[210]
Ionic Liquid Based MMMs (ILMMMs)	PSF/[EMIM][BF_4]	1-ethyl-3-methylimidazolium tetrafluoroborate (10–40 wt%)	+ 30.4–98.3% vs. PSF	—	—	—	[134]
	PSF/ZIF 67/ [APTMS][Ac] −30	ZIF 67/ [APTMS][Ac] −30	22.34 ± 1.12	—	72.06 ± 1.08	—	[186]
	PSF/[Tf2N] @ ZIF-67 (1.5 wt%)	[Tf2N] @ ZIF-67 (1.5 wt%)	46.4 GPU	—	25.9	—	[227]

(continued on next page)

Table 7 (*continued*)

Membrane Type	Composition	Additive / Feature	Permeability (Barrer)		Selectivity		Reference
			P_{CO_2}	P_{H_2S}	P_{CO_2}/P_{CH_4}	P_{H_2S}/P_{CH_4}	
	PSF/[Tf2N] @ ZIF-67 (2 wt%)	[Tf2N] @ ZIF-67 (2 wt%)	60.5 GPU	—	26.1	—	[227]
	PSF/Cu-BTC (1 wt%)/ [Bmim][Tf2N] (5 wt%)	Cu-BTC (1 wt%)/ [Bmim][Tf2N] (5 wt%)	32 GPU	—	26	—	[230]
	PSF/[Dmim][Cl] (5 wt%)	[Dmim][Cl] (5 wt%)	17 GPU	—	16.5	—	[230]

"—" data is not available (limited literature)

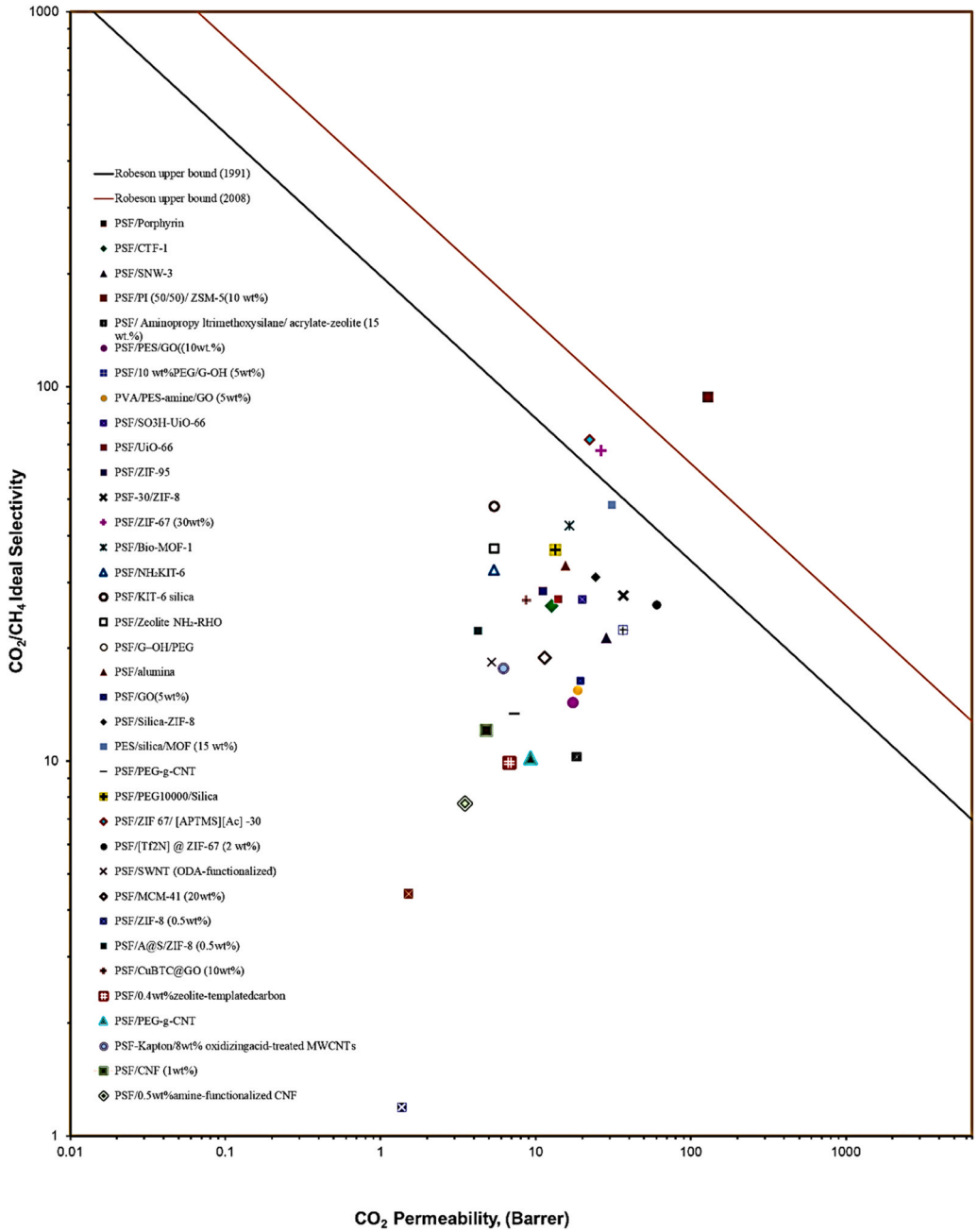

Fig. 25. Separation performance of hybrid/ MMM with Robeson's upper limit.

polymers such as PSF and PI [252]. From the 2000s onward, computational approaches expanded to mechanistic investigations of MMMs, including simulations of nanoporous fillers (e.g., zeolites, MOFs) and kinetic/MC analyses of two-phase transport [253,254]. High-performance computing in the 2010s enabled large-scale MD simulations, adsorption modeling, and the emergence of early machine learning models to predict permeability and complete material databases [252,255]. In the 2020 s, AI-driven screening, interpretable machine learning, and advanced quantum algorithms accelerate discovery, while interfacial structures in MMMs are engineered and quantified at the molecular-level [168,256]. Fig. 26 illustrates a graphical timeline of the evolution of computational chemistry in membrane technology,

Table 8
Gas Permeation and Selectivity Benchmarks for CO_2 and H_2S Separation from CH_4.

Polymer / Membrane Type	Permeability (Barrer)		Selectivity		Reference
	P_{H_2S}	P_{CO_2}	P_{H_2S}/P_{CH_4}	P_{CO_2}/P_{CH_4}	
PSF (DMAC solvent, M3 membrane)	~119,000	–	1.56	–	[92]
PSF (THF solvent)	–	62.3	–	48	[86]
CA	25	~10	25–40	30–40	[245]
Modified CA (VTMS-grafted)	~165	~140	~27	~20	[245]
Polyimide (6FDA-based)	~30	10–20	10–20	60–80	[245]
Polyimide (6FDA-durene copolymer)	~10	~10	~23	~27	[245]
PIM-1 (amidoxime functionalized)	4300	800	74	13	[245]
Crosslinked PEG (rubbery polymer)	–	–	65–116	15–58	[246]
PEO-based rubbery polymer	200–400	150–300	10–15	15–25	[245]
Supported Ionic Liquid Membrane (PVDF + $BMImBF_4$)	160–1100	30–180	130–260	25–45	[247]

highlighting milestones from early solution-diffusion models to modern AI-driven membrane design.

5.4.1. *Molecular simulation*

Molecular simulation provides a window into atomic and molecular-level phenomena, complementing experimental studies. MD and MC simulations can track polymer chain dynamics, cavity formation, and gas-polymer interactions, offering mechanistic insights that explain macroscopic transport behavior [257,258–260]. These techniques allow researchers to predict gas permeability, selectivity, swelling, and plasticization based on the polymer's molecular architecture, filler properties, and functional groups [261]. Fig. 27 summarizes the key benefits of MD simulation, including its ability to capture atomic-level dynamics, free volume distributions, and gas-polymer interactions, which are critical for understanding and predicting membrane performance.

For example, simulations of PSF and its derivatives revealed that para isomers have larger cavity sizes than meta isomers, leading to enhanced gas transport [262]. By using the COMPASS force field and equilibrating multiple initial polymer configurations, these studies linked atomic-level free volume distribution to experimentally measured permeabilities. Similarly, MD studies of PSU, PESU, and Ultem demonstrated how polymer chain mobility and hydrogen bonding sites influence water sorption and gas-induced swelling [263,264]. These findings illustrate that atomistic packing and dynamic behavior, rather than just bulk composition, govern transport properties.

Grand Canonical Monte Carlo (GCMC) simulations further complemented MD by capturing gas adsorption in confined polymer and nanocomposite environments, reproducing sorption isotherms and elastic responses at the molecular scale [265]. Studies incorporating single-walled carbon nanotubes (SWNTs) or silica nanoparticles into PSF matrices showed that filler-induced modifications of local free volume, interfacial interactions, and polymer chain orientation significantly affect gas diffusivity and selectivity [265–268]. These atomistic insights explain why certain filler types, loadings, or functionalizations improve

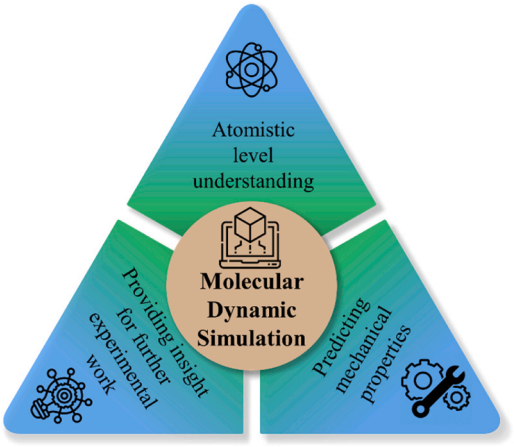

Fig. 27. Key advantages of MD simulation in membrane research.

CO_2 permeability or CO_2/CH_4 selectivity.

MD simulations combined with design of experiment (DOE) approaches further elucidated how temperature, pressure, and filler content modulate polymer-filler-gas interactions [150]. In PSF/PEG/SiO_2 MMMs, Fig. 28 illustrates the molecular representation of PEG and PSF monomers, polymer chains, silica nanoparticles, and the final membrane configuration. The simulations captured how filler distribution and polymer conformations create diffusion pathways and influence gas transport.

In PSF/PDMS MMMs with ZnO nanoparticles, MD and GCMC studies revealed that enhanced CO_2/N_2 and CO_2/CH_4 selectivities arose from optimized free volume, polymer flexibility, and preferential gas-filler interactions [269]. Recent studies have developed computational frameworks capable of simulating non-ideal effects, such as CO_2

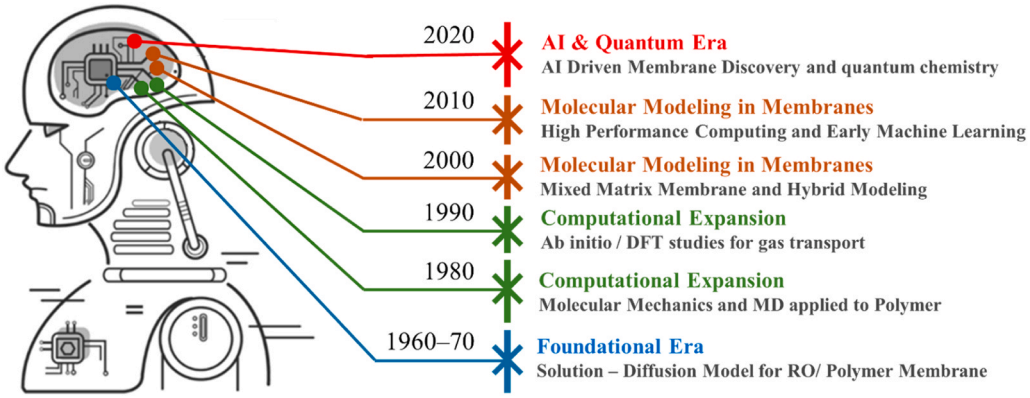

Fig. 26. The evaluation of computational chemistry in membrane technology.

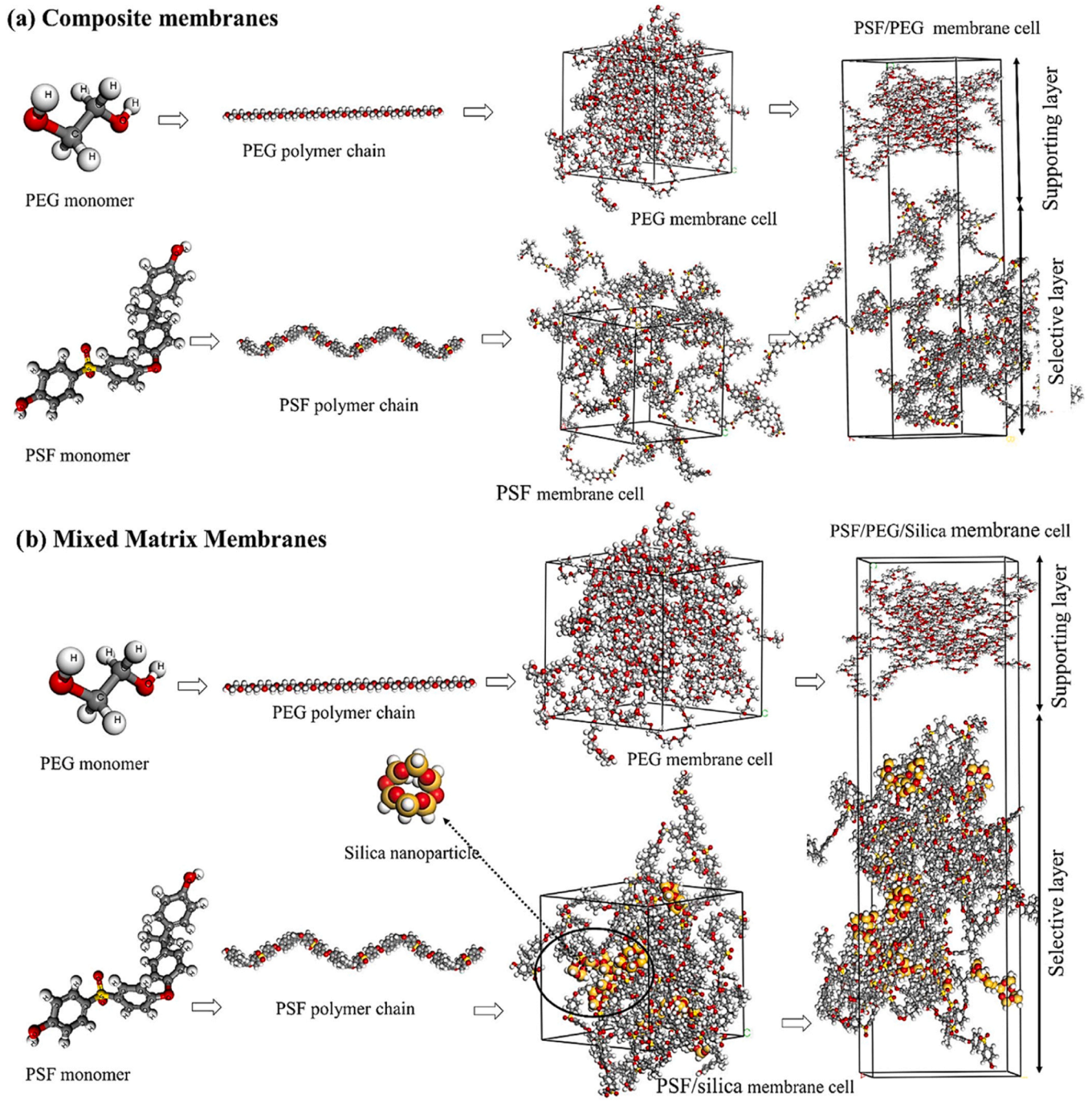

Fig. 28. Representation of PEG and PSF monomers and polymer chains and the added silica nanoparticles as well as the final configuration of constructed membranes (a) composite membranes and (b) MMMs. The selective and supporting layers are shown in the Figure [150].Copyright 2021, Elsevier.

plasticization and confinement in ultrathin membranes, enabling mechanistic predictions of gas separation performance under realistic conditions [270–274].

As membrane simulation studies are scarce, particularly focused on PSF-based membranes so the summary of the PSF and other membranes related simulation-based studies on the CO_2/CH_4 and H_2S/CH_4 separation performance of filler/polymer/MMMs is discussed in Table 8. The Table demonstrates that incorporating inorganic and nanostructured fillers into polymer matrices significantly enhances gas transport properties, with substantial variations in permeability and selectivity depending on filler type, loading percentage, and operating pressure. Notably, high-permeability systems such as pristine single-walled carbon nanotube (SWCNT) composites exhibit dramatic increases in CO_2 transport. Whereas hybrid structures like ZIF-7 NCPMs and ZnO-reinforced PSF achieve more balanced improvements in both permeability and selectivity, highlighting the importance of optimizing filler-polymer interfacial interactions for membrane performance.

Overall, molecular simulations provide atomistic-level mechanistic understanding, how polymer chain conformation, cavity connectivity, functional groups, and filler interfaces govern transport, swelling, and selectivity. These insights allow the rational design of next-generation PSF membranes and MMMs, guiding choices of polymer chemistry, filler type, functionalization, and processing conditions for optimal separation performance.

Table 9 summarizes reported simulation studies on the separation performance of CO_2 and H_2S using various polymeric and MMMs under

different operating conditions. The results show that the incorporation of inorganic fillers such as silica, amine-functionalized silica, ZnO, α-cristobalite, FAU zeolite, ZIF-7, and carbon nanotubes into polymer matrices (e.g., PSF, PEBA, PDMS blends) significantly influences gas transport properties. In general, CO_2 permeability varies widely depending on filler type and loading, ranging from very low values (e.g., Extem XH1015) to exceptionally high values in CNT-based systems. Among the reported systems, ZIF-7/NCPMs are notable for providing simultaneous CO_2 and H_2S permeability data, demonstrating balanced selectivity for both gas pairs. However, most studies primarily focus on CO_2 permeability and CO_2/CH_4 selectivity, while H_2S permeability and H_2S/CH_4 selectivity data remain scarce. This highlights that, even in simulation studies, systematic evaluation of H_2S separation performance is still limited compared to CO_2, emphasizing the need for more comprehensive investigations on simultaneous acid gas separation. These findings align with recent MD simulation studies, which reveal that gas transport behavior in mixed $CO_2/CH_4/H_2S$ systems is strongly influenced by pressure, temperature, and polymer–gas interactions. For example, MD and Monte Carlo simulations have shown that gas diffusion and solubility coefficients vary significantly with operating conditions, directly impacting separation performance [279].

6. Challenges in PSF-based membranes

6.1. Stability, purity and scalability issues

The long term stability and purity of PSF-based MMMs remain critical for demanding gas separation applications, including CO_2 capture and ternary $H_2S/CO_2/CH_4$ separations. PSF membranes can undergo physical or chemical degradation over time, which is intensified by poorly dispersed or incompatible fillers, potentially reducing separation efficiency [47,280]. Maintaining high gas purity is particularly challenging in ultrathin MMMs, where minor interfacial defects or polymer-filler mismatches create non-selective pathways. Structural integrity under prolonged exposure to high pressures, aggressive gases, and temperature fluctuations is essential for industrial viability [281, 282], with the choice of chemically and thermally stable PSF-filler combinations being crucial for multicomponent gas streams [245, 283]. Scaling PSF-based MMMs from laboratory to industrial applications introduces technical and economic challenges. Membrane fouling, limited lifespan, solvent effects on filler dispersion, and the delicate balance between permeability and selectivity complicate large-scale fabrication [63,86,268,280,284,285]. Achieving uniform performance across extensive membrane areas requires precise control of fabrication parameters, filler loading, and interfacial compatibility, highlighting the importance of optimizing both membrane stability and scalability for reliable industrial deployment [9,86].

6.2. Selectivity, permeability, and material development

Enhancing selectivity, permeability, and long term stability in PSF-based MMMs remains a central challenge in membrane science. PSF, while mechanically robust and thermally stable, exhibits moderate intrinsic gas separation performance. To overcome these limitations, recent efforts have focused on embedding functional fillers into the PSF matrix to improve separation efficiency, particularly for CO_2 capture applications [47,196]. However, the development of durable PSF-based MMMs that maintain high purity levels under harsh operating conditions is complex. Filler incorporation must be carefully engineered to avoid interfacial defects and ensure compatibility with PSF's chemical structure. Teixeira Cardoso *et al.* (2022) emphasized the importance of designing membranes that retain performance under extreme pressures, temperatures, and chemically aggressive environments [9]. Recent breakthroughs include the use of nanocomposites, tailored polymer blends, and MOFs that synergize with PSF to enhance gas transport properties. These materials offer improved selectivity and permeability while preserving structural integrity during prolonged operation [164, 286], [197]. Nonetheless, achieving consistent performance across varying gas compositions and industrial conditions requires further refinement in material design and membrane architecture. The incorporation of fillers into PSF-based MMM has attracted considerable interest for enhancing CO_2 and CH_4 separation performance; however, the fabrication of defect-free membranes remains a major challenge. The hydrophobic nature and rigid backbone of PSF often lead to poor interfacial adhesion with polar or structurally incompatible fillers, resulting in interfacial voids that act as non-selective transport pathways and degrade separation efficiency [148]. In addition, inadequate filler dispersion and nanoparticle agglomeration can disrupt polymer morphology, reduce effective surface area, and create localized stress regions, further limiting membrane performance. Despite the application of surface functionalization and solvent optimization strategies, achieving uniform compatibility between PSF and diverse filler chemistries remains difficult [139].

6.3. Plasticization, conditioning, and aging

PSF-based MMMs used in CO_2 separation are prone to several degradation mechanisms, including penetrant-induced plasticization, physical aging, and conditioning-related instability. These phenomena significantly affect membrane performance and long term operational reliability, particularly in natural gas separation processes [63,287]. Plasticization occurs when CO_2, which has high solubility in PSF, interacts with the polymer matrix and increases chain mobility. This leads to elevated permeability but reduced selectivity, especially under high-pressure conditions typical of CO_2/CH_4 and H_2S/CH_4 separations [245,288]. The presence of fillers in MMMs can either mitigate or exacerbate this effect depending on their compatibility and interaction

Table 9
Simulation studies for CO_2 and H_2S separation performance of fillers/ polymer/ MMMs.

Membrane	Filler Loading %	Operating Conditions T(C), P(bar)	Permeability (Barrer)		Selectivity		Reference
			P_{CO_2}	P_{H_2S}	P_{CO_2}/P_{CH_4}	P_{H_2S}/P_{CH_4}	
PEBA-1657/Faujasite (FAU)	20	25, 1	89.2	——	20.5	——	[275]
Silica/PSF	20	35, 1	22.57	——	18.2	——	[266]
Pristine single-walled carbon nanotubes (p- SWCNT)	0.5–3	25, 2	7838	——	8.12	——	[276]
ZIF-7/nanocomposite polymeric membranes (NCPMs)	22	25, 3.75	128.3	54.78	21.86	9.33	[277]
Silica/PSF	25	35, 1	25.35	——	11.7	——	[274]
Amine-functionalized silica/PSF	20	35, 1	62	——	10.9	——	[267]
Extem XH1015	2	35, 1	3.28	——	25.2	——	[278]
SWNTs/PSF	10	35, 0.01–18	5.19	——	18.41	——	[265]
PSF-25 wt% α-Cristobalite	25	55, 1	39.98	——	16.65	——	[268]
PSF-PEG- silica	20	25, 10	14.76	——	25.44	——	[150]
80%PSf + 20%PDMS/6 wt%ZnO	6	25, 16	78.02	——	27.3	——	[269]
Xeon/PSF~100	——	35, 2	1.839	——	22.937	——	[271]

with the PSF matrix. Physical aging is another concern, particularly in glassy polymers like PSF. Over time, the polymer structure undergoes densification, resulting in a reduction of free volume and a corresponding decline in gas permeability. This aging process drives the membrane toward a more thermodynamically stable state, which compromises its separation efficiency [245,289]. Swelling under high CO_2 pressures further contributes to plasticization. The polymer matrix may expand, altering the filler-polymer interface and introducing non-selective pathways. This effect is particularly pronounced in MMMs where filler dispersion is uneven or interfacial adhesion is weak, leading to performance deterioration over time [290,291].

6.4. Integration of PSF-based MMM with conventional processes and technological advancement

Integrating PSF-based MMMs into conventional gas separation systems, such as cryogenic distillation, adsorption, and absorption units, presents several engineering and operational challenges. These systems require membrane modules that are compatible with existing infrastructure while maintaining high-performance under variable industrial conditions [292]. PSF is a favorable matrix due to its mechanical strength and thermal stability, making it suitable for hollow fiber configurations. However, the incorporation of fillers introduces additional complexity. Issues such as interfacial defects, inconsistent permeability, and mechanical heterogeneity can hinder seamless integration. Advancements in spinning techniques, module design, and filler alignment are necessary to ensure that PSF-based MMMs deliver reliable selectivity and permeability in demanding environments [31,293,294]. To enable large-scale deployment, PSF-based MMMs must also meet criteria related to energy efficiency, operational cost, and long term durability. These requirements call for coordinated efforts in membrane formulation, process design, and hybrid system development. Simulation-guided optimization and modular retrofitting strategies are increasingly being explored to bridge the gap between laboratory performance and industrial implementation.

6.5. Environmental impacts/ issues

The generation and disposal of PSF membranes have repercussions to the environment because these are non-degradable materials. Further, the manufacturing process employs organic solvents as well as other chemicals which are also dangerous to the environment [295,296]. Further, the study helps to improve real CO_2/CH_4 separation in the future design and concept of functionalized MMMs using molecular simulation and empirical modeling strategies [267]. However, the aim of precisely forecasting emergent events at both atomistic and macroscopic sizes remains unfulfilled [260].

The multidisciplinary collaborations of materials science, engineering, process and environment is becoming more pronounced in membrane research [297]. The prospects for membrane technology in CO_2/CH_4 and H_2S/CH_4 separation seem good, with ongoing developments. Recent investigations, as highlighted in several references, have shown major patterns and emphasis topics for future research. Such as the progress in the development of materials and membranes tailored to maximize efficiency under difficult conditions is expected [9], tailoring the CO_2/CH_4 separation performance using MMMs is growing, with greater efficiency compared to standard polymeric membranes [298], selection of innovative technologies [299]. Molecular simulation techniques are among the most advanced and reliable tools in membrane research, offering predictive insights into gas transport and polymer-filler interactions [268,300–302]. However, their application is often constrained by high computational costs, limited scalability to complex multicomponent systems, and challenges in accurately translating simulation outcomes to real-world membrane performance.

The combined efforts undertaken indicate a dynamic trajectory for membrane technology in gas separation, overcoming hurdles and opening the path for increasingly efficient and discriminating processes.

7. Future prospective in PSF-based membranes

7.1. Advanced polymer engineering, surface functionalization, and hybrid integration

Future advancements in PSF-based membranes are expected to arise from the integrated application of advanced polymer blending, surface functionalization, hybrid separation technologies, and sustainable fabrication practices. The incorporation of high-performance additives such as GO, MOFs, and ILs into PSF matrices has demonstrated strong potential to enhance polymer compatibility, regulate microphase separation, and alleviate the trade-off between permeability and selectivity. These approaches have enabled improved separation performance for challenging gas pairs, including CO_2/CH_4 and O_2/N_2 [163]. For example, GO-PSF MMMs exhibited approximately a 14% increase in CO_2 permeance, along with selectivity enhancements of 158% for CO_2/N_2 and 74% for CO_2/CH_4, which were attributed to strengthened interfacial interactions and tailored microstructural organization within the polymer matrix [139]. Maintaining controlled phase morphology remains essential for achieving consistent performance across varying operating conditions. In parallel, membrane durability and operational stability can be significantly improved through surface modification techniques such as plasma treatment, chemical grafting, and nanoparticle deposition, which impart anti-fouling, anti-plasticization, and oxidation-resistant properties [241,303]. The complementary roles of polymer blending in enhancing selectivity and surface functionalization in improving durability and fouling resistance are illustrated in Figs. 29 (a) and 29(b), respectively. Beyond material design, the integration of PSF membranes into hybrid gas separation systems combining membranes with adsorption, cryogenic distillation, or chemical absorption offers a pathway to overcome the intrinsic limitations of standalone membrane processes and improve overall separation efficiency and energy performance [31]. Concurrently, increasing emphasis is being placed on environmentally sustainable fabrication strategies, including the use of bio-based or less toxic solvents, solvent-free processing routes, and recyclable membrane modules, in line with industrial sustainability goals [127,304,305]. Despite these advances, critical challenges remain, including ensuring long term interfacial stability between PSF and diverse fillers, developing scalable and reproducible fabrication methods, and achieving a deeper mechanistic understanding of polymer-filler interactions under dynamic industrial conditions. Addressing these gaps through predictive modeling, sustainable processing, and hybrid system integration will be essential to fully realize the potential of PSF-based MMMs for large-scale gas separation applications.

7.2. Computational-experimental Co-design frameworks/ machine learning

PSF-based membrane innovation is progressively embracing integrated computational and data-driven methodologies to shift development from empirical trial-and-error toward predictive, co-design workflows. At the molecular-level, atomistic simulations (MD, MC, soft-confinement models) offer detailed insights into gas transport phenomena, including solubility, diffusivity, and permeance under industrially relevant temperature and pressure conditions [273,274]. For PSF MMMs with silica or other inorganic fillers, these tools clarify how filler content alters free volume and separation behavior under mixed-gas feeds. At the module and process scale, mathematical modeling is instrumental for predicting performance in hollow fiber modules and industrial separation systems. This modeling captures multicomponent flows, concentration polarization, and real-world separation behavior, enabling scale-up design and optimization [306,307]. On the

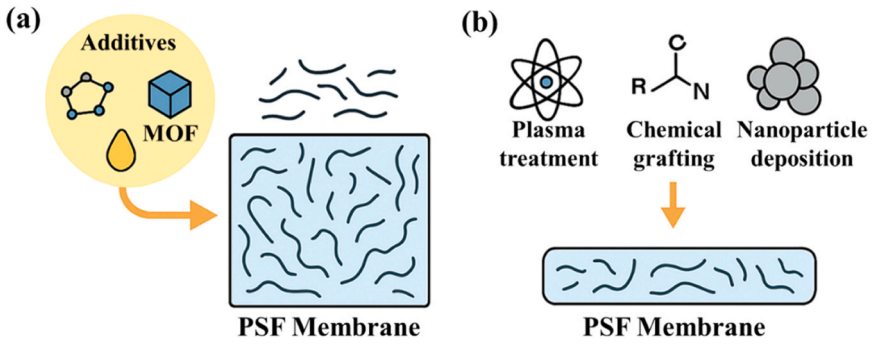

Fig. 29. (a) Polymer blending for enhanced selectivity (b) Surface functionalization for anti-fouling and long term stability.

data-driven front, ML models such as artificial neural network (ANN) [308] and graph neural network (GNN) [309] trained on comprehensive datasets including compositional, structural, and operational variables have shown promising accuracy in forecasting PSF membrane permeability and selectivity (R^2: 0.79–0.85), and effectively classifying top-performing membranes [310]. These computational advancements are progressively being incorporated into autonomous experimental platforms, wherein robotic systems undertake the synthesis, processing, and testing of the most promising candidates identified through simulations. This closed-loop methodology is shortening development timelines from years to mere months, representing a significant transformation in the discovery and validation of membrane materials. As depicted in Fig. 30, this integrated co-design loop demonstrates the dynamic interaction between quantum-level simulations, ML techniques (including GNN-based property prediction), robotic synthesis, and experimental feedback. This dynamic framework enables a continuously optimized membrane development cycle.

8. Conclusion

PSF-based membranes represent a mature and highly robust platform for CO_2 and H_2S separation from natural gas, offering superior thermal, mechanical, and chemical stability compared with conventional polymeric membranes. Their durability, scalability, and tunable interfacial chemistry make them particularly suitable for industrial sour gas processing under aggressive operating conditions. This review provides a critical evaluation of PSF membrane synthesis techniques, evaluated in terms of fabrication complexity and separation performance, identifying phase inversion as the most widely adopted and viable technique. Recent advances in PSF-based MMM, incorporating functionalized fillers such as GO, MOF, and ILs, have enabled concurrent improvements in permeability and selectivity while suppressing interfacial defects through enhanced chemical compatibility. In parallel, polymer blending and surface functionalization strategies have been shown to improve fouling resistance, and plasticization stability. Most PSF-based MMMs cluster is between permeability approximately 5–100 Barrer and selectivity between 10 and 80. Some advanced systems (e.g., ZIF-67, porphyrin-modified membranes) approach the 2008 upper bound and very few exceed the 2008 limit, meaning the trade-off still exists. It is noteworthy that H_2S permeability data remain underreported in PSF-based membrane studies, despite their critical relevance in sour gas processing. This gap in experimental data highlights the need for more systematic investigations on CO_2 and H_2S separation under realistic operating conditions. This review introduces a predictive analytical framework that transforms fragmented experimental observations on PSF-based membranes into a unified design assessment tool for sour gas applications. The framework systematically links structural, chemical, and thermo-mechanical indicators to membrane stability. It reveals that chemically engineered PSF systems outperform pristine and physically blended membranes due to simultaneous enhancement of interfacial compatibility and plasticization resistance. By reducing trial-and-error experimentation, the framework provides a transferable methodology for guiding the rational design of next-generation membranes for aggressive CO_2/H_2S environments. These insights contribute to the advancement of durable, energy-efficient membrane systems for sustainable gas purification. From a practical perspective, PSF-based membranes position them as strong candidates for industrial deployment in natural gas processing, particularly for simultaneous CO_2 and H_2S removal. Their compatibility with existing membrane module designs and potential integration into hybrid separation systems further

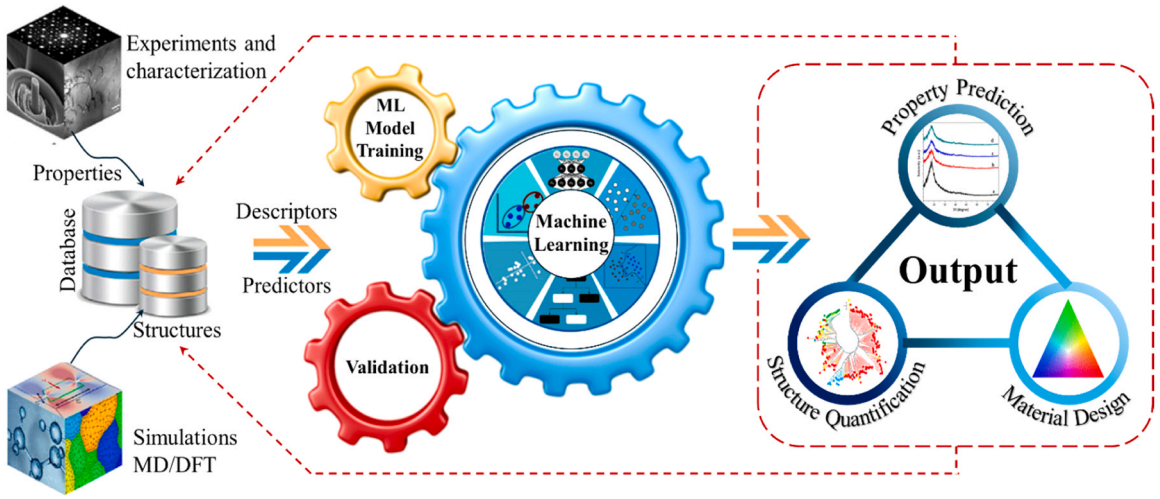

Fig. 30. Closed-loop ML-driven co-design for PSF membrane development.

enhance their applicability in large-scale operations. Moreover, the development of predictive frameworks and AI-assisted design strategies can significantly reduce development time and operational costs, supporting the transition toward more efficient and economically viable gas separation technologies. Furthermore, the sensitivity analysis of the predictive framework is also conducted that confirms it effectiveness representing a key novelty of this study and providing a practical tool for guiding future membrane design and optimization. Despite these advancements, significant challenges remain, particularly the scarcity of long term mixed-gas studies under realistic conditions, limited techno-economic and life-cycle assessments, and an incomplete understanding of fouling and aging at scale. Addressing these gaps will require integrated experimental and computational strategies, including in-situ characterization, multiscale modeling, and pilot-scale validation. Looking forward, PSF membranes are expected to be integrated into hybrid separation systems and multi-stage membrane modules for bulk CO_2 removal followed by selective H_2S polishing. They are also promising for compact offshore gas treatment units, where mechanical robustness and corrosion resistance are critical. In addition, the adoption of green fabrication routes and AI-assisted molecular and process design is expected to accelerate their industrial deployment. Collectively, these developments position PSF-based membranes as next-generation, sustainable separation materials. They show strong potential for efficient sour gas purification and global carbon mitigation. Although the present study demonstrates promising outcomes, further research is needed to improve the robustness and applicability of the proposed model. Incorporating broader datasets and conducting experimental validation under diverse operating conditions will enhance its predictive reliability. Moreover, extending this framework to other polymeric and MMM systems represents a promising direction for enabling wider applicability and more optimized membrane design.

Table of Abbreviations

CA	Cellulose acetate
CNF	Carbon nano-fiber
DFT	Density functional theory
LbL	Layer-by-layer
ZIF	Zeolitic imidazolate frameworks
AFM	Atomic force microscopy
ANN	Artificial neural network
CAS	Chemical abstract service
CMS	Carbon molecular sieve
COMPASS	Condensed-phase optimized molecular potentials for atomistic simulation studies
DOE	Design of experiment
DSC	Differential scanning calorimetry
EIPS	Evaporation-induced phase separation
GCMC	Grand Canonical Monte Carlo
GO	Graphene oxide
IL	Ionic liquids
IP	Interfacial polymerization
LAL	Laser ablation in liquid
LIG	Laser-induced graphene
MC	Monte Carlo
MD	Molecular dynamic
MMM	Mixed matrix membrane
MOF	Metal organic framework
NIOSH	National institute for occupational safety and health
NIPS	Non-solvent induced phase separation
O&M	Operation and maintenance
PLAL	Pulsed laser ablation in liquid
PVP	Poly vinyl chloride and cellulose
QEHS	Quality, environment, health, and safety
SEM	Scanning electron microscopy
TEM	Transmission Electron Microscopy
TFC	Thin-film composite
TIPS	Thermal-induced phase separation
VIPS	Vapor-induced phase separation
RTIL	Room temperature ionic liquid
FESEM	Field emission scanning electron microscopy
FTIR	Fourier transform infrared spectroscopy

Disclosure

The authors wish to acknowledge the use of AI-based language assistance, specifically OpenAI's ChatGPT, for paraphrasing and enhancing the readability of the manuscript. This support was limited to language refinement, and all scientific ideas, analyses, and conclusions presented in this work are solely those of the authors.

CRediT authorship contribution statement

Suhaib Umer Ilyas: Writing – review & editing. **Mehtab Ali Darban:** Writing – review & editing. **Syed Abdul Moiz Hashmi:** Writing – review & editing, Methodology. **Lydia Anggraini:** Writing – review & editing. **Waqar Hussain:** Writing – original draft, Visualization, Methodology, Data curation, Conceptualization. **Serene Sow Mun Lock:** Writing – review & editing, Supervision, Resources, Project administration, Investigation, Funding acquisition, Formal analysis. **Lam Ghai Lim:** Writing – review & editing. **Lian See Tan:** Writing – review & editing. **Mee Kee Wong:** Writing – review & editing.

Funding

We want to acknowledge the financial support provided by YUTP Fundamental Research Grant (Cost Centre: 015LC0-498 and 015LC0-618).

Declaration of Competing Interest

The authors declare that they have no known competing financial interests or personal relationships that could have appeared to influence the work reported in this paper.

Appendix A. Supporting information

Supplementary data associated with this article can be found in the online version at doi:10.1016/j.jece.2026.122520.

Data Availability

No data was used for the research described in the article.

References

[1] EIA, Natural Gas Information: Overview, 2021. ⟨https://www.iea.org/reports/natural-gas-information-overview/demand⟩ (accessed September 24, 2024).
[2] Rystad Energy / International Gas Union / Snam, Global Gas Report 2024, 2024. ⟨https://www.igu.org/resources/global-gas-report-2024-edition/⟩ (accessed September 24, 2024).
[3] S.T. Revankar, Chemical Energy Storage, Elsevier Inc, 2019, https://doi.org/10.1016/B978-0-12-813975-2.00006-5.
[4] M.S. Shah, M. Tsapatsis, J.I. Siepmann, Hydrogen sulfide capture: from absorption in polar liquids to oxide, zeolite, and metal-organic framework adsorbents and membranes, Chem. Rev. 117 (2017) 9755–9803, https://doi.org/10.1021/acs.chemrev.7b00095.
[5] J. Siažik, M. Malcho, Accumulation of primary energy into natural gas hydrates, Procedia Eng. 192 (2017) 782–787, https://doi.org/10.1016/j.proeng.2017.06.135.
[6] J. Ayaburi, S. Sharma, M. Bazilian, Comparative analysis of selected African natural gas markets and related policies, Energy Sustain. Dev. 63 (2021) 67–77, https://doi.org/10.1016/j.esd.2021.05.007.
[7] USGS, What is associated vs. non-associated natural gas? | U.S. Geological Survey. ⟨https://www.usgs.gov/faqs/what-associated-vs-non-associated-natural-gas⟩ (accessed October 9, 2024).

[8] M. Zheng, J. Li, X. Wu, S. Wang, Q. Guo, J. Yu, M. Zheng, N. Chen, Q. Yi, China's conventional and unconventional natural gas resources: potential and exploration targets, J. Nat. Gas. Geosci. 3 (2018) 295–309, https://doi.org/10.1016/j.jnggs.2018.11.007.

[9] A.R. Teixeira Cardoso, A. Ambrosi, M. Di Luccio, D. Hotza, Membranes for separation of CO_2/CH_4 at harsh conditions, J. Nat. Gas. Sci. Eng. 98 (2022) 104388, https://doi.org/10.1016/j.jngse.2021.104388.

[10] T.N.A.T. Hassan, A.M. Shariff, M.M.M. Pauzi, M.S. Khidzir, A. Surmi, Insights on cryogenic distillation technology for simultaneous CO_2 and H_2S removal for sour gas fields, Molecules 27 (2022), https://doi.org/10.3390/molecules27041424.

[11] A. Groysman, Corrosion problems and solutions in oil, gas, refining and petrochemical industry, Koroze a Ochr. Mater. 61 (2017) 100–117, https://doi.org/10.1515/kom-2017-0013.

[12] M. Vakili, P. Koutník, J. Kohout, Addressing hydrogen sulfide corrosion in oil and gas industries: a sustainable perspective, Sustain 16 (2024), https://doi.org/10.3390/su16041661.

[13] A. Mondal, C. Bhattacharjee, Membrane transport for gas separation, Diffus. Found. 23 (2019) 138–150, https://doi.org/10.4028/www.scientific.net/df.23.138.

[14] K. Abbass, M.Z. Qasim, H. Song, M. Murshed, H. Mahmood, I. Younis, A review of the global climate change impacts, adaptation, and sustainable mitigation measures, Environ. Sci. Pollut. Res. 29 (2022) 42539–42559, https://doi.org/10.1007/s11356-022-19718-6.

[15] A. Amouzad Khalili, S. Yeganegi, Molecular simulations of the adsorption and separation of hydrogen sulfide, carbon dioxide, methane, and nitrogen and their binary mixtures (H_2S/CH_4), (CO_2/CH_4) on NUM-3a metal-organic frameworks, J. Mol. Model 27 (2021), https://doi.org/10.1007/s00894-021-04709-0.

[16] M. Rostamizadeh, B. Sadatnia, S. Norouzbahari, A. Ghadimi, Enhancing the gas separation properties of mixed matrix membranes via impregnation of sieve phases with metal and nonmetal promoters, Sep. Purif. Technol. 245 (2020) 116859, https://doi.org/10.1016/j.seppur.2020.116859.

[17] R. Ansari, S. Rouhi, S. Ajori, Molecular dynamics simulations of the polymer/amine functionalized single-walled carbon nanotubes interactions, Appl. Surf. Sci. 455 (2018) 171–180, https://doi.org/10.1016/j.apsusc.2018.04.133.

[18] Hydrogen Sulfide - Hazards | Occupational Safety and Health Administration. ⟨https://www.osha.gov/hydrogen-sulfide/hazards⟩ (accessed October 2, 2024).

[19] W. Hussain, S. Khan, A.H. Mover, Development of quality, environment, health, and safety (QEHS) management system and its integration in operation and maintenance (O&M) of onshore wind energy industries, Renew. Energy 196 (2022) 220–233, https://doi.org/10.1016/j.renene.2022.06.138.

[20] A.R. Rumane, Taylor & Francis Group. Quality Management in Oil and Gas Projects, CRC Press, 2021, pp. 1–94, https://doi.org/10.1201/9781003145059.

[21] I. Othman, M. Napiah, M.F. Nuruddin, M.M.A. Klufallah, Effectiveness of safety management in oil and gas project, Appl. Mech. Mater. 815 (2015) 429–433, https://doi.org/10.4028/www.scientific.net/amm.815.429.

[22] P.N. Okonkwo, J.A. Wium, Investigating the effectiveness of health and safety management systems within construction organizations, Int. J. Occup. Saf. Erg. 29 (2023) 785–795, https://doi.org/10.1080/10803548.2022.2082137.

[23] S. Küfeoğlu, SDG-7 Affordable and Clean Energy, (2022) 305–330. https://doi.org/10.1007/978-3-031-07127-0_9.

[24] O.E. Aksyutin, A.G. Ishkov, K.V. Romanov, V.A. Grachev, The role of natural gas in achieving sustainable development goals, Int. J. Energy Econ. Policy 10 (2020) 463–472, https://doi.org/10.32479/ijeep.9359.

[25] M. Wang, Z. Wang, S. Zhao, J. Wang, S. Wang, Recent advances on mixed matrix membranes for CO_2 separation, Chin. J. Chem. Eng. 25 (2017) 1581–1597, https://doi.org/10.1016/j.cjche.2017.07.006.

[26] S.A.M. Hashmi, H. Moiz, W. Hussain, M. Mumtaz, Enhanced CO_2/CH_4 separation using hydroxyl functionalized Mg-MOF-74, Chem. Eng. Commun. 212 (2025) 1839–1855, https://doi.org/10.1080/00986445.2025.2503004.

[27] B. Yang, H. Jiang, L. Bai, Y. Bai, T. Song, X. Zhang, Application of ionic liquids in the mixed matrix membranes for CO_2 separation: an overview, Int. J. Greenh. Gas. Control 121 (2022) 103796, https://doi.org/10.1016/j.ijggc.2022.103796.

[28] A.R. Nabais, A.P.S. Martins, V.D. Alves, J.G. Crespo, I.M. Marrucho, L.C. Tomé, L. A. Neves, Poly(ionic liquid)-based engineered mixed matrix membranes for CO_2/H_2 separation, Sep. Purif. Technol. 222 (2019) 168–176, https://doi.org/10.1016/j.seppur.2019.04.018.

[29] S. Sreenath, A.A. Sam, Hybrid membrane-cryogenic CO_2 capture technologies: a mini-review, Front. Energy Res. 11 (2023) 1–9, https://doi.org/10.3389/fenrg.2023.1167024.

[30] M. Babar, A. Mukhtar, M. Mubashir, S. Saqib, S. Ullah, A.H.A. Quddusi, M. A. Bustam, P.L. Show, Development of a novel switched packed bed process for cryogenic CO_2 capture from natural gas, Process Saf. Environ. Prot. 147 (2021) 878–887, https://doi.org/10.1016/j.psep.2021.01.010.

[31] A. Imtiaz, M.H.D. Othman, A. Jilani, I.U. Khan, R. Kamaludin, J. Iqbal, A.G. Al-Sehemi, Challenges, opportunities and future directions of membrane technology for natural gas purification: a critical review, Membrane 12 (2022), https://doi.org/10.3390/membranes12070646.

[32] Z. Dai, L. Deng, Membranes for CO_2 capture and separation: progress in research and development for industrial applications, Sep. Purif. Technol. 335 (2024) 126022, https://doi.org/10.1016/j.seppur.2023.126022.

[33] P. Gkotsis, E. Peleka, A. Zouboulis, Membrane-based technologies for post-combustion CO_2 capture from flue gases: recent progress in commonly employed membrane materials, Membrane 13 (2023), https://doi.org/10.3390/membranes13120898.

[34] G. Ji, M. Zhao, Membrane separation technology in carbon capture, Recent Adv. Carbon Capture Storage (2017), https://doi.org/10.5772/65723.

[35] V. Muthukumaraswamy Rangaraj, M.A. Wahab, K.S.K. Reddy, G. Kakosimos, O. Abdalla, E.P. Favvas, D. Reinalda, F. Geuzebroek, A. Abdala, G.N. Karanikolos, Metal organic framework — based mixed matrix membranes for carbon dioxide separation: recent advances and future directions, Front. Chem. 8 (2020) 1–25, https://doi.org/10.3389/fchem.2020.00534.

[36] W.Fen Yong, C.Z. Liang, C.R. Pocha, Application of membrane technology for CO_2 capture and separation, carbon dioxide capture convers, Adv. Mater. Process (2022) 257–289, https://doi.org/10.1016/B978-0-323-85585-3.00007-9.

[37] Y. Han, W.S.W. Ho, Polymeric membranes for CO_2 separation and capture, J. Memb. Sci. 628 (2021) 119244, https://doi.org/10.1016/j.memsci.2021.119244.

[38] M.D. Guiver, M. Yahia, M.M. Dal-Cin, G.P. Robertson, S.S. Garakani, N. Du, N. Tavajohi, Gas transport in a polymer of intrinsic microporosity (PIM-1) substituted with pseudo-ionic liquid tetrazole-type structures, Macromolecules 53 (2020) 8951–8959, https://doi.org/10.1021/acs.macromol.0c01321.

[39] Y. Gu, E.L. Cussler, T.P. Lodge, ABA-triblock copolymer ion gels for CO_2 separation applications, J. Memb. Sci. 423–424 (2012) 20–26, https://doi.org/10.1016/j.memsci.2012.07.011.

[40] G.O. Yahaya, A. Hayek, A. Alsamah, Y.A. Shalabi, M.M. Ben Sultan, R.H. Alhajry, Copolyimide membranes with improved H_2S/CH_4 selectivity for high-pressure sour mixed-gas separation, Sep. Purif. Technol. 272 (2021) 118897, https://doi.org/10.1016/j.seppur.2021.118897.

[41] A.K. Sekizkardes, V.A. Kusuma, J.S. McNally, D.W. Gidley, K. Resnik, S.R. Venna, D. Hopkinson, Microporous polymeric composite membranes with advanced film properties: Pore intercalation yields excellent CO_2 separation performance, J. Mater. Chem. A 6 (2018) 22472–22477, https://doi.org/10.1039/c8ta07424k.

[42] X. Guo, Z. Qiao, D. Liu, C. Zhong, Mixed-matrix membranes for CO_2 separation: role of the third component, J. Mater. Chem. A 7 (2019) 24738–24759, https://doi.org/10.1039/c9ta09012f.

[43] T. Araújo, G. Bernardo, A. Mendes, Cellulose-based carbon molecular sieve membranes for gas separation: a review, Molecules 25 (2020) 1–33, https://doi.org/10.3390/molecules25153532.

[44] D. De Meis, M. Richetta, E. Serra, Microporous inorganic membranes for gas separation and purification, Inter. Int. Ceram. Rev. 67 (2018) 16–21, https://doi.org/10.1007/s42411-018-0023-2.

[45] A.B. Alayande, H. Jee, D. Kang, J.K. Jang, K.J. Chae, M.H. Hwang, C. Kim, S. Chae, I.S. Kim, C.Y. Chuah, E. Yang, Membrane and adsorption technologies for efficient hydrogen sulfide removal from biogas: a review focused on the advancement of key components, Process Saf. Environ. Prot. 186 (2024) 448–473, https://doi.org/10.1016/j.psep.2024.04.018.

[46] Z. Dai, L. Ansaloni, L. Deng, Recent advances in multi-layer composite polymeric membranes for CO_2 separation: a review, Green. Energy Environ. 1 (2016) 102–128, https://doi.org/10.1016/j.gee.2016.08.001.

[47] C.A. Scholes, Challenges for CO_2 capture by membranes, Elsevier Inc, 2020, https://doi.org/10.1016/B978-0-12-819657-1.00016-5.

[48] A. Hayek, A. Alsamah, Q. Saleem, R.H. Alhajry, A.A. Alsuwailem, Enhanced H_2S and CO_2 selectivities through bromo-substitution of polyimide membranes for sour natural gas upgrading, J. Memb. Sci. 721 (2025) 123807, https://doi.org/10.1016/j.memsci.2025.123807.

[49] Q. Qian, A.M. Wright, H. Lee, M. Dincă, Z.P. Smith, Low-Temperature $H_2S/CO_2/CH_4$ separation in mixed-matrix membranes containing MFU-4, Chem. Mater. 33 (2021) 6825–6831, https://doi.org/10.1021/acs.chemmater.1c01533.

[50] S. Rao, X. Deng, C. Zou, B. Prasad, Y. Han, L.C. Lin, W.S.W. Ho, Kinetic H_2S/CO_2 selectivity in an exceptionally sterically hindered amine membrane, J. Mater. Chem. A 12 (2024) 29138–29144, https://doi.org/10.1039/d4ta04997g.

[51] S. Zakariya, Y.F. Yeong, N. Jusoh, L.S. Tan, Performance of multilayer composite hollow membrane in separation of CO_2 from CH_4 in mixed gas conditions, Polymers 14 (2022) 1–13, https://doi.org/10.3390/polym14071480.

[52] Z. Bashir, S.S.M. Lock, N. e Hira, S.U. Ilyas, L.G. Lim, I.S.M. Lock, C.L. Yiin, M. A. Darban, A review on recent advances of cellulose acetate membranes for gas separation, RSC Adv. 14 (2024) 19560–19580, https://doi.org/10.1039/d4ra01315h.

[53] I. Coelhoso, F. Freitas, V.D. Alves, M.A.M. Reis, Biodegradable Organic Matter, 2012. https://doi.org/10.1007/978-3-642-40872-4_52-1.

[54] M.M.H. Shah Buddin, A.L. Ahmad, A review on metal-organic frameworks as filler in mixed matrix membrane: recent strategies to surpass upper bound for CO_2 separation, J. CO_2 Util. 51 (2021) 101616, https://doi.org/10.1016/j.jcou.2021.101616.

[55] Y. Dai, Z. Niu, W. Luo, Y. Wang, P. Mu, J. Li, A review on the recent advances in composite membranes for CO_2 capture processes, Sep. Purif. Technol. 307 (2023) 122752, https://doi.org/10.1016/j.seppur.2022.122752.

[56] A.R. Kamble, C.M. Patel, Z.V.P. Murthy, A review on the recent advances in mixed matrix membranes for gas separation processes, Renew. Sustain. Energy Rev. 145 (2021) 111062, https://doi.org/10.1016/j.rser.2021.111062.

[57] M.I.F. Zainuddin, A.L. Ahmad, Mixed matrix membrane development progress and prospect of using 2D nanosheet filler for CO_2 separation and capture, J. CO_2 Util. 62 (2022) 102094, https://doi.org/10.1016/j.jcou.2022.102094.

[58] C.Y. Chuah, W.C. Poon, Breaking boundaries: innovations in two- and three-dimensional metal-organic framework (MOF)-based mixed-matrix membranes for effective post-combustion CO_2 Capture, J. Chem. Eng. Jpn. 57 (2024), https://doi.org/10.1080/00219592.2024.2350748.

[59] C.S.Q. Christensen, N. Hansen, M. Motadayen, N. Lock, M.L. Henriksen, J. Quinson, A review of metal-organic frameworks and polymers in mixed matrix membranes for CO_2 capture, Beilstein J. Nanotechnol. 16 (2025) 155–186, https://doi.org/10.3762/bjnano.16.14.

[60] L.M. Robeson, The upper bound revisited, J. Memb. Sci. 320 (2008) 390–400, https://doi.org/10.1016/j.memsci.2008.04.030.
[61] F. Kadirkhan, G.P. Sean, A.F. Ismail, W.N.F. Wan Mustapa, M.H.M. Halim, S. W. Kian, Y.S. Yean, CO_2 plasticization resistance membrane for natural gas sweetening process: defining optimum operating conditions for stable operation, Polymers 14 (2022), https://doi.org/10.3390/polym14214537.
[62] H. Pang, Y. Qiu, W. Sheng, Long-term stability of PVDF-SiO_2-HDTMS composite hollow fiber membrane for carbon dioxide absorption in gas–liquid contacting process, Sci. Rep. 13 (2023) 1–10, https://doi.org/10.1038/s41598-023-31428-8.
[63] F. Kadirkhan, P.S. Goh, A.F. Ismail, W.N.F. Wan Mustapa, M.H.M. Halim, W. K. Soh, S.Y. Yeo, Recent advances of polymeric membranes in tackling plasticization and aging for practical industrial CO_2/CH_4 applications—a review, Membrane 12 (2022), https://doi.org/10.3390/membranes12010071.
[64] K. Mizrahi Rodriguez, S. Lin, A.X. Wu, K.R. Storme, T. Joo, A.F. Grosz, N. Roy, D. Syar, F.M. Benedetti, Z.P. Smith, Penetrant-induced plasticization in microporous polymer membranes, Chem. Soc. Rev. 53 (2024) 2435–2529, https://doi.org/10.1039/d3cs00235g.
[65] R. Naim, a F. Ismail, H. Saidi, E. Saion, Development of sulfonated polysulfone membranes as a material for Proton Exchange Membrane (PEM), Proc. Reg. Symp. Membr. Sci. Technol. (2004) 1–17. ⟨https://www.researchgate.net/profile/Elias-Saion/publication/239924456_Development_of_sulfonated_polysulfone_membranes_as_a_material_for_Proton_Exchange_Membrane_PEM/links/00b4952834926062200000000/Development-of-sulfonated-polysulfone-membranes-as-a-material-for-Proton-Exchange-Membrane-PEM.pdf⟩.
[66] X.X. Zheng, A.J. Böttger, K.M.B. Jansen, J. van Turnhout, J. van Kranendonk, Aging of polyphenylene sulfide-glass composite and polysulfone in highly oxidative and strong alkaline environments, Front. Mater. 7 (2020) 1–12, https://doi.org/10.3389/fmats.2020.610440.
[67] G. Sherif, D.I. Chukov, V.V. Tcherdyntsev, V.G. Torokhov, D.D. Zherebtsov, Effect of glass fibers thermal treatment on the mechanical and thermal behavior of polysulfone based composites, Polymers 12 (2020), https://doi.org/10.3390/POLYM12040902.
[68] A. Igder, S. Pye, A.H. Mohammed Al-Antaki, A. Keshavarz, C.L. Raston, A. Nosrati, Vortex fluidic mediated synthesis of polysulfone, RSC Adv. 10 (2020) 14761–14767, https://doi.org/10.1039/d0ra00602e.
[69] O. Dumbrava, A. Filimon, L. Marin, Tailoring properties and applications of polysulfone membranes by chemical modification: Structure-properties-applications relationship, Eur. Polym. J. 196 (2023) 112316, https://doi.org/10.1016/J.EURPOLYMJ.2023.112316.
[70] A.M. Dobos, A. Popa, C.M. Rimbu, A. Filimon, Structure-bioactivity relationship of the functionalized polysulfone with triethylphosphonium pendant groups: perspective for biomedical applications, Polymers 15 (2023), https://doi.org/10.3390/polym15040877.
[71] S. Karki, G. Hazarika, D. Yadav, P.G. Ingole, Polymeric membranes for industrial applications: Recent progress, challenges and perspectives, Desalination 573 (2024) 117200, https://doi.org/10.1016/j.desal.2023.117200.
[72] M. Liu, L.B. Zhao, L.Y. Yu, Y.M. Wei, Z.L. Xu, Structure and properties of PSf hollow fiber membranes with different molecular weight hyperbranched polyester using pentaerythritol as core, Polymers 12 (2020), https://doi.org/10.3390/polym12020383.
[73] R.H. Alasfar, V. Kochkodan, S. Ahzi, N. Barth, M. Koç, Preparation and characterization of polysulfone membranes reinforced with cellulose nanofibers, Polymers 14 (2022), https://doi.org/10.3390/polym14163317.
[74] B. Hazarika, M. Ahmaruzzaman, M.S. Santosh, D. Barceló, S. Rtimi, Advances in polymer-based nanocomposite membranes for water remediation: preparation methods, critical issues and mechanisms, J. Environ. Chem. Eng. 11 (2023), https://doi.org/10.1016/j.jece.2023.111401.
[75] A. Ammar, A.M. Al-Enizi, M.A.A. AlMaadeed, A. Karim, Influence of graphene oxide on mechanical, morphological, barrier, and electrical properties of polymer membranes, Arab. J. Chem. 9 (2016) 274–286, https://doi.org/10.1016/j.arabjc.2015.07.006.
[76] Q. Zeng, Z. Wan, Y. Jiang, J. Fortner, Enhanced polysulfone ultrafiltration membrane performance through fullerol Addition: a study towards optimization, Chem. Eng. J. 431 (2022) 134071, https://doi.org/10.1016/J.CEJ.2021.134071.
[77] Y. Jia, S. Sun, S. Li, Z. Wang, F. Wen, C. Li, H. Matsuyama, S. Hu, Improved performance of polysulfone ultrafiltration membrane using TCPP by post-modification method, Membrane 10 (2020), https://doi.org/10.3390/membranes10040066.
[78] M.B.M.Y. Ang, V.J. Lau, Y.L. Ji, S.H. Huang, Q.F. An, A.R. Caparanga, H.A. Tsai, W.S. Hung, C.C. Hu, K.R. Lee, J.Y. Lai, Correlating PSf support physicochemical properties with the formation of piperazine-based polyamide and evaluating the resultant nanofiltration membrane performance, Polymers 9 (2017) 1–17, https://doi.org/10.3390/polym9100505.
[79] E. Soo, F. Schaefer, Dialysis in Inborn Errors of Metabolism, Handb. Dial. Ther. Fifth Ed. (2017) 948–954.e1, https://doi.org/10.1016/B978-0-323-39154-2.00082-5.
[80] E.R. Radu, S.I. Voicu, V.K. Thakur, Polymeric membranes for biomedical applications, Polymers 15 (2023), https://doi.org/10.3390/polym15030619.
[81] D.I. Chukov, S.G. Nematulloev, V.V. Tcherdyntsev, V.G. Torokhov, A. A. Stepashkin, M.Y. Zadorozhnyy, D.D. Zherebtsov, G. Sherif, Structure and properties of polysulfone filled with modified twillweave carbon fabrics, Polymers 12 (2020) 13–15, https://doi.org/10.3390/polym12010050.
[82] B. Leonard, H. Loh, D. Lu, E.A. Ogbuoji, I.C. Escobar, Sustainable additive manufacturing of polysulfone membranes for liquid separations Journal of Physics: Energy OPEN ACCESS Sustainable additive manufacturing of polysulfone membranes for liquid separations, (2024).
[83] S. Kheirieh, M. Asghari, M. Afsari, Application and modification of polysulfone membranes, Rev. Chem. Eng. 34 (2018) 657–693, https://doi.org/10.1515/revce-2017-0011.
[84] Y.W. Jeon, D.H. Lee, Gas membranes for CO_2/CH_4 (biogas) separation: a review, Environ. Eng. Sci. 32 (2015) 71–85, https://doi.org/10.1089/ees.2014.0413.
[85] S. Pakdel, H. Erfan-Niya, J. Azamat, CO_2/CH_4 mixed-gas separation through carbon nitride membrane: a molecular dynamics simulation, Colloids Surf. A Physicochem. Eng. Asp. 650 (2022) 129643, https://doi.org/10.1016/J.COLSURFA.2022.129643.
[86] R.M. Almuhtaseb, A. Awadallah-F, S.A. Al-Muhtaseb, M. Khraisheh, Influence of casting solvents on CO_2/CH_4 separation using polysulfone membranes, Membrane 11 (2021), https://doi.org/10.3390/membranes11040286.
[87] O.S. Serbanescu, S.I. Voicu, V.K. Thakur, Polysulfone functionalized membranes: Properties and challenges, Mater. Today Chem. 17 (2020) 100302, https://doi.org/10.1016/j.mtchem.2020.100302.
[88] N. Vainrot, M. Li, A.M. Isloor, M.S. Eisen, New preparation methods for pore formation on polysulfone membranes, Membrane 11 (2021), https://doi.org/10.3390/membranes11040292.
[89] S. Hermans, R. Bernstein, A. Volodin, I.F.J. Vankelecom, Study of synthesis parameters and active layer morphology of interfacially polymerized polyamide-polysulfone membranes, React. Funct. Polym. 86 (2015) 199–208, https://doi.org/10.1016/j.reactfunctpolym.2014.09.013.
[90] H.T.V. Nguyen, T.H.A. Ngo, K.D. Do, M.N. Nguyen, N.T.T. Dang, T.T.H. Nguyen, V. Vien, T.A. Vu, Preparation and characterization of a hydrophilic polysulfone membrane using graphene oxide, J. Chem. 2019 (2019) 15–20, https://doi.org/10.1155/2019/3164373.
[91] O.M.A. Shahlol, H. Isawi, M.G. El-Malky, A.E.H.M. Al-Aassar, A. El zwai, Performance evaluation of the different nano-enhanced polysulfone membranes via membrane distillation for produced water desalination in Sert Basin-Libya, Arab. J. Chem. 13 (2020) 5118–5136, https://doi.org/10.1016/j.arabjc.2020.02.011.
[92] A. Shokri, Synthesize and characterization of polysulfone membrane for the separation of hydrogen sulfide from natural gas, Surf. Interfaces 25 (2021) 101233, https://doi.org/10.1016/j.surfin.2021.101233.
[93] L. Jiang, Y. Meng, S. Xu, H. Yu, X. Hou, Preparation and gas separation performance of polysulfone mixed matrix membrane, J. Nanomater 2021 (2021), https://doi.org/10.1155/2021/9934118.
[94] Q. Ma, D. Liu, B. Wang, W. Liu, G. Xiong, J. Liu, Cellulose acetate-promoted polymer-in-salt electrolytes for solid-state lithium batteries, J. Solid State Electrochem 27 (2023) 1–11, https://doi.org/10.1007/s10008-023-05414-z.
[95] S. LOEB, S. SOURIRAJAN, Sea Water Demineralization by Means of an Osmotic Membrane, in: Saline Water Conversion—II, AMERICAN CHEMICAL SOCIETY, 1963, pp. 117–132, https://doi.org/10.1021/ba-1963-0038.ch009.
[96] A.F. Ismail, K.C. Khulbe, T. Matsuura, Gas separation membranes: polymeric and inorganic, Gas. Sep. Membr. Polym. Inorg. (2015) 1–331, https://doi.org/10.1007/978-3-319-01095-3.
[97] C.B. Urducea, A.C. Nechifor, I.A. Dimulescu, O. Oprea, G. Nechifor, E.E. Totu, I. Isildak, P.C. Albu, S.G. Bungău, Control of nanostructured polysulfone membrane preparation by phase inversion method, Nanomaterials 10 (2020) 1–21, https://doi.org/10.3390/nano10122349.
[98] D. Nayeri, A. Jafari, A review on the recent development of carbon nanotubes (CNTs) application for polymeric mixed-matrix membranes: synthesis, performance, and future challenges, J. Inorg. Organomet. Polym. Mater. 34 (2024) 3315–3345, https://doi.org/10.1007/s10904-024-03036-0.
[99] N. Peng, N. Widjojo, P. Sukitpaneenit, M.M. Teoh, G.G. Lipscomb, T.S. Chung, J. Y. Lai, Evolution of polymeric hollow fibers as sustainable technologies: past, present, and future, Prog. Polym. Sci. 37 (2012) 1401–1424, https://doi.org/10.1016/j.progpolymsci.2012.01.001.
[100] C. Cohen, G.B. Tanny, S. Prager, Diffusion-controlled formation of porous structures in ternary polymer systems, J. Polym. Sci. Polym. Phys. Ed. 17 (1979) 477–489, https://doi.org/10.1002/pol.1979.180170312.
[101] L. Yilmaz, A.J. McHugh, Analysis of nonsolvent–solvent–polymer phase diagrams and their relevance to membrane formation modeling, J. Appl. Polym. Sci. 31 (1986) 997–1018, https://doi.org/10.1002/app.1986.070310404.
[102] A.J. Reuvers, C.A. Smolders, Formation of membranes by means of immersion precipitation, Part Ii. Mech. Form. Membr. Prep. Syst. Cellul. acetate-acetone-Water J. Memb. Sci. 34 (1987) 67–86, https://doi.org/10.1016/S0376-7388(00)80021-6.
[103] Y.D. Kim, J.Y. Kim, H.K. Lee, S.C. Kim, A new modeling of asymmetric membrane formation in rapid mass transfer system, J. Memb. Sci. 190 (2001) 69–77, https://doi.org/10.1016/S0376-7388(01)00420-3.
[104] Y. Termonia, Monte Carlo diffusion model of polymer coagulation, Phys. Rev. Lett. 72 (1994) 3678–3681, https://doi.org/10.1103/PhysRevLett.72.3678.
[105] X.L. Wang, H.J. Qian, L.J. Chen, Z.Y. Lu, Z.S. Li, Dissipative particle dynamics simulation on the polymer membrane formation by immersion precipitation, J. Memb. Sci. 311 (2008) 251–258, https://doi.org/10.1016/j.memsci.2007.12.024.
[106] L.G. Tiron, C. Pintilie, M. Vlad, I.G. Birsan, Baltă, Characterization of polysulfone membranes prepared with thermally induced phase separation technique, IOP Conf. Ser. Mater. Sci. Eng. 209 (2017). https://iopscience.iop.org/article/10.1088/1757-899X/209/1/012013.
[107] H. qing Liang, H. nan Li, H. hao Yu, Y. ting Zhou, Z. kang Xu, Polysulfone membranes via thermally induced phase separation (English Ed.), Chin. J. Polym. Sci. 35 (2017) 846–856, https://doi.org/10.1007/s10118-017-1943-4.

[108] A. Rahimpour, M.S. Kebria, M. Dadashi Firouzjaei, M. Mozafari, M. Elliott, M. Sadrzadeh, in: P.I. Khayet (Ed.), Chapter 1 - Nonsolvent-induced phase separation, Elsevier, 2024, pp. 1–36, https://doi.org/10.1016/B978-0-323-95628-4.00009-4 (N. Tavajohi, M.B.T.-P.M.F. by).

[109] A. Dehqan, S. Paziresh, V. Vatanpour, in: P.I. Khayet (Ed.), Chapter 4 - Evaporation-induced phase separation, Elsevier, 2024, pp. 125–139, https://doi.org/10.1016/B978-0-323-95628-4.00005-7 (N. Tavajohi, M.B.T.-P.M.F. by).

[110] N. Ismail, A. Venault, J.P. Mikkola, D. Bouyer, E. Drioli, N. Tavajohi Hassan Kiadeh, Investigating the potential of membranes formed by the vapor induced phase separation process, J. Memb. Sci. 597 (2020) 117601, https://doi.org/10.1016/j.memsci.2019.117601.

[111] S. Yousef, A. Tonkonogovas, S.I. Lukošiūtė, A. Mohamed, Gas permeation and selectivity characteristics of sponge-like and finger-like structures of polysulfone membranes, Fuel 347 (2023), https://doi.org/10.1016/j.fuel.2023.128476.

[112] S. Kluge, T. Kose, M. Tutuş, Tuning the morphology and gas separation properties of polysulfone membranes, Membrane 12 (2022), https://doi.org/10.3390/membranes12070654.

[113] M.N.A. Seman, M. Khayet, N. Hilal, Nanofiltration thin-film composite polyester polyethersulfone-based membranes prepared by interfacial polymerization, J. Memb. Sci. 348 (2010) 109–116, https://doi.org/10.1016/j.memsci.2009.10.047.

[114] A. Awad, I.H. Aljundi, Interfacial polymerization of facilitated transport polyamide membrane prepared from PIP and IPC for gas separation applications, Korean J. Chem. Eng. 35 (2018) 1700–1709, https://doi.org/10.1007/s11814-018-0079-8.

[115] F. Yuan, Z. Wang, S. Li, J. Wang, S. Wang, Formation-structure-performance correlation of thin film composite membranes prepared by interfacial polymerization for gas separation, J. Memb. Sci. 421–422 (2012) 327–341, https://doi.org/10.1016/j.memsci.2012.07.035.

[116] H. Xu, W. Feng, M. Sheng, Y. Yuan, B. Wang, J. Wang, Z. Wang, Covalent organic frameworks-incorporated thin film composite membranes prepared by interfacial polymerization for efficient CO_2 separation, Chin. J. Chem. Eng. 43 (2022) 152–160, https://doi.org/10.1016/j.cjche.2022.02.014.

[117] W.J. Lau, A.F. Ismail, Progress in interfacial polymerization technique on composite membrane preparation, in: Proc. 2011 2nd Int. Conf. Environ. Eng. Appl. (ICEEA 2011), 2011: pp. 586–588. ⟨https://scholar.google.com/scholar?hl=en&as_sdt=0%2C5&q=W.J.+Lau%2C+A.F.+Ismail%2C+Progress+in+interfacial+polymerization+technique+on+composite+membrane+preparation%2C+in%3A+Proc.+2011+2nd+Int.+Conf.+Environ.+Eng.+Appl.+%28ICEEA+2011%29%2C+2011%3A+pp.+58⟩.

[118] N.M. Mwenze, M. Juma, M. Maaza, Z. Birech, M. Dhlamini, Laser liquid ablation for silver nanoparticles synthesis and conjugation with hydroxychloroquine for Covid-19 treatment, Mater. Today Proc. (2023), https://doi.org/10.1016/j.matpr.2023.08.195.

[119] A. Hakan Yilmaz, B. Ortaç, S. Mutlu, S. Savaskan Yilmaz, Synthesis of polyethylene-based materials, ion exchanger, superabsorbent, radiation shielding, and laser ablation applications, Polyethyl. - N. Dev. Appl. [Work. Title (2023), https://doi.org/10.5772/intechopen.1003665.

[120] M. Navarro, B. Seoane, E. Mateo, R. Lahoz, G.F. De La Fuente, J. Coronas, ZIF-8 micromembranes for gas separation prepared on laser-perforated brass supports, J. Mater. Chem. A 2 (2014) 11177–11184, https://doi.org/10.1039/c4ta00547c.

[121] N. Mintcheva, D.K. Subbiah, M.E. Turabayev, S.O. Gurbatov, J.B.B. Rayappan, A. A. Kuchmizhak, S.A. Kulinich, Gas sensing of laser-produced hybrid TiO_2-ZnO nanomaterials under room-temperature conditions, Nanomaterials 13 (2023), https://doi.org/10.3390/nano13040670.

[122] N.K. Mishra, N. Patil, M. Anas, X. Zhao, B.A. Wilhite, M.J. Green, Highly selective laser-induced graphene (LIG)/polysulfone composite membrane for hydrogen purification, Appl. Mater. Today 22 (2021) 100971, https://doi.org/10.1016/j.apmt.2021.100971.

[123] S. Nazari, A. Abdelrasoul, Impact of membrane modification and surface immobilization techniques on the hemocompatibility of hemodialysis membranes: a critical review, Membrane 12 (2022), https://doi.org/10.3390/membranes12111063.

[124] V. Vasagar, M.K. Hassan, M. Khraisheh, Membrane surface modification and functionalization, Membranes 11 (2021) 391–416, https://doi.org/10.3390/membranes11110877.

[125] R.A. Roslan, W.J. Lau, A.K. Zulhairun, P.S. Goh, A.F. Ismail, Improving CO_2/CH_4 and O_2/N_2 separation by using surface-modified polysulfone hollow fiber membranes, J. Polym. Res. 27 (2020), https://doi.org/10.1007/s10965-020-02104-6.

[126] B. Sasikumar, S. Bisht, G. Arthanareeswaran, A.F. Ismail, M.H.D. Othman, Performance of polysulfone hollow fiber membranes encompassing ZIF-8, SiO_2/ZIF-8, and amine-modified SiO_2/ZIF-8 nanofillers for CO_2/CH_4 and CO_2/N_2 gas separation, Sep. Purif. Technol. 264 (2021), https://doi.org/10.1016/j.seppur.2021.118471.

[127] S.H. Alkandari, B. Castro-Dominguez, Advanced and sustainable manufacturing methods of polymer-based membranes for gas separation: a review, Front. Membr. Sci. Technol. 3 (2024) 1–26, https://doi.org/10.3389/frmst.2024.1390599.

[128] H.Y. Chong, S.A.H. Muhammad, S.N. Norazmi, Z.H. Chang, Y.H. Teoh, A review on membrane fabrication: structure, properties and performance relationship, J. Appl. Membr. Sci. Technol. 29 (2025) 73–97, https://doi.org/10.11113/jamst.v29n1.311.

[129] J. Jaafar, A.M. Nasir, Grand challenge in membrane fabrication: membrane science and technology, Front. Membr. Sci. Technol. 1 (2022) 1–6, https://doi.org/10.3389/frmst.2022.883913.

[130] S.R. Ravichandran, C.D. Venkatachalam, M. Sengottian, S. Sekar, B. S. Subramaniam Ramasamy, M. Narayanan, A.V. Gopalakrishnan, S. Kandasamy, R. Raja, A review on fabrication, characterization of membrane and the influence of various parameters on contaminant separation process, Chemosphere 306 (2022) 135629, https://doi.org/10.1016/j.chemosphere.2022.135629.

[131] Y. Liu, D. Nakamura, J. Gao, K. Imamura, S. Aki, Y. Nagai, I. Taniguchi, K. Fujiwara, R. Horii, Y. Miura, Y. Hoshino, Laser patterning of porous support membranes to enhance the effective surface area of thin-film composite-facilitated transport membranes for CO_2 separation, ACS Appl. Mater. Interfaces 16 (2024) 29112–29120, https://doi.org/10.1021/acsami.4c01260.

[132] M. Alsaady, S. Waqas, M.A. Almarshoud, K. Maqsood, Polysulfone / Graphene Oxide Mixed Matrix Membranes for Improved CO2/CH4 Separation, (2025) 1–17.

[133] A. Bednarska, M. Grądkowski, 2016 problemy eksploatacji-maintenance problems scanning electron microscopy (Sem) in the analysis of the structure of polymeric nanofiltration, Membr. Probl. Eksploat. 1 (2016) 119–128. ⟨https://scholar.google.com/scholar?hl=en&as_sdt=0%2C5&q=A.+Bednarska%2C+M.+Grądkowski%2C+-2016+Problemy+Eksploatacji-Maintenance+Problems+Scanning+Electron+Microscopy+%28Sem%29+in+the+Analysis+of+the+Structure+of+Polymeric+Nanofiltration+Membranes%2C+Prob⟩.

[134] M. Farrokhara, F. Dorosti, New high permeable polysulfone/ionic liquid membrane for gas separation, Chin. J. Chem. Eng. 28 (2020) 2301–2311, https://doi.org/10.1016/j.cjche.2020.04.002.

[135] K. Tulugan, P. Tian, X. Li, W. Zhao, X. Zhang, Y.Bin Zhao, PSF/GO filtering membrane fabricated by electro-spinning applied on arsenic contaminated underground water, J. Eng. Res. (2024), https://doi.org/10.1016/j.jer.2024.01.001.

[136] N.S. Fadaly, F. Aziz, Preparation and characterization of mixed matrix membrane based on Polysulfone (PSF) and lanthanum orthoferrite ($LaFeO_3$) for gas separation, J. Appl. Membr. Sci. Technol. 24 (2020) 27–38, https://doi.org/10.11113/amst.v24n1.169.

[137] Z. Jamian, M.H. Tajuddin, N. Yusof, F.E. Che Othman, Development of polysulfone/activated carbon nanofibers mixed matrix membrane for CO_2/CH4 separation, J. Appl. Membr. Sci. Technol. 22 (2018) 11–17, https://doi.org/10.11113/amst.v22n1.114.

[138] S.H. Ding, T.Y.Siew Ng, T.L. Chew, P.C. Oh, A.L. Ahmad, C.D. Ho, Evaluation of the properties, gas permeability, and selectivity of mixed matrix membrane based on polysulfone polymer matrix incorporated with KIT-6 silica, Polymers 11 (11) (2019) 1, https://doi.org/10.3390/polym11111732.

[139] K. Zahri, K.C. Wong, P.S. Goh, A.F. Ismail, Graphene oxide/polysulfone hollow fiber mixed matrix membranes for gas separation, RSC Adv. 6 (2016) 89130–89139, https://doi.org/10.1039/c6ra16820e.

[140] N.A.H.M. Nordin, A.F. Ismail, A. Mustafa, R.Surya Murali, T. Matsuura, Utilizing low ZIF-8 loading for an asymmetric PSf/ZIF-8 mixed matrix membrane for CO_2/CH_4 separation, RSC Adv. 5 (2015) 30206–30215, https://doi.org/10.1039/c5ra00567a.

[141] N.A.H.M. Nordin, A.F. Ismail, A. Mustafa, Synthesis and preparation of asymmetric PSf/ZIF-8 mixed matrix membrane for CO_2/CH_4 separation, J. Teknol. (Sci. Eng. 69 (2014) 73–76, https://doi.org/10.11113/jt.v69.3400.

[142] Y. Alqaheem, A.A. Alomair, Microscopy and spectroscopy techniques for characterization of polymeric membranes, 2020. https://doi.org/10.3390/MEMBRANES10020033.

[143] F.H. Akhtar, M. Kumar, L.F. Villalobos, H. Vovusha, R. Shevate, U. Schwingenschlögl, K.V. Peinemann, Polybenzimidazole-based mixed membranes with exceptionally high water vapor permeability and selectivity, J. Mater. Chem. A 5 (2017) 21807–21819, https://doi.org/10.1039/c7ta05081j.

[144] T. Corrado, Z. Huang, J. Aboki, R. Guo, Microporous polysulfones with enhanced separation performance via integration of the triptycene moiety, Ind. Eng. Chem. Res. 59 (2020) 5351–5361, https://doi.org/10.1021/acs.iecr.9b04861.

[145] Y. Zhao, C. Zhou, C. Kong, L. Chen, Ultrathin reduced graphene oxide/organosilica hybrid membrane for gas separation, JACS Au 1 (2021) 328–335, https://doi.org/10.1021/jacsau.0c00073.

[146] T.L. Chew, S.H. Ding, P.C. Oh, A.L. Ahmad, C.D. Ho, Functionalized KIT-6/polysulfone mixed matrix membranes for enhanced CO_2/CH_4 gas separation, Polymers 12 (2020) 1–11, https://doi.org/10.3390/polym12102312.

[147] M. Alsaady, S. Waqas, M.H. Zeeshan, M.A. Almarshoud, K. Maqsood, A. Abdulrahman, Y. Yan, Efficient CO_2/CH_4 separation using polysulfone/NH_2-MIL-125(Ti) mixed matrix membranes, ACS Omega 10 (2025) 11972–11979, https://doi.org/10.1021/acsomega.4c09251.

[148] L.D. Anbealagan, T.Y.S. Ng, T.L. Chew, Y.F. Yeong, S.C. Low, Y.T. Ong, C.D. Ho, Z. A. Jawad, Modified zeolite/polysulfone mixed matrix membrane for enhanced CO_2/CH_4 separation, Membranes 11 (2021) 1–17, https://doi.org/10.3390/membranes11080630.

[149] A. Imtiaz, R. Kamaludin, M.H.D. Othman, A. Jilani, I.U. Khan, M. Ayub, O. Samuel, M. Iftikhar, Synthesis and performance analysis of a polysulfone braid-supported hollow fiber membrane for natural gas purification, J. Mater. Sci. (2023), https://doi.org/10.1007/s10853-023-09208-6.

[150] I. Salahshoori, A. Seyfaee, A. Babapoor, F. Neville, R. Moreno-Atanasio, Evaluation of the effect of silica nanoparticles, temperature and pressure on the performance of PSF/PEG/SiO_2 mixed matrix membranes: a molecular dynamics simulation (MD) and design of experiments (DOE) study, J. Mol. Liq. 333 (2021) 115957, https://doi.org/10.1016/j.molliq.2021.115957.

[151] P. Natarajan, B. Sasikumar, S. Elakkiya, G. Arthanareeswaran, A.F. Ismail, W. Youravong, E. Yuliwati, Pillared cloisite 15A as an enhancement filler in polysulfone mixed matrix membranes for CO_2/N_2 and O_2/N_2 gas separation, J. Nat. Gas. Sci. Eng. 86 (2021) 103720, https://doi.org/10.1016/j.jngse.2020.103720.

[152] W. Zhao, Y. Li, Q. Li, Y. Wang, G. Wang, Investigation of the structure-property effect of phosphorus-containing polysulfone on decomposition and flame retardant epoxy resin composites, Polymers 11 (2019), https://doi.org/10.3390/POLYM11020380.
[153] A. Jonnalagedda, B.V.R. Kuncharam, Novel mixed matrix membranes with indium-based 2D and 3D MOFs as fillers and polysulfone for CO_2/CH_4 mixed gas separation, RSC Adv. 15 (2025) 2996–3007, https://doi.org/10.1039/d4ra08557d.
[154] A. Gómez-Avilés, V. Muelas-Ramos, J. Bedia, J.J. Rodriguez, C. Belver, Thermal post-treatments to enhance the water stability of NH_2-MIL-125(Ti), Catalysts 10 (2020), https://doi.org/10.3390/catal10060603.
[155] N. Nordin, A.F. Ismail, N. Misdan, N.A.M. Nazri, Modified ZIF-8 mixed matrix membrane for CO_2, AIP Conf. Proc. 1891 (2017) 322–334. ⟨https://pubs.aip.org/aip/acp/article/1891/1/020091/886522/Modified-ZIF-8-mixed-matrix-membrane-for-CO2-CH4⟩.
[156] M. Farnam, H. bin Mukhtar, A. bin Mohd Shariff, Highly permeable and selective polymeric blend mixed matrix membranes for CO_2/CH_4 separation, Chem. Pap. 75 (2021) 5663–5685, https://doi.org/10.1007/s11696-021-01744-2.
[157] Y. Ding, Perspective on gas separation membrane materials from process economics point of view, Ind. Eng. Chem. Res. 59 (2020) 556–568, https://doi.org/10.1021/acs.iecr.9b05975.
[158] X. Cao, H. Xu, S. Dong, J. Xu, Z. Qiao, S. Zhao, J. Wang, Z. Wang, Preparation of high-performance and pressure-resistant mixed matrix membranes for CO_2/H_2 separation by modifying COF surfaces with the groups or segments of the polymer matrix, J. Memb. Sci. 601 (2020) 117882, https://doi.org/10.1016/j.memsci.2020.117882.
[159] S. Singh, A.M. Varghese, K.S.K. Reddy, G.E. Romanos, G.N. Karanikolos, Polysulfone mixed-matrix membranes comprising poly(ethylene glycol)-grafted carbon nanotubes: mechanical properties and co2 separation performance, Ind. Eng. Chem. Res. 60 (2021) 11289–11308, https://doi.org/10.1021/acs.iecr.1c02040.
[160] J. Ahn, W.J. Chung, I. Pinnau, M.D. Guiver, Polysulfone/silica nanoparticle mixed-matrix membranes for gas separation, J. Memb. Sci. 314 (2008) 123–133, https://doi.org/10.1016/j.memsci.2008.01.031.
[161] E. Boyraz, F. Yalcinkaya, Preparation of Nanofibrous Membranes for Oil/ Water Separation Diplomová práce 3106T017-Clothing and Textile Engineering, Technical University of Liberec, 2019. ⟨https://d1wqtxts1xzle7.cloudfront.net/84048513/BoyrazEvren_DP-libre.pdf?1649837037=&response-content-disposition=inline%3B+filename%3DPreparation_of_NanofibrousMembranes_for.pdf&Expires=1774761143&Signature=BK5mVGICrGB-ppRz-16m6eF6vkBiLKsEiBCpAv75Ie0D8uFWp7KtYwukeMEvs5uyciliLbb9zWjgQCFtXhxM8PXK3L8HhdedIU3bZBt1TGmwC0kBYYA9LG1MX7BlWzUJCWpI7iMTRP89ZPpyZT4NvIxETOMDZRBftCZDhRrI—~V4~LaObj6-k5IUUWYCQ1qDiggSIQNVMqo53iSj4IDvl-ayv9u-YMDZyqpJa5DyCx1~hFy1iXa86RaX~vMEDeFdCgeuEgGR2LGeqyJL9kTupIEWqnD6UOMPivEbbj4FQXVB~9NiWVPfei-82C~9~y8bGrGP7sm6ivrSeJU5tRtQ_&Key-Pair-Id=APKAJLOHF5GGSLRBV4ZA⟩.
[162] T.S. Chung, L.Y. Jiang, Y. Li, S. Kulprathipanja, Mixed matrix membranes (MMMs) comprising organic polymers with dispersed inorganic fillers for gas separation, Prog. Polym. Sci. 32 (2007) 483–507, https://doi.org/10.1016/j.progpolymsci.2007.01.008.
[163] G. Dong, H. Li, V. Chen, Challenges and opportunities for mixed-matrix membranes for gas separation, J. Mater. Chem. A 1 (2013) 4610–4630, https://doi.org/10.1039/c3ta00927k.
[164] H. Roafi, S. Farrukh, Z. Salahuddin, A. Raza, S.S. Karim, H. Waheed, Fabrication and permeation analysis of polysulfone (PSf) Modified Cellulose Triacetate (CTA) Blend Membranes for CO_2 Separation from Methane (CH_4), J. Polym. Environ. 32 (2024) 2414–2430, https://doi.org/10.1007/s10924-023-03125-0.
[165] S. Dey, S. Bügel, S. Sorribas, A. Nuhnen, A. Bhunia, J. Coronas, C. Janiak, Synthesis and characterization of covalent triazine framework CTF-1@ polysulfone mixed matrix membranes and their gas separation studies, Front. Chem. 7 (2019) 1–8, https://doi.org/10.3389/fchem.2019.00693.
[166] S.A.M. Hashmi, W. Hussain, H. Bhanbhro, H. Rasool, Engineering hierarchical zeolites: mechanistic insights, predictive framework, and deployment pathways, Comments Inorg. Chem. (2025) 1–81, https://doi.org/10.1080/02603594.2025.2569055.
[167] H. Daglar, S. Keskin, Combining Machine learning and molecular simulations to unlock gas separation potentials of MOF Membranes and MOF/Polymer MMMs, ACS Appl. Mater. Interfaces 14 (2022) 32134–32148, https://doi.org/10.1021/acsami.2c08977.
[168] J. Yang, L. Tao, J. He, J.R. McCutcheon, Y. Li, Machine learning enables interpretable discovery of innovative polymers for gas separation membranes, Sci. Adv. 8 (2022) 1–14, https://doi.org/10.1126/sciadv.abn9545.
[169] L. Pilz, C. Natzeck, J. Wohlgemuth, N. Scheuermann, S. Spiegel, S. Oßwald, A. Knebel, S. Bräse, C. Wöll, M. Tsotsalas, N. Prasetya, Utilizing machine learning to optimize metal-organic framework-derived polymer membranes for gas separation, J. Mater. Chem. A 11 (2023) 24724–24737, https://doi.org/10.1039/d3ta05235d.
[170] S. Velioğlu, H.E. Karahan, B. Tantekin-Ersolmaz, Predictive transport modelling in polymeric gas separation membranes: From additive contributions to machine learning, Sep. Purif. Technol. 340 (2024), https://doi.org/10.1016/j.seppur.2024.126743.
[171] C.Y. Chuah, K. Goh, Y. Yang, H. Gong, W. Li, H.E. Karahan, M.D. Guiver, R. Wang, T.H. Bae, Harnessing filler materials for enhancing biogas separation membranes, Chem. Rev. 118 (2018) 8655–8769, https://doi.org/10.1021/acs.chemrev.8b00091.
[172] I. Douna, S. Farrukh, A. Hussain, Z. Salahuddin, T. Noor, E. Pervaiz, M. Younas, X. F. Fan, Experimental investigation of polysulfone modified cellulose acetate membrane for CO_2/H_2 gas separation, Korean J. Chem. Eng. 39 (2022) 189–197, https://doi.org/10.1007/s11814-021-0900-7.
[173] Y. Ma, H. Guo, R. Selyanchyn, B. Wang, L. Deng, Z. Dai, X. Jiang, Hydrogen sulfide removal from natural gas using membrane technology: a review, J. Mater. Chem. A 9 (2021) 20211–20240, https://doi.org/10.1039/d1ta04693d.
[174] K. Staszak, Membrane processes, Phys. Sci. Rev. 2 (2017) 1–18, https://doi.org/10.1515/psr-2017-0142.
[175] X.M. Tan, D. Rodrigue, A review on porous polymeric membrane preparation. Part I: Production techniques with polysulfone and poly (vinylidene fluoride), Polymers 11 (2019), https://doi.org/10.3390/polym11071160.
[176] R.W. Baker, B.T. Low, Gas separation membrane materials: a perspective, Macromolecules 47 (2014) 6999–7013, https://doi.org/10.1021/ma501488s.
[177] S. Dong, Z. Wang, M. Sheng, Z. Qiao, J. Wang, High-performance multi-layer composite membrane with enhanced interlayer compatibility and surface crosslinking for CO_2 separation, J. Memb. Sci. 610 (2020) 118221, https://doi.org/10.1016/j.memsci.2020.118221.
[178] S. Maghami, M. Sadeghi, S. Baghersad, B. Zornoza, Influence of solvent, Lewis acid–base complex, and nanoparticles on the morphology and gas separation properties of polysulfone membranes, Polym. Eng. Sci. 61 (2021) 1931–1942, https://doi.org/10.1002/pen.25708.
[179] S. Karimi, E. Firouzfar, M.R. Khoshchehreh, Assessment of gas separation properties and CO_2 plasticization of polysulfone/polyethylene glycol membranes, J. Pet. Sci. Eng. 173 (2019) 13–19, https://doi.org/10.1016/j.petrol.2018.10.012.
[180] D. Nasirian, I. Salahshoori, M. Sadeghi, N. Rashidi, M. Hassanzadeganroudsari, Investigation of the gas permeability properties from polysulfone/polyethylene glycol composite membrane, Polym. Bull. 77 (2020) 5529–5552, https://doi.org/10.1007/s00289-019-03031-3.
[181] M.A. Abd. Hamid, Y.T. Chung, R. Rohani, M.U. Mohd. Junaidi, Miscible-blend polysulfone/polyimide membrane for hydrogen purification from palm oil mill effluent fermentation, Sep. Purif. Technol. 209 (2019) 598–607, https://doi.org/10.1016/j.seppur.2018.07.067.
[182] C.Z. Liang, T.S. Chung, J.Y. Lai, A review of polymeric composite membranes for gas separation and energy production, Prog. Polym. Sci. 97 (2019) 101141, https://doi.org/10.1016/j.progpolymsci.2019.06.001.
[183] H. Mahdavi, F. Moradi-garakani, Effect of mixed matrix membranes comprising a novel trinuclear zinc MOF, fumed silica nanoparticles and PES on CO 2 / CH 4 separation, Chem. Eng. Res. Des, Chem. Eng. Res. Des. 125 (2017) 156–165, https://doi.org/10.1016/j.cherd.2017.07.007.
[184] H.A. Mannan, D.F. Mohshim, H. Mukhtar, T. Murugesan, Z. Man, M.A. Bustam, Journal of Industrial and Engineering Chemistry Synthesis, characterization, and CO 2 separation performance of polyether sulfone /[EMIM][Tf 2 N] ionic liquid-polymeric membranes (ILPMs), J. Ind. Eng. Chem. 54 (2017) 98–106, https://doi.org/10.1016/j.jiec.2017.05.022.
[185] M. Farrokhara, F. Dorosti, Chinese Journal of Chemical Engineering New high permeable polysulfone / ionic liquid membrane for gas separation, 28 (2020) 2301–2311.
[186] I. Yasmeen, A. Ilyas, Z. Shamair, M.A. Gilani, S. Rafiq, M.R. Bilad, A.L. Khan, Synergistic effects of highly selective ionic liquid confined in nanocages: exploiting the three component mixed matrix membranes for CO_2 capture, Chem. Eng. Res. Des. 155 (2020) 123–132, https://doi.org/10.1016/j.cherd.2020.01.006.
[187] M.S. Suleman, K.K. Lau, Y.F. Yeong, Enhanced gas separation performance of PSF membrane after modification to PSF/PDMS composite membrane in CO_2/CH_4 separation, J. Appl. Polym. Sci. 135 (2018) 1–9, https://doi.org/10.1002/app.45650.
[188] H.A. Mannan, H. Mukhtar, T. Murugesan, Preparation and characterization of newly developed polysulfone/polyethersulfone blend membrane for CO_2 Separation, Appl. Mech. Mater. 699 (2014) 325–330, https://doi.org/10.4028/www.scientific.net/amm.699.325.
[189] F. Dorosti, M.R. Omidkhah, M.Z. Pedram, F. Moghadam, Fabrication and characterization of polysulfone / polyimide – zeolite mixed matrix membrane for gas separation, Chem. Eng. J. 171 (2011) 1469–1476, https://doi.org/10.1016/j.cej.2011.05.081.
[190] S.V. Prasad, G. Arthanareeswaran, Embedding Porous MXene into the selective layer of pebax-based thin-film nanocomposite membranes for enhanced CO_2 removal performance, ACS Appl. Polym. Mater. 7 (2025) 6042–6054, https://doi.org/10.1021/acsapm.5c00372.
[191] S. Li, Y. Liu, D.A. Wong, J. Yang, Recent advances in polymer-inorganic mixed matrix membranes for co 2 separation, Polymers 13 (2021) 2539, https://doi.org/10.3390/polym13152539.
[192] M. Vinoba, M. Bhagiyalakshmi, Y. Alqaheem, A.A. Alomair, A. Pérez, M.S. Rana, Recent progress of fillers in mixed matrix membranes for CO_2 separation: a review, Sep. Purif. Technol. 188 (2017) 431–450, https://doi.org/10.1016/j.seppur.2017.07.051.
[193] A. Nuhnen, C. Janiak, in: M.J.M. Abadie, M. Pinteala, A. Rotaru (Eds.), Mixed-Matrix Membranes BT - New Trends in Macromolecular and Supramolecular Chemistry for Biological Applications, Springer International Publishing, Cham, 2021, pp. 87–113, https://doi.org/10.1007/978-3-030-57456-7_5.
[194] K. Asif, S.S.M. Lock, S.A.A. Taqvi, N. Jusoh, C.L. Yiin, B.L.F. Chin, A molecular simulation study on amine-functionalized silica/polysulfone mixed matrix

membrane for mixed gas separation, Chemosphere 311 (2023) 1–28, https://doi.org/10.1016/j.chemosphere.2022.136936.
[195] M.R.A. Hamid, H.K. Jeong, Recent advances on mixed-matrix membranes for gas separation: opportunities and engineering challenges, Korean J. Chem. Eng. 35 (2018) 1577–1600, https://doi.org/10.1007/s11814-018-0081-1.
[196] J.H. Kim, Grand challenges in membrane applications—gas and vapor, Front. Membr. Sci. Technol. 1 (2022) 1–3, https://doi.org/10.3389/frmst.2022.853402.
[197] M. Ding, X. Cai, H.L. Jiang, Improving MOF stability: approaches and applications, Chem. Sci. 10 (2019) 10209–10230, https://doi.org/10.1039/c9sc03916c.
[198] X. Liu, X. Wang, A.V. Bavykina, L. Chu, M. Shan, A. Sabetghadam, H. Miro, F. Kapteijn, J. Gascon, Molecular-scale hybrid membranes derived from metal-organic polyhedra for gas separation, ACS Appl. Mater. Interfaces 10 (2018) 21381–21389, https://doi.org/10.1021/acsami.8b07045.
[199] S. Saqib, S. Rafiq, N. Muhammad, A.L. Khan, A. Mukhtar, S. Ullah, M.H. Nawaz, F. Jamil, C. Zhang, V. Ashokkumar, Sustainable mixed matrix membranes containing porphyrin and polysulfone polymer for acid gas separations, J. Hazard. Mater. 411 (2021) 125155, https://doi.org/10.1016/j.jhazmat.2021.125155.
[200] S. Shafiq, B.A. Al-Maythalony, M. Usman, M.S. Ba-Shammakh, A.A. Al-Shammari, ZIF-95 as a filler for enhanced gas separation performance of polysulfone membrane, RSC Adv. 11 (2021) 34319–34328, https://doi.org/10.1039/d1ra06271a.
[201] I.U. Khan, M.H.D. Othman, A. Jilani, A.F. Ismail, H. Hashim, J. Jaafar, A. K. Zulhairun, M.A. Rahman, G.U. Rehman, ZIF-8 based polysulfone hollow fiber membranes for natural gas purification, Polym. Test. 84 (2020) 106415, https://doi.org/10.1016/j.polymertesting.2020.106415.
[202] K. Papchenko, G. Risaliti, M. Ferroni, M. Christian, M.G. De Angelis, An analysis of the effect of zif-8 addition on the separation properties of polysulfone at various temperatures, Membr. (Basel) 11 (2021), https://doi.org/10.3390/membranes11060427.
[203] S. Negi, A.K. Suresh, Intricacies of CO 2 removal from mixed gases and biogas using polysulfone / ZIF-8 mixed matrix, (2024) 30529–30542. https://doi.org/10.1039/d4ra04477k.
[204] X. Mei, S. Yang, P. Lu, Y. Zhang, J. Zhang, Improving the Selectivity of ZIF-8/Polysulfone-Mixed Matrix Membranes by Polydopamine Modification for H_2/CO_2 Separation, Front. Chem. 8 (2020) 1–10, https://doi.org/10.3389/fchem.2020.00528.
[205] P.D. Sutrisna, E. Savitri, M.A. Gunawan, I.H.F. Putri, S.G.B. de Rozari, Synthesis, characterization, and gas separation performances of polysulfone and cellulose acetate-based mixed matrix membranes, Polym. Technol. Mater. 59 (2020) 1300–1307, https://doi.org/10.1080/25740881.2020.1738471.
[206] S. Ishaq, R. Tamime, M.R. Bilad, A.L. Khan, Mixed matrix membranes comprising of polysulfone and microporous Bio-MOF-1: preparation and gas separation properties, Sep. Purif. Technol. 210 (2019) 442–451, https://doi.org/10.1016/j.seppur.2018.08.031.
[207] A.A. Amusa, A.L. Ahmad, A.K. Jimoh, Enhanced gas separation prowess using functionalized lignin-free lignocellulosic biomass/polysulfone composite membranes, Membr. (Basel) 11 (2021), https://doi.org/10.3390/membranes11030202.
[208] M. Raouf, R. Abedini, M. Omidkhah, E. Nezhadmoghadam, A favored CO_2 separation over light gases using mixed matrix membrane comprising polysulfone/polyethylene glycol and graphene hydroxyl nanoparticles, Process Saf. Environ. Prot. 133 (2020) 394–407, https://doi.org/10.1016/j.psep.2019.11.002.
[209] N. Gholamipour, M. Sadeghi, M. Shafiei, Effect of Silica Nanoparticles on the Performance of Polysulfone Membranes for Olefin-Paraffin Separation, Chem. Eng. Technol. 42 (2019) 2292–2301, https://doi.org/10.1002/ceat.201800147.
[210] M. Najafi, M. Sadeghi, A.A. Shamsabadi, M. Dinari, M. Soroush, Polysulfone Membranes Incorporated with Reduced Graphene Oxide Nanoparticles for Enhanced Olefin/Paraffin Separation, ChemistrySelect 5 (2020) 3675–3681, https://doi.org/10.1002/slct.202000240.
[211] R. Lin, L. Ge, H. Diao, V. Rudolph, Z. Zhu, Ionic liquids as the MOFs/polymer interfacial binder for efficient membrane separation, ACS Appl. Mater. Interfaces 8 (2016) 32041–32049, https://doi.org/10.1021/acsami.6b11074.
[212] T. Numpilai, L.K.H. Pham, T. Witoon, Advances in Ionic Liquid Technologies for CO_2 Capture and Conversion: A Comprehensive Review, Ind. Eng. Chem. Res. 63 (2024) 19865–19915, https://doi.org/10.1021/acs.iecr.4c02072.
[213] J. Tao, X. Chen, G. Chen, X. Meng, N. Yang, Recent progress on ionic liquid-based mixed-matrix membranes for CO_2 capture: disclosing the roles of ionic liquids, Sep. Purif. Technol. 376 (2025) 134150, https://doi.org/10.1016/j.seppur.2025.134150.
[214] M. Khraisheh, K.M. Zadeh, A.I. Alkhouzaam, D. Turki, M.K. Hassan, F.Al Momani, S.M.J. Zaidi, Characterization of polysulfone/diisopropylamine 1-alkyl-3-methylimidazolium ionic liquid membranes: high pressure gas separation applications, Greenh. Gases Sci. Technol. 10 (2020) 795–808, https://doi.org/10.1002/ghg.2006.
[215] P. Ortiz-Albo, T.J. Ferreira, C.F. Martins, V. Alves, I.A.A.C. Esteves, L. Cunha-Silva, I. Kumakiri, J. Crespo, L.A. Neves, Impact of ionic liquid structure and loading on gas sorption and permeation for zif-8-based composites and mixed matrix membranes, Membranes 12 (2022) 1–39, https://doi.org/10.3390/membranes12010013.
[216] Q. Liu, J. Liu, M. Li, T. Yu, M. Hu, P. Jia, N. Qi, Z. Chen, Plasticization of a novel polysulfone based mixed matrix membrane with high-performance CO_2 separation studied by positron annihilation, Colloids Surf. A Physicochem. Eng. Asp. 654 (2022) 130108, https://doi.org/10.1016/j.colsurfa.2022.130108.
[217] X. Xu, J. Wang, A. Zhou, S. Dong, K. Shi, B. Li, J. Han, D. O'Hare, High-efficiency CO_2 separation using hybrid LDH-polymer membranes, Nat. Commun. 12 (2021) 1–10, https://doi.org/10.1038/s41467-021-23121-z.
[218] M. Alsaady, M.F. Usman, H.A. Mannan, M.A.Ben Ali, A. Abdulrahman, A. Ahmed, S.U. Ilyas, Effect of VTMS-Modified TiO_2 Nanoparticles on CO_2 separation performance of polysulfone-based mixed matrix membranes, Membranes 15 (2025) 1–19, https://doi.org/10.3390/membranes15120360.
[219] H.B. Tanh Jeazet, C. Staudt, C. Janiak, Metal–organic frameworks in mixed-matrix membranes for gas separation, J. Chem. Soc Dalt. Trans. 41 (2012) 14003–14027, https://doi.org/10.1039/c2dt31550e.
[220] B. Sasikumar, G. Arthanareeswaran, Construction of selective gas permeation channels in polymeric membranes using nanocage tuned ionic liquid/MIL-53 (Al) filler nanoparticles for effective CO_2 separation, J. Nat. Gas. Sci. Eng. 106 (2022) 104728, https://doi.org/10.1016/j.jngse.2022.104728.
[221] B.D. Reid, F.A. Ruiz-Trevino, I.H. Musselman, K.J. Balkus, J.P. Ferraris, Gas permeability properties of polysulfone membranes containing the mesoporous molecular sieve MCM-41, Chem. Mater. 13 (2001) 2366–2373, https://doi.org/10.1021/cm000931+.
[222] A. Junaidi, U. Zulfiani, S. Khomariyah, T. Gunawan, N. Widiastuti, N. Sazali, W.N. W. Salleh, Utilization of polyphenylene sulfide as an organic additive to enhance gas separation performance in polysulfone membranes, RSC Adv. 14 (2024) 2311–2319, https://doi.org/10.1039/d3ra06136a.
[223] M. Raouf, R. Abedini, M. Omidkhah, A favored CO_2 separation over light gases using mixed matrix membrane comprising polysulfone / polyethylene glycol and graphene hydroxyl nanoparticles, Process Saf. Environ. Prot. 133 (2020) 394–407.
[224] S. Ebrahimi, S. Mollaiy-berneti, H. Asadi, PVA / PES-amine-functional graphene oxide mixed matrix membranes for CO_2/CH_4 separation: experimental and modeling, Chem. Eng. Res. Des. 9 (2016) 647–656.
[225] Z. Tahir, M. Aslam, M. Amjad, M. Roil, Separation and Puri fi cation Technology SO_3H functionalized UiO-66 nanocrystals in Polysulfone based mixed matrix membranes, Synth. Appl. e ffi Cient. CO_2 capture 224 (2019) 524–533.
[226] N.A.H.M. Nordin, A.F. Ismail, A. Mustafa, R.S. Murali, T. Matsuura, Utilizing low ZIF-8 loading for asymmetric PSf/ZIF-8 mixed matrix membrane for CO_2/CH_4 Separation, RCS Adv. (2015).
[227] B. Sasikumar, G. Arthanareeswaran, Concurrent enhancement of CO_2-philic pathway and interfacial compatibilization in ZIF-67 based polysulfone membranes through [Bmim][Tf2N] for CO_2 separation, Appl. Surf. Sci. 606 (2022), https://doi.org/10.1016/j.apsusc.2022.154900.
[228] K. Sainath, A. Modi, J. Bellare, In-situ growth of zeolitic imidazolate framework-67 nanoparticles on polysulfone/graphene oxide hollow fiber membranes enhance CO_2/CH_4 separation, J. Memb. Sci. 614 (2020) 118506, https://doi.org/10.1016/j.memsci.2020.118506.
[229] A. Azizi, E.A. Feijani, Z. Ghorbani, A. Tavasoli, Fabrication and characterization of highly efficient three component CuBTC/graphene oxide/PSF membrane for gas separation application, Int. J. Hydrog. Energy 46 (2021) 2244–2254, https://doi.org/10.1016/j.ijhydene.2020.10.025.
[230] B. Sasikumar, G. Arthanareeswaran, Interfacial design of polysulfone/Cu-BTC membrane using [Bmim][Tf2N] and [Dmim][Cl] RTILs for CO_2 separation: performance assessment for single and mixed gas separation, Sep. Purif. Technol. 295 (2022) 121315, https://doi.org/10.1016/j.seppur.2022.121315.
[231] R. Wijiyanti, A.N. Ubaidillah, T. Gunawan, Z.A. Karim, A.F. Ismail, S. Smart, R. Lin, N. Widiastuti, Polysulfone mixed matrix hollow fiber membranes using zeolite templated carbon as a performance enhancement filler for gas separation, Chem. Eng. Res. Des. 150 (2019) 274–288, https://doi.org/10.1016/j.cherd.2019.08.004.
[232] S. Castarlenas, C. Téllez, J. Coronas, Gas separation with mixed matrix membranes obtained from MOF UiO-66-graphite oxide hybrids, J. Memb. Sci. 526 (2017) 205–211, https://doi.org/10.1016/j.memsci.2016.12.041.
[233] P.S.G, A.F.I.K. Zahri, The incorporation of graphene oxide into polysulfone mixed matrix membrane for CO_2/CH_4 separation, 325–123, IOP Conf. Ser. Earth Environ. Sci. 36 (2016), https://doi.org/10.1088/1755-1315/36/1/012007.
[234] S. Sorribas, B. Zornoza, C. Téllez, J. Coronas, Mixed matrix membranes comprising silica-(ZIF-8) core-shell spheres with ordered meso-microporosity for natural- and bio-gas upgrading, J. Memb. Sci. 452 (2014) 184–192, https://doi.org/10.1016/j.memsci.2013.10.043.
[235] R. Wijiyanti, A.R.K. Wardhani, R.A. Roslan, T. Gunawan, Z.A. Karim, A.F. Ismail, N. Widiastuti, Enhanced gas separation performance of polysulfone membrane by incorporation of zeolite-templated carbon, Malays. J. Fundam. Appl. Sci. 16 (2020) 128–134, https://doi.org/10.11113/mjfas.v16n2.1472.
[236] H. Mahdavi, F. Moradi-garakani, Effect of mixed matrix membranes comprising a novel trinuclear zinc MOF, fumed silica nanoparticles and PES on CO 2 / CH 4 separation, 5, Chem. Eng. Res. Des. (2017) 156–165.
[237] S.F. Soleymanipour, A.H.S. Dehaghani, V. Pirouzfar, A. Alihosseini, The morphology and gas-separation performance of membranes comprising multiwalled carbon nanotubes/polysulfone-Kapton, J. Appl. Polym. Sci. 133 (2016) 1–8, https://doi.org/10.1002/app.43839.
[238] S. Kim, L. Chen, J.K. Johnson, E. Marand, Polysulfone and functionalized carbon nanotube mixed matrix membranes for gas separation: Theory and experiment, J. Memb. Sci. 294 (2007) 147–158, https://doi.org/10.1016/j.memsci.2007.02.028.
[239] O. Choi, S. Karki, R.R. Pawar, S. Hazarika, P.G. Ingole, A new perspective of functionalized MWCNT incorporated thin film nanocomposite hollow fiber membranes for the separation of various gases, J. Environ. Chem. Eng. 9 (2021) 104774, https://doi.org/10.1016/j.jece.2020.104774.

[240] A. Dehghani Kiadehi, A. Rahimpour, M. Jahanshahi, A.A. Ghoreyshi, Novel carbon nano-fibers (CNF)/polysulfone (PSf) mixed matrix membranes for gas separation, J. Ind. Eng. Chem. 22 (2015) 199–207, https://doi.org/10.1016/j.jiec.2014.07.011.
[241] A.D. Kiadehi, M. Jahanshahi, A. Rahimpour, S.A.A. Ghoreyshi, The effect of functionalized carbon nano-fiber (CNF) on gas separation performance of polysulfone (PSf) membranes, Chem. Eng. Process. Process. Intensif. 90 (2015) 41–48, https://doi.org/10.1016/j.cep.2015.02.005.
[242] I. Salahshoori, D. Nasirian, N. Rashidi, M.K. Hossain, A. Hatami, M. Hassanzadeganroudsari, The effect of silica nanoparticles on polysulfone–polyethylene glycol (PSF/PEG) composite membrane on gas separation and rheological properties of nanocomposites, Springe Berl. Heidelb. (2021), https://doi.org/10.1007/s00289-020-03255-8.
[243] H. Kulak, R. Thür, I.F.J. Vankelecom, MOF/polymer mixed-matrix membranes preparation: effect of main synthesis parameters on co2/ch4 separation performance, Membrane 12 (2022), https://doi.org/10.3390/membranes12040425.
[244] Y. Cheng, Y. Ying, L. Zhai, G. Liu, J. Dong, Y. Wang, M.P. Christopher, S. Long, Y. Wang, D. Zhao, Mixed matrix membranes containing MOF@COF hybrid fillers for efficient CO_2/CH_4 separation, J. Memb. Sci. 573 (2019) 97–106, https://doi.org/10.1016/j.memsci.2018.11.060.
[245] S. Rao, B. Prasad, Y. Han, W.S.W. Ho, Polymeric Membranes for H_2S and CO_2 Removal from Natural Gas for Hydrogen Production: A Review, Energies 16 (2023), https://doi.org/10.3390/en16155713.
[246] D.J. Harrigan, J.A. Lawrence, H.W. Reid, J.B. Rivers, J.T. O'Brien, S.A. Sharber, B. J. Sundell, Tunable sour gas separations: Simultaneous H_2S and CO_2 removal from natural gas via crosslinked telechelic poly(ethylene glycol) membranes, J. Memb. Sci. 602 (2020) 117947, https://doi.org/10.1016/j.memsci.2020.117947.
[247] Y.I. Park, B.S. Kim, Y.H. Byun, S.H. Lee, E.W. Lee, J.M. Lee, Preparation of supported ionic liquid membranes (SILMs) for the removal of acidic gases from crude natural gas, Desalination 236 (2009) 342–348, https://doi.org/10.1016/j.desal.2007.10.085.
[248] M. Heiranian, H. Fan, L. Wang, X. Lu, M. Elimelech, Mechanisms and models for water transport in reverse osmosis membranes: history, critical assessment, and recent developments, Chem. Soc. Rev. 52 (2023) 8455–8480, https://doi.org/10.1039/d3cs00395g.
[249] L. Wang, T. Cao, J.E. Dykstra, S. Porada, P.M. Biesheuvel, M. Elimelech, Salt and water transport in reverse osmosis membranes: beyond the solution-diffusion model, Environ. Sci. Technol. 55 (2021) 16665–16675, https://doi.org/10.1021/acs.est.1c05649.
[250] D.N. Theodorou, U.W. Suter, Atomistic modeling of mechanical properties of polymeric glasses, Macromolecules 19 (1986) 139–154, https://doi.org/10.1021/ma00155a022.
[251] D. Račko, S. Capponi, F. Alvarez, J. Colmenero, J. Bartoš, The free-volume structure of a polymer melt, poly(vinyl methylether) from molecular dynamics simulations and cavity analysis, J. Chem. Phys. 131 (2009), https://doi.org/10.1063/1.3193727.
[252] N. Vergadou, D.N. Theodorou, Molecular modeling investigations of sorption and diffusion of small molecules in Glassy polymers, Membr. (Basel) 9 (2019), https://doi.org/10.3390/membranes9080098.
[253] S. Keskin, S.A. Altinkaya, A review on computational modeling tools for MOF-based mixed matrix membranes, Computation 7 (2019), https://doi.org/10.3390/computation7030036.
[254] D. Schneider, F. Kapteijn, R. Valiullin, Transport properties of mixed-matrix membranes: a kinetic Monte Carlo Study, Phys. Rev. Appl. 12 (2019) 1, https://doi.org/10.1103/PhysRevApplied.12.044034.
[255] Q. Yuan, M. Longo, A.W. Thornton, N.B. McKeown, B. Comesaña-Gándara, J. C. Jansen, K.E. Jelfs, Imputation of missing gas permeability data for polymer membranes using machine learning, J. Memb. Sci. 627 (2021), https://doi.org/10.1016/j.memsci.2021.119207.
[256] G. Zhu, C. Kim, A. Chandrasekarn, J.D. Everett, R. Ramprasad, R.P. Lively, Polymer genome-based prediction of gas permeabilities in polymers, J. Polym. Eng. 40 (2020) 451–457, https://doi.org/10.1515/polyeng-2019-0329.
[257] S. Majumdar, B. Tokay, V. Martin-Gil, J. Campbell, R. Castro-Muñoz, M. Z. Ahmad, V. Fila, Mg-MOF-74/Polyvinyl acetate (PVAc) mixed matrix membranes for CO_2 separation, Sep. Purif. Technol. 238 (2020) 116411, https://doi.org/10.1016/j.seppur.2019.116411.
[258] B.J. Befort, R.S. DeFever, E.J. Maginn, A.W. Dowling, Machine Learning-Enabled Optimization of Force Fields for Hydrofluorocarbons, Comput. Aided Chem. Eng. 49 (2022) 1249–1254, https://doi.org/10.1016/B978-0-323-85159-6.50208-6.
[259] F. Cailliez, P. Pernot, F. Rizzi, R. Jones, O. Knio, G. Arampatzis, P. Koumoutsakos, Bayesian calibration of force fields for molecular simulations, Uncertain. Quantif. Multiscale Mater. Model (2020) 169–227, https://doi.org/10.1016/B978-0-08-102941-1.00006-7.
[260] G. Ciccotti, C. Dellago, M. Ferrario, E.R. Hernández, M.E. Tuckerman, Molecular simulations: past, present, and future (a Topical Issue in EPJB), Eur. Phys. J. B 95 (2022), https://doi.org/10.1140/epjb/s10051-021-00249-x.
[261] A. Owhal, V. Belwanshi, T. Roy, S. Goel, Strain softening observed during nanoindentation of Equimolar- Ratio Co-Mn-Fe-Cr-Ni High Entropy Alloy, J. Micro 20 (2023). ⟨https://www.researchgate.net/profile/Saurav-Goel/publication/375890792⟩.
[262] X.Y. Wang, P.J. In'T Veld, Y. Lu, B.D. Freeman, I.C. Sanchez, A molecular simulation study of cavity size distributions and diffusion in para and meta isomers, Polym. (Guildf.) 46 (2005) 9155–9161, https://doi.org/10.1016/j.polymer.2005.06.122.
[263] G. Marque, J. Verdu, V. Prunier, D. Brown, A molecular dynamics simulation study of three polysulfones in dry and hydrated states, J. Polym. Sci. Part B Polym. Phys. 48 (2010) 2312–2336, https://doi.org/10.1002/polb.22117.
[264] M. Heuchel, M. Böhning, O. Hölck, M.R. Siegert, D. Hofmann, Atomistic packing models for experimentally investigated swelling states induced by CO_2 in glassy polysulfone and poly(ether sulfone), J. Polym. Sci. Part B Polym. Phys. 44 (2006) 1874–1897, https://doi.org/10.1002/POLB.20844.
[265] O. Hölck, M.R. Siegert, M. Heuchel, M. Böhning, CO_2 sorption induced dilation in polysulfone: Comparative analysis of experimental and molecular modeling results, Macromolecules 39 (2006) 9590–9604, https://doi.org/10.1021/ma061562r.
[266] K. Golzar, S. Amjad-Iranagh, M. Amani, H. Modarress, Molecular simulation study of penetrant gas transport properties into the pure and nanosized silica particles filled polysulfone membranes, J. Memb. Sci. 451 (2014) 117–134, https://doi.org/10.1016/j.memsci.2013.09.056.
[267] K. Asif, S.S.M. Lock, S.A.A. Taqvi, N. Jusoh, C.L. Yiin, B.L.F. Chin, A molecular simulation study on amine-functionalized silica/polysulfone mixed matrix membrane for mixed gas separation, Chemosphere 311 (2023) 136936, https://doi.org/10.1016/j.chemosphere.2022.136936.
[268] S.S.M. Lock, K.K. Lau, N. Jusoh, A.M. Shariff, C.H. Gan, C.L. Yiin, An atomistic simulation towards molecular design of silica polymorphs nanoparticles in polysulfone based mixed matrix membranes for CO_2/CH_4 gas separation, Polym. Eng. Sci. 60 (2020) 3197–3215, https://doi.org/10.1002/pen.25547.
[269] R. Soleimani, A.H. Saeedi Dehaghani, A theoretical probe into the separation of $CO_2/CH_4/N_2$ mixtures with polysulfone/polydimethylsiloxane–nano zinc oxide MMM, Sci. Rep. 13 (2023) 1–15, https://doi.org/10.1038/s41598-023-36051-1.
[270] S.S.M. Lock, K.K. Lau, A.M. Shariff, Y.F. Yeong, M.A. Bustam, Computational insights on the role of film thickness on the physical properties of ultrathin polysulfone membranes, RSC Adv. 7 (2017) 44376–44393, https://doi.org/10.1039/c7ra07277e.
[271] S.S.M. Lock, K.K. Lau, A.M. Shariff, Y.F. Yeong, M.A. Bustam, Thickness dependent penetrant gas transport properties and separation performance within ultrathin polysulfone membrane: Insights from atomistic molecular simulation, J. Polym. Sci. Part B Polym. Phys. 56 (2018) 131–158, https://doi.org/10.1002/polb.24523.
[272] S.S.M. Lock, K.K. Lau, A.M. Shariff, Y.F. Yeong, M.A. Bustam, N. Jusoh, F. Ahmad, An atomistic simulation towards elucidation of operating temperature effect in CO_2 swelling of polysulfone polymeric membranes, J. Nat. Gas. Sci. Eng. 57 (2018) 135–154, https://doi.org/10.1016/j.jngse.2018.07.002.
[273] S.S.M. Lock, K.K. Lau, N. Jusoh, A.M. Shariff, Y.F. Yeong, C.L. Yiin, S.A. Ammar Taqvi, Physical property and gas transport studies of ultrathin polysulfone membrane from 298.15 to 328.15 K and 2–50 bar: atomistic molecular simulation and empirical modelling, RSC Adv. 10 (2020) 32370–32392, https://doi.org/10.1039/d0ra05836j.
[274] K. Asif, S.S.M. Lock, S.A.A. Taqvi, N. Jusoh, C.L. Yiin, B.L.F. Chin, A.C.M. Loy, A molecular simulation study of silica/polysulfone mixed matrix membrane for mixed gas separation, Polymers 13 (2021), https://doi.org/10.3390/polym13132199.
[275] M. Dehghani, M. Asghari, A.H. Mohammadi, M. Mokhtari, Molecular simulation and Monte Carlo study of structural-transport-properties of PEBA-MFI zeolite mixed matrix membranes for CO_2, CH_4 and N_2 separation, Comput. Chem. Eng. 103 (2017) 12–22, https://doi.org/10.1016/j.compchemeng.2017.03.002.
[276] K. Golzar, H. Modarress, S. Amjad-Iranagh, Effect of pristine and functionalized single- and multi-walled carbon nanotubes on CO_2 separation of mixed matrix membranes based on polymers of intrinsic microporosity (PIM-1): a molecular dynamics simulation study, J. Mol. Model 23 (2017), https://doi.org/10.1007/s00894-017-3436-3.
[277] K. Golzar, H. Modarress, S. Amjad-Iranagh, Separation of gases by using pristine, composite and nanocomposite polymeric membranes: a molecular dynamics simulation study, J. Memb. Sci. 539 (2017) 238–256, https://doi.org/10.1016/j.memsci.2017.06.010.
[278] J. Xia, S. Liu, P.K. Pallathadka, M.L. Chng, T.S. Chung, Structural determination of extem XH 1015 and its gas permeability comparison with polysulfone and ultem via molecular simulation, Ind. Eng. Chem. Res. 49 (2010) 12014–12021, https://doi.org/10.1021/ie901906p.
[279] H. Li, X. Zhang, H. Chu, G. Qi, H. Ding, X. Gao, J. Meng, Molecular simulation on permeation behavior of $CH_4/CO_2/H_2S$ Mixture Gas in PVDF at service conditions, Polymers 14 (2022), https://doi.org/10.3390/polym14030545.
[280] H.D. Patel, N.K. Acharya, Transport properties of polymer blends and composite membranes for selective permeation of hydrogen, Int. J. Hydrog. Energy 48 (2023) 37796–37810, https://doi.org/10.1016/J.IJHYDENE.2022.11.304.
[281] N. Saini, K. Pandey, K. Awasthi, Conjugate polymer-based membranes for gas separation applications: current status and future prospects, Mater. Today Chem. 22 (2021) 100558, https://doi.org/10.1016/j.mtchem.2021.100558.
[282] F. Weigelt, S. Escorihuela, A. Descalzo, A. Tena, S. Escolástico, S. Shishatskiy, J. M. Serra, T. Brinkmann, Novel polymeric thin-film composite membranes for high-temperature gas separations, Membrane 9 (2019), https://doi.org/10.3390/membranes9040051.
[283] N.N. Nyamweya, Applications of polymer blends in drug delivery, Futur. J. Pharm. Sci. 7 (2021), https://doi.org/10.1186/s43094-020-00167-2.
[284] L. Wang, Y. Wang, L. Wu, G. Wei, Fabrication, Properties, Performances, and Separation Application of Polymeric Pervaporation Membranes: A Review, Polylers 12 (2020) 1–30, https://doi.org/10.3390/polym12071466.
[285] X. Dong, D. Lu, T.A.L. Harris, I.C. Escobar, Polymers and solvents used in membrane fabrication: A review focusing on sustainable membrane development, Membrane 11 (2021), https://doi.org/10.3390/membranes11050309.

[286] N. Abdul, H. Nordin, A.F. Ismail, N. Misdan, Modified ZIF-8 mixed matrix membrane for Modified ZIF-8 Mixed Matrix Membrane for CO_2/CH_4 Separation, 2nd, Int. Conf. Appl. Sci. Technol. (2017), 020091 (202AD) 020091–1–020091–6.
[287] J.K. Adewole, A.L. Ahmad, S. Ismail, C.P. Leo, Current challenges in membrane separation of CO_2 from natural gas: A review, Int. J. Greenh. Gas. Control 17 (2013) 46–65, https://doi.org/10.1016/j.ijggc.2013.04.012.
[288] K. Farahdila, P.S. Goh, A.F. Ismail, N.F.W.M. Wan, H.M.H. Mohd, W.K. Soh, S. Y. Yeo, Challenges in Membrane Process for Gas Separation from Natural Gas, J. Appl. Membr. Sci. Technol. 25 (2021) 89–105, https://doi.org/10.11113/amst.v25n2.222.
[289] G.O. Yahaya, A. Hayek, A. Alsamah, Y.A. Shalabi, M.M. Ben Sultan, R.H. Alhajry, Copolyimide membranes with improved H_2S/CH_4 selectivity for high-pressure sour mixed-gas separation, Sep. Purif. Technol. 272 (2021) 118897, https://doi.org/10.1016/j.seppur.2021.118897.
[290] J.C. Guerrero Piña, D. Alpízar, P. Murillo, M. Carpio-Chaves, R. Pereira-Reyes, J. Vega-Baudrit, C. Villarreal, Advances in mixed-matrix membranes for biorefining of biogas from anaerobic digestion, Front. Chem. 12 (2024) 1–11, https://doi.org/10.3389/fchem.2024.1393696.
[291] X. Du, S. Zhao, Y. Qu, H. Jia, S. Xu, M. Zhang, G. Geng, Preparation of polyimide/ionic liquid hybrid membrane for CO_2/CH_4 Separation, Polymers 16 (2024), https://doi.org/10.3390/polym16030393.
[292] N. Kabay, M.M.A. Shirazi, E. Güler, M. Bryjak, Grand challenges in membrane modules and processes, Front. Membr. Sci. Technol. 1 (2022) 1–4, https://doi.org/10.3389/frmst.2022.913597.
[293] K.C. Khulbe, T. Matsuura, Thin film composite and/or thin film nanocomposite hollow fibermembrane forwater treatment, pervaporation, and gas/vapor separation, Polymers 10 (2018) 1–22, https://doi.org/10.3390/polym10101051.
[294] L. Li, G. Ma, Z. Pan, N. Zhang, Z. Zhang, Research progress in gas separation using hollow fiber membrane contactors, Membrers 10 (2020) 1–20, https://doi.org/10.3390/membranes10120380.
[295] P. Yadav, N. Ismail, M. Essalhi, M. Tysklind, D. Athanassiadis, N. Tavajohi, Assessment of the environmental impact of polymeric membrane production, J. Memb. Sci. 622 (2021) 118987, https://doi.org/10.1016/j.memsci.2020.118987.
[296] A. Dedvukaj, P. Van den Mooter, I.F.J. Vankelecom, Solvent-resistant uv-cured polysulfone support membranes using a green solvent, Membrane 12 (2022), https://doi.org/10.3390/membranes12010001.
[297] E. Favre, The future of membrane separation processes: a prospective analysis, Front. Chem. Eng. 4 (2022) 1–5, https://doi.org/10.3389/fceng.2022.916054.
[298] N.H. Suhaimi, Y.F. Yeong, C.W.M. Ch'ng, N. Jusoh, Tailoring CO_2/CH_4 separation performance of mixed matrix membranes by using ZIF-8 particles functionalized with different amine groups, Polymers 11 (2019) 1–19, https://doi.org/10.3390/polym11122037.
[299] X. Zhang, Z. Tu, H. Li, K. Huang, X. Hu, Y. Wu, D.R. MacFarlane, Selective separation of H_2S and CO_2 from CH_4 by supported ionic liquid membranes, J. Memb. Sci. 543 (2017) 282–287, https://doi.org/10.1016/j.memsci.2017.08.033.
[300] A.M.M. Gomes, P.J. Costa, M. Machuqueiro, Recent advances on molecular dynamics-based techniques to address drug membrane permeability with atomistic detail, BBA Adv. 4 (2023), https://doi.org/10.1016/j.bbadva.2023.100099.
[301] S.L. Watkins, Current trends and changes in use of membrane molecular dynamics simulations within academia and the pharmaceutical industry, Membranes 13 (2023), https://doi.org/10.3390/membranes13020148.
[302] C.Y. Yee, L.G. Lim, S.S.M. Lock, N. Jusoh, C.L. Yiin, B.L.F. Chin, Y.H. Chan, A.C. M. Loy, M. Mubashir, A systematic review of the molecular simulation of hybrid membranes for performance enhancements and contaminant removals, Chemosphere 307 (2022) 135844, https://doi.org/10.1016/J.CHEMOSPHERE.2022.135844.
[303] A. Rawal, T. Hazarika, B. Kakati, D. Pal, Low-temperature DC argon plasma treatment of polysulfone membranes to enhance anti-fouling properties in oil-water emulsion separation, Surf. Interfaces 64 (2025) 106406, https://doi.org/10.1016/j.surfin.2025.106406.
[304] A. Mohamed, S. Yousef, A. Tonkonogovas, V. Makarevicius, Thin-film composite membranes with tailored pore structures for enhanced gas separation performance, J. Environ. Chem. Eng. 13 (2025) 115527, https://doi.org/10.1016/j.jece.2025.115527.
[305] A. Figoli, T. Marino, S. Simone, E. Di Nicolò, X.M. Li, T. He, S. Tornaghi, E. Drioli, Towards non-toxic solvents for membrane preparation: a review, Green. Chem. 16 (2014) 4034–4059, https://doi.org/10.1039/c4gc00613e.
[306] J.Y. Jeon, B.R. Park, J.H. Kim, Numerical Simulation and Optimization of 4-Component LDG separation in the steelmaking industry using polysulfone hollow fiber membranes, Membranes 12 (2022), https://doi.org/10.3390/membranes12010097.
[307] H. Abdul Mannan, H. Mukhtar, M. Shima Shaharun, M. Roslee Othman, T. Murugesan, Polysulfone/poly(ether sulfone) blended membranes for CO_2 separation, J. Appl. Polym. Sci. 133 (2016) 1–9, https://doi.org/10.1002/app.42946.
[308] M. Zhao, C. Zhang, Y.-X. Weng, Improved artificial neural networks (ANNs) for predicting the gas separation performance of polyimides, J. Memb. Sci. 681 (2023) 121765, https://doi.org/10.1016/j.memsci.2023.121765.
[309] A. Li, J. Chu, S. Huang, Y. Liu, M. He, X. Liu, Machine learning-assisted development of gas separation membranes: a review, Carbon Capture Sci. Technol. 14 (2025), https://doi.org/10.1016/j.ccst.2025.100374.
[310] T. Liu, L. Liu, F. Cui, F. Ding, Q. Zhang, Y. Li, Predicting the performance of polyvinylidene fluoride, polyethersulfone and polysulfone filtration membranes using machine learning, J. Mater. Chem. A 8 (2020) 21862–21871, https://doi.org/10.1039/d0ta07607d.